

Calcination of Gypsum Plasterboard under Fire Exposure

by

Chu Nguong, Ngu

Supervised by:

Associate Professor Andy Buchanan
and
Hans Gerlich

Fire Engineering Research Report 04/6

May 2004

This report is similar to a thesis submitted in partial fulfilment of the requirements for the degree of Master of Engineering in Fire Engineering

Department of Civil Engineering
University of Canterbury
Private Bag 4800
Christchurch, New Zealand

For a full list of reports please visit http://www.civil.canterbury.ac.nz/fire/fe_resrch_reps.html

Abstract

The area of post-flashover fire investigation using the degradation or calcination of gypsum plasterboard has attracted interest in many countries. Many fire investigators often see the results of the calcination of gypsum plasterboard that can be particularly useful tool as an indicator of fire origin and fire severity. This thesis examines the depth of calcination of gypsum plasterboard under simulated fire exposure conditions and develops a practical method of assessing the calcination.

Past methods were found only concerned about the relative calcination depths hence the actual calcination measurements are of little importance and measurements taken often depend on the testing personnel. For this purpose, constant force probe was developed to give a better representation of the actual calcination depth and consistent measurement due to its constant penetrating force into the fire damaged plasterboard. The relative changes; increasing or decreasing in calcination depth measurements at different local positions after the room burnout can be used to predict the likely fire origin and fire development scenarios. Bench scale cone calorimeter tests were carried out to expose gypsum plasterboards to different heat fluxes for varying exposure time, establishing the depth of calcination.

A method of predicting the time when the fire has been put out and the calcination depth for complete burnout of a compartment has been established. This is based on a correlation between the calcination depth and fire severity obtained from the experimental data and the radiant exposure area correlation concept. Further validation is required to ensure the method is reliable by conducting full scale compartment tests. The full scale compartment tests would also provide the use of calcination depth of gypsum plasterboard in real fires as an indicator of fire severity.

Acknowledgements

First of all, I would like to give a special word of thanks to my supervisors, Dr Andy Buchanan (University of Canterbury) and Hans Gerlich (Winstone Wallboards Ltd.) for their guidance, constant encouragement and enthusiasm and Winstone Wallboards Ltd. of providing all the necessary materials throughout my research. The project would not be possible without them.

Special thanks to Grant Dunlop and Russell Peoples for their technical service and expertise, particularly for helping me to cut the samples, building the tools, running the cone calorimeter etc.

Thank you to Clara Sumner (Winstone Wallboards Ltd.) for sending the gypsum plasterboards and providing useful background information.

Additional thanks go to Roger Harrison, Andrew Tsui and Michael Spearpoint (University of Canterbury) for their support and advice during my research and many thanks to all of the 2003 Fire Engineering class for all the enjoyable times.

Finally, my deepest gratitude is extended to many people, especially to my family; Mum and Dad, Brothers, Sister and Chan Hung, without their reassurance and caring, the completion of my course of study would have been more arduous.

Table of Contents

Abstract	ii
Acknowledgements	iii
Table of Contents	iv
List of Figures	vii
List of Tables	x
Chapter 1 Introduction	1
1.1 Background	1
1.2 Gypsum Wallboards in New Zealand.....	3
1.3 Manufacture.....	6
1.4 Chemistry	7
1.5 Project Objectives.....	8
Chapter 2 Literature Review	11
2.1 Fire Properties and Performance	11
2.1.1 Ryan (1962).....	11
2.1.2 Lawson (1977).....	11
2.1.3 Buchanan and Gerlich (1997).....	12
2.1.4 Alfawakhiri et al (1999)	13
2.1.5 Thomas (2002)	16
2.1.6 Goncalves et al (1996).....	17
2.1.7 National Research Council of Canada.....	18
2.2 Fire Modeling.....	18
2.2.1 Mehaffey et al (1994).....	19
2.2.2 Gerlich (1995)	19
2.2.3 Sultan (1996)	19
2.2.4 Cooper (1997).....	20
2.2.5 Takeda and Mehaffey (1998).....	20

2.2.6 McGraw (1998)	20
2.2.7 Jones (2001)	21
2.2.8 Thomas (2002)	21
2.3 Post-flashover Analysis	22
2.3.1 Posey and Posey (1983)	22
2.3.2 McGraw (1998)	22
2.3.3 Schroeder and Williamson (2000)	23
2.3.4 Kennedy et al (2003)	24
Chapter 3 Methods of Measuring Calcination Depth.....	25
3.1 Probe Survey Methods	25
3.2 Visual Observation	27
3.3 Hand Scraping	27
3.4 Spring Force Probe	28
3.5 Constant Force Probe	32
3.6 Methods of Measuring Calcination Depth Conclusions.....	39
Chapter 4 Room Fires.....	40
4.1 General	40
4.2 Stages in Enclosure Fire Development.....	40
4.3 Fire Severity	44
4.3.1 Equal Area Concept.....	45
4.3.2 Time-Equivalent Concept.....	47
4.4 Design Fires.....	47
Chapter 5 Experimental Program.....	51
5.1 General	51
5.2 Cone Calorimeter Test.....	51
5.2.1 Cone Heater	54
5.2.2 Sample Mounting	56
5.3 Experimental Procedures.....	58
5.3.1 Calibration	58

5.3.2 Sample preparation.....	59
5.3.3 Design of experiments.....	62
5.3.4 Testing procedure.....	63
Chapter 6 Analysis of Results	66
6.1 Analysis Procedures and Calculations.....	66
6.1.1 Mass Loss.....	66
6.1.2 Calcination Depth.....	66
6.1.3 Temperature profile.....	71
6.2 Results.....	71
6.2.1 Mass Loss.....	71
6.2.2 Calcination Depth and Fire Severity Correlation.....	72
6.2.3 Calcination Depth in Pre-flashover Stage.....	75
6.2.4 Calcination Depth in Post-flashover Stage.....	77
6.2.5 Temperature profile.....	83
Chapter 7 Discussion.....	85
7.1 Mass Loss.....	85
7.2 Correlation between Calcination Depth and Fire Severity.....	85
7.3 Effect of Pre-flashover Stage on Calcination Depth.....	86
7.4 Effect of Post-flashover Stage on Calcination Depth.....	87
7.5 Temperature Profile.....	91
Chapter 8 Conclusions.....	93
8.1 Conclusions.....	93
8.2 Recommendations.....	95
Chapter 9 References.....	96
Appendix A Sample Test Scenarios.....	102
Appendix B Summary of Mass Loss and Calcination Depths.....	104
Appendix C Mass Loss Curves.....	107

List of Figures

Figure 1.1 Gypsum wallboard or gypsum plasterboard	1
Figure 1.2 Annual shipments of gypsum wallboard from U.S. manufacturers.....	2
Figure 1.3 Available thickness, width and length for GIB® Products (Taken from GIB® website)	5
Figure 1.4 Typical production process for gypsum plasterboard (Figure taken from Buchanan and Gerlich 1997)	6
Figure 1.5 Gypsum plasterboard exposed to fire heat flux (Mowrer 2001).....	9
Figure 2.1 Comparison of New Zealand and North American boards when used in symmetrical non load bearing wood stud walls (Reproduced from Buchanan and Gerlich (1997))	13
Figure 2.2 Specific Heat of Type X Gypsum Board (Reproduced from Sultan (1996))	14
Figure 2.3 Thermal Conductivity of Gypsum Board (Reproduced from Sultan (1996)).....	14
Figure 2.4 Specific Heat of Gypsum Plaster (Reproduced from Cooper (1997)).....	15
Figure 2.5 Thermal Conductivity of Gypsum Plaster (Reproduced from Cooper (1997))	15
Figure 2.6 Revised specific heat as used (Reproduced from Thomas (2002))	16
Figure 2.7 Revised thermal conductivity as used (Reproduced from Thomas (2002))	17
Figure 3.1 Test probe – Depth gauge (Kennedy et al 2003)	26
Figure 3.2 Test probe – Vernier Calliper	26
Figure 3.3 Examining the depth of calcination using the naked eye.....	27
Figure 3.4 Examining the depth of calcination by using “hand scraping” method.....	28
Figure 3.5 Electronic digital calliper and the main body	29
Figure 3.6 Pin attached to the end of the probe with spring inside the main body	29
Figure 3.7 Complete view of the spring-force probe	30
Figure 3.8 Different pin shapes; sharp, blunt and flat (from left to right)	30
Figure 3.9 Constant-force spring.....	33
Figure 3.10 Typical load/deflection curves.....	33

Figure 3.11 Constant-force springs arrangement in order to multiply spring load	34
Figure 3.12 Constant force probe made	35
Figure 3.13 Different pin sizes made	36
Figure 3.14 Calcination depth measurements at different pressures for probe test 1 – 10 mm Standard board under 50 kW/m ² and 15 minutes	37
Figure 3.15 Calcination depth measurements at different pressures for probe test 2 – 10 mm Fyreline board under 50 kW/m ² and 15 minutes	38
Figure 3.16 Calcination depth measurements at different pressures for probe test 3 – 10 mm Noiseline board under 50 kW/m ² and 15 minutes	39
Figure 4.1 Idealized temperature history showing all 5 stages of fire growth	41
Figure 4.2 Rate of temperature decay in EC1 parametric fires	50
Figure 5.1 The cone calorimeter test apparatus	52
Figure 5.2 Complete schematic representation of the cone calorimeter apparatus (Figure taken from Nyman 2001)	53
Figure 5.3 Radiator cone (Figure taken from BS 476)	54
Figure 5.4 Cone heater schematic (Figure taken from Nyman 2001)	55
Figure 5.5 Illustration of how the samples were mounted during the fire testing	56
Figure 5.6 Masking plate (left) and sample holder with baseboard (right)	57
Figure 5.7 Calibration curve for the cone heater	58
Figure 5.8 Samples storage ready for cone calorimeter testing	60
Figure 5.9 Steel plate with five circular openings	61
Figure 5.10 Thermocouples placement in thicker gypsum plasterboards	62
Figure 6.1 Radiant exposure area correlation	67
Figure 6.2 Determining the fire severity for pre-flashover period	70
Figure 6.3 Influence of exposure duration on mass loss for 10 mm Fyreline Board	71
Figure 6.4 Mass loss during heating and cooling under 50 kW/m ² exposure	72
Figure 6.5 Correlation between calcination depth and fire severity for 10 mm Standard Board	73

Figure 6.6 Correlation between calcination depth and fire severity for 10 mm Fyrelite Board ...	74
Figure 6.7 Correlation between calcination depth and fire severity for 10 mm Noiseline Board .	74
Figure 6.8 Correlation between calcination depth and fire severity for 19 mm Fyrelite Board ...	75
Figure 6.9 Fire severity curves for ventilation factor of 0.02 and different fuel loads	77
Figure 6.10 Fire severity curves for ventilation factor of 0.04 and different fuel loads	78
Figure 6.11 Fire severity curves for ventilation factor of 0.08 and different fuel loads	79
Figure 6.12 Fire severity curves for ventilation factor of 0.12 and different fuel loads	79
Figure 6.13 Calcination depth curves for 10 mm Standard board with ventilation factor of 0.04.	80
Figure 6.14 Calcination depth curves for 10 mm Standard board with ventilation factor of 0.08.	81
Figure 6.15 Thermocouples data collected at different depth below the upper surface of the sample under 50 kW/m ² fire exposure	83
Figure 6.16 Thermocouples data collected at different depth below the upper surface of the sample under 65 kW/m ² fire exposure	84
Figure 7.1 Illustration in determining the time of fire extinguishment	89
Figure 7.2 Horizontal lines showing water dehydration; Top (50 kW/m ²) and Bottom (65 kW/m ²)	92

List of Tables

Table 2.1 Test results for gypsum board materials	12
Table 2.2 Mechanical properties of Australian manufactured plasterboards.....	18
Table 3.1 Depth of calcination measurements by using spring-force probe and hand scraping....	31
Table 3.2 Pressure calculations	36
Table 3.3 Fire tests to determine the depth of calcination by different pin sizes.....	37
Table 5.1 Calibration data	59
Table 5.2 Measured densities of gypsum plasterboards.....	60
Table 5.3 Matrix of sample specifications for testing	63
Table 6.1 Fire growth rates for t^2 fires	69
Table 6.2 The relationship between the calcination depth and fire severity	75
Table 6.3 Determined calcination depth before flashover occurs for ventilation factor of 0.02 ...	76
Table 6.4 Determined calcination depth before flashover occurs for ventilation factor of 0.04 ...	76
Table 6.5 Determined calcination depth before flashover occurs for ventilation factor of 0.08 ...	76
Table 6.6 Determined calcination depth before flashover occurs for ventilation factor of 0.12 ...	77
Table 6.7 Predicted calcination depth of 10 mm Standard board for complete room burnout	81
Table 6.8 Predicted calcination depth of 10 mm Fyreline board for complete room burnout	81
Table 6.9 Predicted calcination depth of 10 mm Noiseline board for complete room burnout	82
Table 6.10 Predicted calcination depth of 19 mm Fyreline board for complete room burnout	82

Chapter 1 Introduction

1.1 Background

The use of gypsum plaster as an interior finish material, similar of that today, was used back to the times of the Egyptians pyramids and tombs at least 4,000 years ago; white lime plaster was used in Greece 3,000 years ago and by the Romans later (Ryan 1962). Gypsum wallboard, as it is known today, was first used in construction in the early 1900's. Gypsum is calcium sulphate dihydrate ($\text{CaSO}_4 \cdot 2\text{H}_2\text{O}$), a white or grey naturally occurring mineral. Gypsum wallboard or gypsum plasterboard consists of a sandwich of a gypsum core between two layers of paper. The paper assists in providing the plasterboard with adequate tensile strength capacity hence to resist forces encountered in handling and use. The production and use of the material in building construction grew at a slow rate until the mid 1940's when the demand particularly for interior linings in domestic housing and commercial office buildings rapidly increased. In 1970's, the use of gypsum wallboard utilizes approximately 90 percent of all buildings within the United States (Lawson 1977).

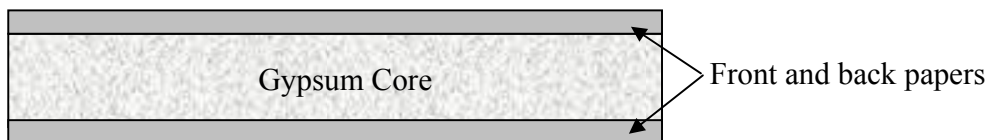


Figure 1.1 Gypsum wallboard or gypsum plasterboard

Figure 1.2 is the collected data from the Gypsum Association showing the annual shipments of 0.5 inches thick gypsum wallboard products in the United States since 1930 (Mowrer 2001). The growth in the annual shipments indicating the use of gypsum products around the United States is observed to increase rapidly since 1950 and continuing through 1997. A total of approximately 25 billion square feet of 0.5 inches thick gypsum wallboard is shipped by United States

Introduction

manufacturers in 1997, which compares to about 3 billion square feet shipped by Canadian manufacturers during the same year (McGraw 1998). The reasons for the widespread use of gypsum wallboards as wall and ceiling linings are due to its ease of installation, economical cost, acoustic, thermal and superior fire-resisting properties.

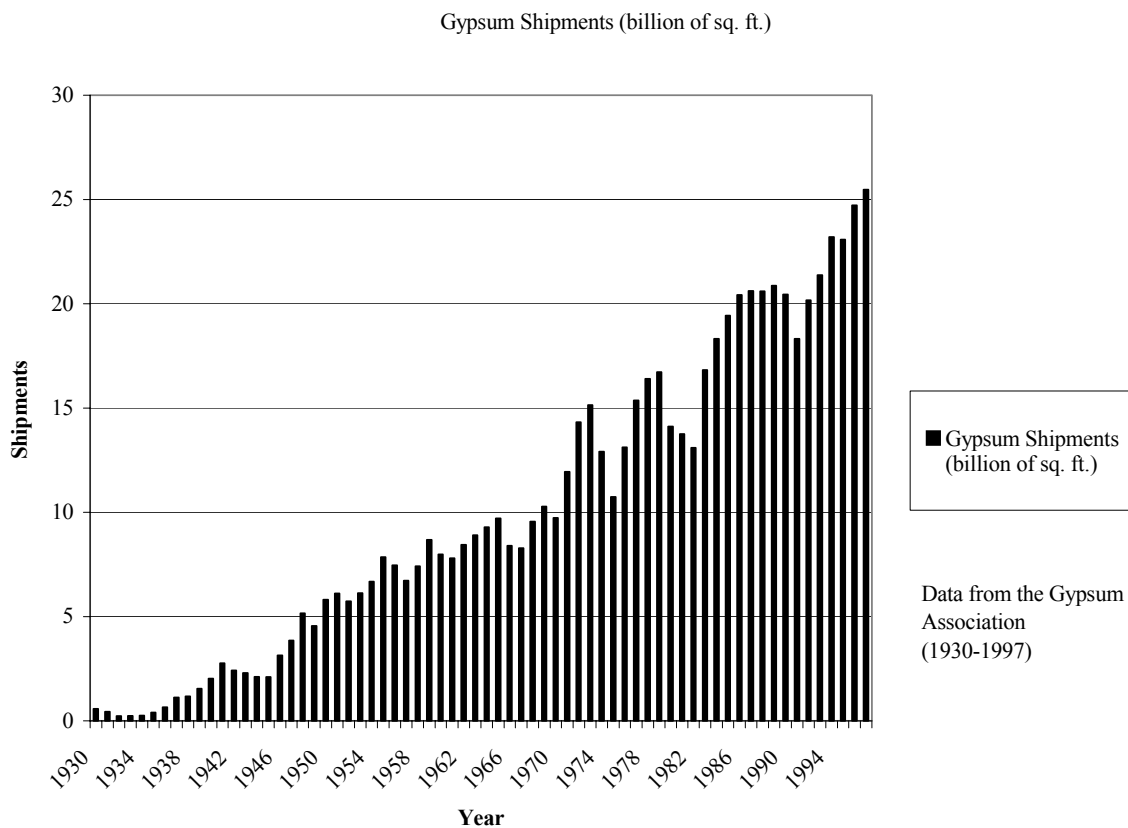


Figure 1.2 Annual shipments of gypsum wallboard from U.S. manufacturers

There are many different types of gypsum wallboard products varying from country to country but generally follows a similar pattern. In North America, there are three broad types of gypsum board, usually known as Regular board, Type X board and Special Purpose board whereas some parts of Europe and Asia only have the first two categories and smaller market areas such as New

Zealand and Australia only have regular board and special purpose board. Buchanan and Gerlich (1997) describes the regular gypsum wallboard has poor performance compared with Type X or Special purpose board. Regular gypsum wallboard is simply a gypsum core between the two paper facings with no reinforcing fibres. Type X gypsum wallboard is a generic term that describes a more fire resistive type of gypsum wallboard, defined by performance rather than by a manufacturing specification. All Type X boards contain some glass fibre reinforcing and may have other additives to improve stability during and after a fire. The glass fibre acts as a reinforcing web to hold the calcinated gypsum together after fire exposure. Special purpose boards are proprietary products made by manufacturers to obtain enhanced fire or structural performance over Regular or Type X boards, for structural bracing, impact resistance, wet area applications or fire resistance. Special purpose board provides more fire resistance than Type X board as it contains more glass fibres and more core additives.

1.2 Gypsum Wallboards in New Zealand

The composition of gypsum plasterboard and hence the properties vary slightly between manufacturers and countries of origin. Gypsum wallboard or gypsum plasterboard is manufactured in New Zealand by Winstone Wallboards Limited (also referred to as “WWB”) under the brand name GIB®. Gib® offers a range of gypsum plasterboards with different properties. There are GIB Board, GIB Braceline, GIB Fyreline, GIB Aqualine, GIB Toughline, GIB Ultraline, GIB Noiseline and GIB Wideline.

GIB Board® is a relatively light board featuring a pure gypsum plaster core encased in a face and backing paper and is available in 10 mm and 13 mm thickness. 10 mm GIB Board is the standard panel used to line internal timber framed and steel framed walls, and ceilings in residential and commercial buildings.

Introduction

GIB Braceline® is a heavier board consisting of reinforced short strands of fibreglass. It is an effective wall bracing sheet for light timber framed buildings which maintains the continuity between wall bracing and wall lining sheets and provides resistance against wind and earthquake forces. It only comes with 10 mm thick which provides continuity with the standard 10 mm GIB Board lining. To aid in identifying GIB Braceline, it has blue face paper.

GIB Fyrelite® is formulated as a high performance fire resistant board and has pink face paper. It contains vermiculite and short glass fibres added to the gypsum plaster core. Vermiculite prevents the plasterboard from shrinkage as it expands at high temperatures and the glass fibres enable the plasterboard to sustain the load and retain some structural integrity or to prevent the gypsum plaster crumbling away after the calcination (Hannant 1978). It is used ideally for dividing walls, lift shafts, stairwells and anywhere that fire could be a threat.

GIB Aqualine® is used for internal lining wet or humid such as bathrooms, kitchens, laundries and toilets. It contains a wax emulsion in addition to the gypsum core which resists water vapour. It is also ideal for the application of paint and wallpaper finishes outside of those areas subject to direct water pressure. GIB Aqualine is produced with green coloured face paper.

GIB Toughline® has a better performance and is found twice as strong as the standard GIB Board of the same thickness. This is because of its special high density core reinforced with a continuous calcium sulphate dehydrate mesh. It is designed for use in areas such as corridors, garages, children's bedrooms and gymnasiums which requiring improved resistance to dents, chips and breakthrough. GIB Toughline has purple face paper.

GIB Ultralite® is a special types of gypsum plasterboard that consists of white surface paper with finer, smoother texture and a special mixture of plaster and calcium sulphate dehydrate□ reinforcing in its core, making it more solid and rigid than 10 mm GIB Board. It is ideally used

Introduction

in areas requiring extra attention that most often visited and seen by visitors such as entranceways, lounges and dining rooms.

GIB Noiseline® is designed specifically to reduce the level of sound transmission between rooms. This is achieved by increasing the density of the gypsum plaster core. It has a smoother and white face paper.

Figure 1.3 shows a table summarizing the thickness, width and length for different types of GIB plasterboards manufactured by Winstone Wallboards Limited that are available in New Zealand. In this research, only 10 mm GIB® Standard, 13 mm GIB® Standard, 10 mm GIB Fyreline®, 13 mm GIB Fyreline®, 16 mm GIB Fyreline®, 19 mm GIB Fyreline® and 10 mm GIB Noiseline® are examined.

PRODUCTS MATRIX																		
TYPE	GIB® Standard		GIB® Ultralite®		GIB® Wideline®	GIB® BraceLine®	GIB® Aqualite®		GIB Fyreline®				GIB® Noiseline®		GIB® Toughline®		GIB X-Block®	
	10.0	13.0	10.0	13.0	10.0	10.0	10.0	13.0	10.0	13.0	16.0	19.0	10.0	13.0	10.0	13.0	13.0	
Thickness mm	1200	1200	1200	1200	1350	1200	1200	1200	1200	1200	1200	1200	1200	1200	1200	1200	1200	
LENGTH (mm)	2400mm	✓♦	✓				✓	✓	✓	✓	✓	✓	✓	✓	✓	✓	✓	
	2700mm	✓	✓				✓	✓	✓	✓	✓		✓	✓		✓		
	3000mm	✓♦	✓	✓	✓		✓	✓	✓	✓	✓	✓	✓		✓	✓	✓	
	3300mm	✓♦	✓								✓	✓		✓				
	3600mm	✓♦	✓	✓♦	✓	♦	✓	✓	✓	✓	✓					✓		
	3900mm	✓	✓															
	4200mm	✓♦	✓															
	4800mm	✓♦	✓	✓	✓	♦												
	6000mm	✓♦		✓		♦												
	Max Weight kg/m ²	6.4	8.5	7.0	8.5	7.0	8.5	7.5	10.0	6.6	9.5	13.7	16.2	8.5	12.7	8.5	11.0	14.6

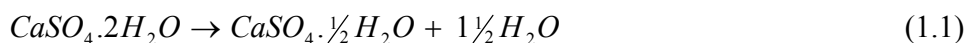
LEGEND
 ✓ Tapered Edge/Tapered Edge ♦ Square Edge/Tapered Edge

Figure 1.3 Available thickness, width and length for GIB® Products (Taken from GIB® website)

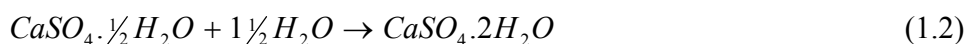
calcination and the calcined gypsum produced is a type of plaster of Paris. When the proper amount of water is added back to the calcined gypsum, the liquid gypsum plaster mixture is poured on to the lower sheet of paper and the upper sheet of paper is applied. The board is then passed through rollers before the plaster sets, forming the plasterboard. The paper becomes chemically and mechanically bonded to the core. At last, the board is cut into the desired size and kiln-dried to remove any excess moisture.

1.4 Chemistry

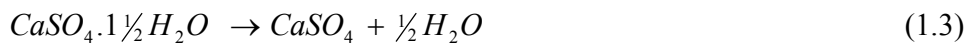
Gypsum consists of a matrix of interlocking elongated crystals (Buchanan and Gerlich 1997). Solid gypsum and gypsum rock is calcium sulphate dihydrate, $\text{CaSO}_4 \cdot 2\text{H}_2\text{O}$, produced from dehydration and re-hydration of a mineral crystal. The two water molecules are chemically bound with calcium sulphate in an orthorhombic crystalline mineral structure (Stanish 1994). Calcium sulphate hemihydrate, $\text{CaSO}_4 \cdot 1/2\text{H}_2\text{O}$, is produced when dihydrate was heated driving off the chemically bound water out of the gypsum rock in a process called calcining. The dehydration reaction, also known as calcination, is an endothermic decomposition reaction which occurs between 100°C and 120°C . When gypsum is heated in a fire, the dehydration follows the reaction in Equation 1.1 as solid gypsum starts to degrade, loses its strength and is eventually transformed back to the powdery material of calcium sulphate hemihydrate.



The above reaction is reversed to become a hydration reaction when the powder is mixed with water and formed into flat sheets of gypsum plaster. The hydration reaction is:



The resulting gypsum contains approximately 21% water content and about 79% calcium sulphate, which is inert below a temperature of 1200°C (Goncalves et al 1996). The bound crystalline moisture content plays a significant role in the excellent fire-resisting behaviour of gypsum plasterboard. It is found that approximately 3% free water is contained inside gypsum plaster, depending on the ambient temperature and relative humidity (Buchanan 2001a). In order to evaporate the free water and create the chemical change which releases the chemically bound water in crystal structure, a large amount of energy is required. If the reaction in Equation 1.1 or calcium sulphate hemihydrate is heated to higher temperature, complete dehydration occurs as follows:



However, this complete dehydration of gypsum plaster does not occur until the temperature of about 700°C (post-flashover fires) is reached and an additional energy input is required for this to occur.

1.5 Project Objectives

After a fire has occurred, fire investigators often see the results of calcination depth of gypsum plasterboard (Figure 1.5). These calcination or fire patterns on gypsum plasterboard can be a particularly useful tool for post-flashover incident analysis or investigation to determine the possible cause of the fire, likely origin and development scenarios. Gypsum plasterboard calcination has also been used as an indicator of fire intensity and duration. Unfortunately, the area of post-flashover fire investigation using the calcination depth of gypsum plasterboard as an investigative tool has not been investigated in detail and a practical paper based on structured research would be of significantly benefit.



Figure 1.5 Gypsum plasterboard exposed to fire heat flux (Mowrer 2001)

The aim of the research is to conduct bench scale cone calorimeter tests exposing gypsum plasterboards to different heat fluxes for varying exposure time and to quantify the depth of calcination. The research's objective is to establish a correlation between the depths of calcination of gypsum plasterboards, fire exposure and exposure duration. Such a correlation can be used as an indication of the fire severity. This also applies to real fires that the depth of calcination of damaged gypsum plasterboard can be assessed to indicate the fire severity of the burning room or compartment.

The research examines the available methods that are used to measure the depth of calcination, which are described in Chapter 3. The research's objective is to identify a practical method or develop an on-site measuring and assessing tool, which can be a good representative of the actual calcination depth. This tool can then be used by fire investigators on fire incidents to measure calcination depth accurately and giving consistent measurements as there appears no consistency at present with other methods; vernier calliper, depth gauge, ruler and visual observation.

The temperature variation across the thickness of gypsum plasterboards under the cone heater fire exposure is proposed by implementing a series of thermocouples into the board at different depths and so to determine the time-temperature history curves. This thermocouple data could

Introduction

provide a useful information for fire properties, heat transfer phenomenon over gypsum plasterboard and computer modelling.

In order to use the information gained from this research, the procedures for measuring the depth of calcination are outlined along with the relationship between the depth of calcination, heat flux and fire exposure time. The information gained from this research would be particularly useful to predict the damage to gypsum plasterboard in real fires and to use the calcination of gypsum plasterboard after a real fire as an indication of the fire severity. All these information has value to fire investigators and fire protection engineers.

Chapter 2 Literature Review

2.1 Fire Properties and Performance

In New Zealand the most common lining material used in light timber frame wall and floor assemblies is gypsum plasterboard. The use of gypsum plasterboard has increased dramatically since the advent of a performance based building code in 1993. Therefore, an evaluation of the fire properties of gypsum plaster is an important aspect in order to obtain an understanding of the material's reaction to a fire environment and these thermal properties of gypsum plaster are required if finite-element thermal calculations are to be made hence developing mass and heat transfer models for wall and floor assemblies.

2.1.1 Ryan (1962)

The earliest study of gypsum plasters when exposed to fire was proposed by Ryan (1962), who examined the effects of mix, aggregate i.e. perlite, vermiculite and sand, and conditioning on the fire endurance, in terms of a limiting temperature rise of gypsum plasters. Experimental results showed that the mix ratio and aggregate density has little effect on the fire performance based under the conditions of specimen size and test conditions conducted. The perlite and vermiculite plasters was found to exhibit significantly longer temperature rise times but shorter times were observed for sanded plasters. The aging or conditioning effect was significant only for the combination of both short aging periods and relatively high humidity conditions. Ryan also proposed the estimates of thermal properties of gypsum plasters at elevated temperatures, which were derived from the data.

2.1.2 Lawson (1977)

Lawson (1977) described four small-scale fire test methods used in order to examine the fire properties of nine generic gypsum board materials in United States. These tests were conducted to determine the potential heat, ease of ignition by flame impingement, rate of heat release and

rate of flame spread as they are the major factors that influence the fire growth in a room. Experimental results determined by Lawson for the nine different gypsum boards are summarized in Table 2.1.

Table 2.1 Test results for gypsum board materials

Fire properties		Values
Potential heat [J/g]		510 – 2670
Average peak heat release [W/cm ²]	Unpiloted 4 W/cm ² exposure	2.5 – 4.8
	Unpiloted 6 W/cm ² exposure	3.9 – 8.2
Time of ignition [s]		42 – 171
Flame spread index		8 – 38

2.1.3 Buchanan and Gerlich (1997)

Buchanan and Gerlich (1997) reported the quality and composition of gypsum plasterboard can have a significant effect on the fire performance of light frame systems. North American Type X board is found to have a better performance than regular board but poorer than special purpose boards. Buchanan and Gerlich concluded that fire performance of gypsum plasterboard can be improved by providing glass fibres to control shrinkage and prevent board fall-off, additives to reduce shrinkage and increased density to increase heat capacity. It is also reported that for the same thickness of gypsum plasterboard, the New Zealand systems perform better than the Australian and North American equivalents (Figure 2.1).

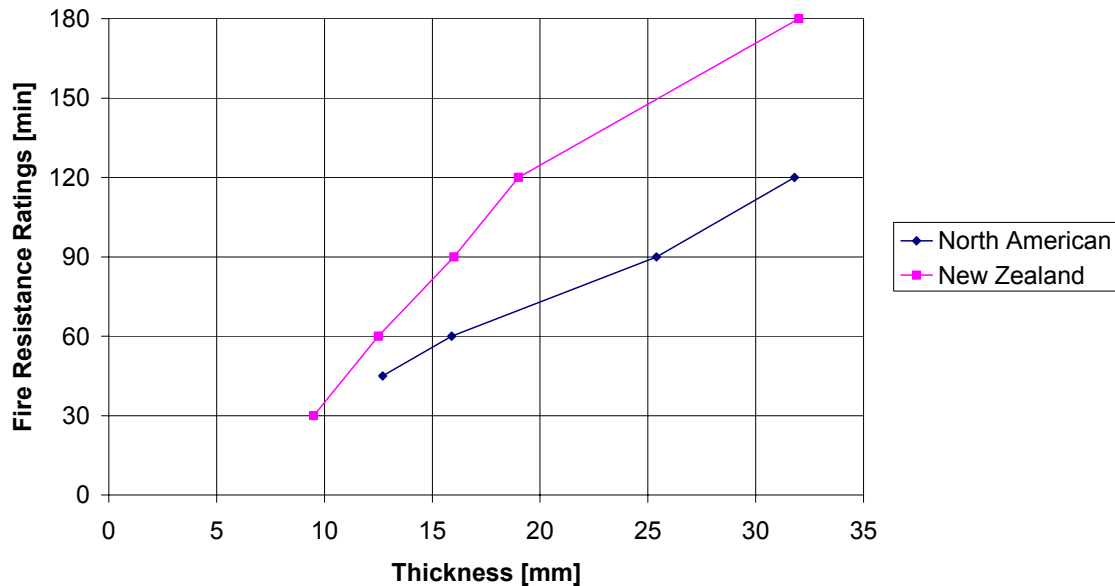


Figure 2.1 Comparison of New Zealand and North American boards when used in symmetrical non load bearing wood stud walls (Reproduced from Buchanan and Gerlich (1997))

2.1.4 Alfawakhiri et al (1999)

Alfawakhiri et al (1999) carried out a literature survey summarizing the information available on topics that are related to the fire resistance of load bearing cold-forming steel stud walls clad with gypsum plasterboard. Alfawakhiri et al illustrated the typical variation of the specific heat and thermal conductivity of Type X gypsum board with temperature as shown in Figure 2.2 and 2.3 respectively. These results are based on the tests by Sultan (1996). The two peaks in the specific heat curve indicate the dehydration of gypsum which appears at temperatures around 100°C and 650°C. These thermal properties of gypsum plasterboard are necessary in order to make any finite-element thermal calculations. Cooper (1997) also published the thermal properties values which are taken from Sultan (1996), and shown in Figure 2.4 and 2.5.

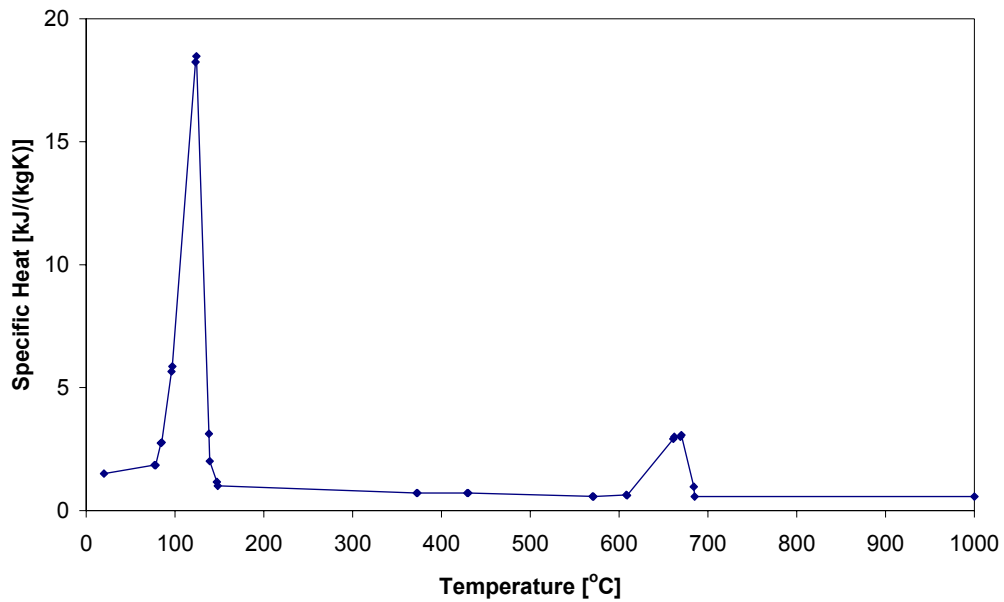


Figure 2.2 Specific Heat of Type X Gypsum Board (Reproduced from Sultan (1996))

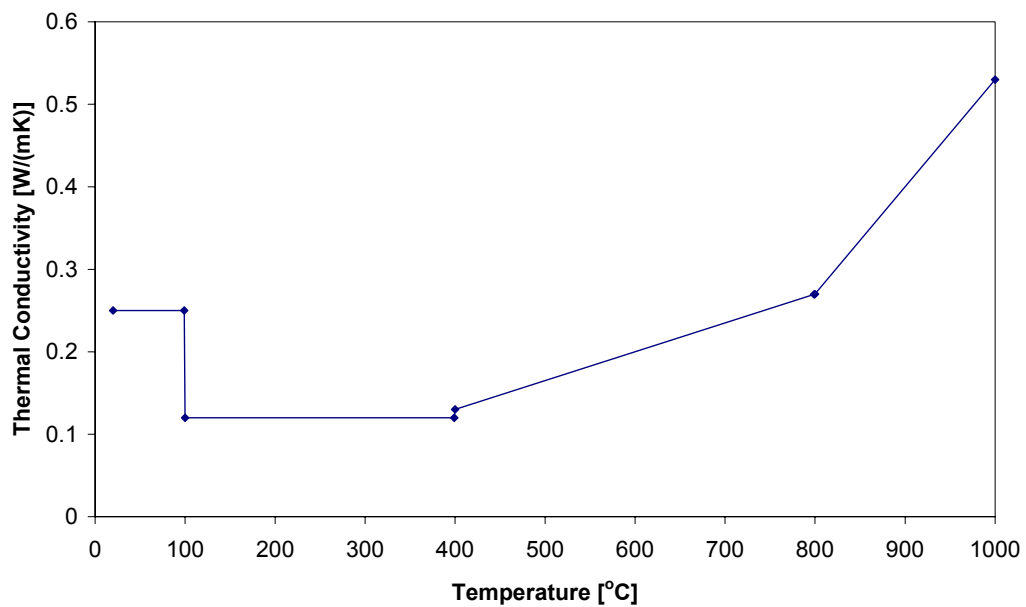


Figure 2.3 Thermal Conductivity of Gypsum Board (Reproduced from Sultan (1996))

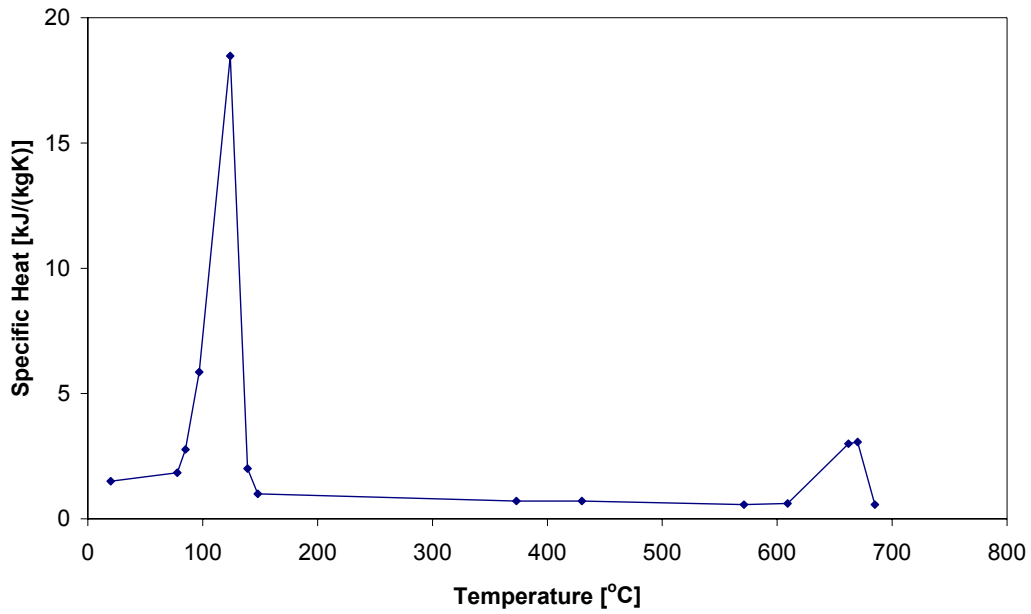


Figure 2.4 Specific Heat of Gypsum Plaster (Reproduced from Cooper (1997))

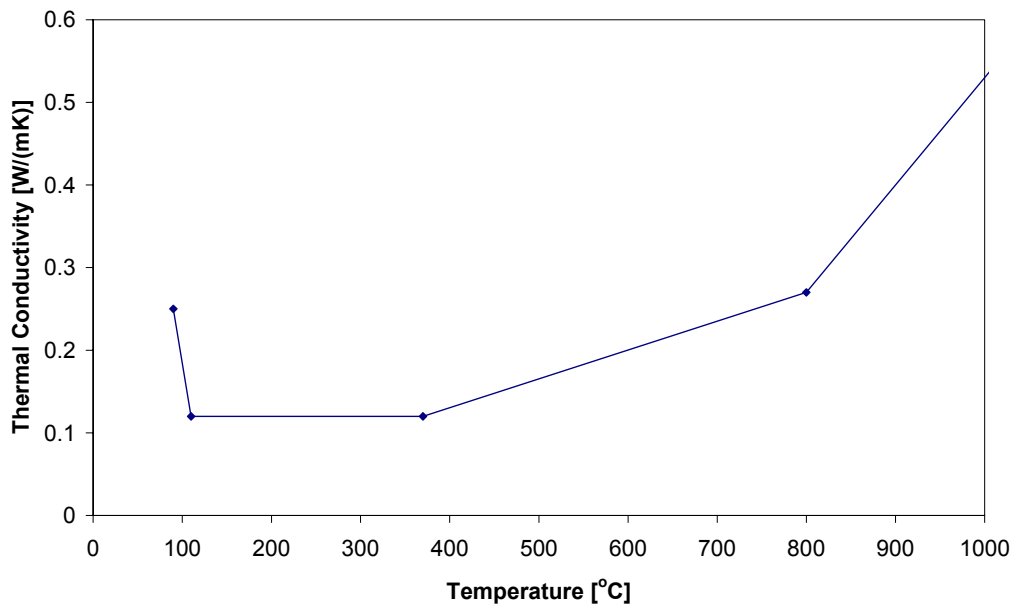


Figure 2.5 Thermal Conductivity of Gypsum Plaster (Reproduced from Cooper (1997))

2.1.5 Thomas (2002)

The information on the thermal properties of gypsum plasterboard at elevated temperatures are limited as they are difficult to measure, subject to transient effects and often the results found vary with the method of measurement used and the rate of temperature change. Thomas (2002) reviewed a number of relevant literatures and modified these thermo-physical properties values that are suitable for use in finite element heat transfer model of light timber frame wall and floor assemblies. These values are calibrated and validated using furnace and fire test data. The recommended thermal properties for gypsum plasterboard for specific heat and thermal conductivity are plotted in Figure 2.6 and 2.7 respectively. However, these figures are quite differing from those determined by Sultan (1996) and Cooper (1997).

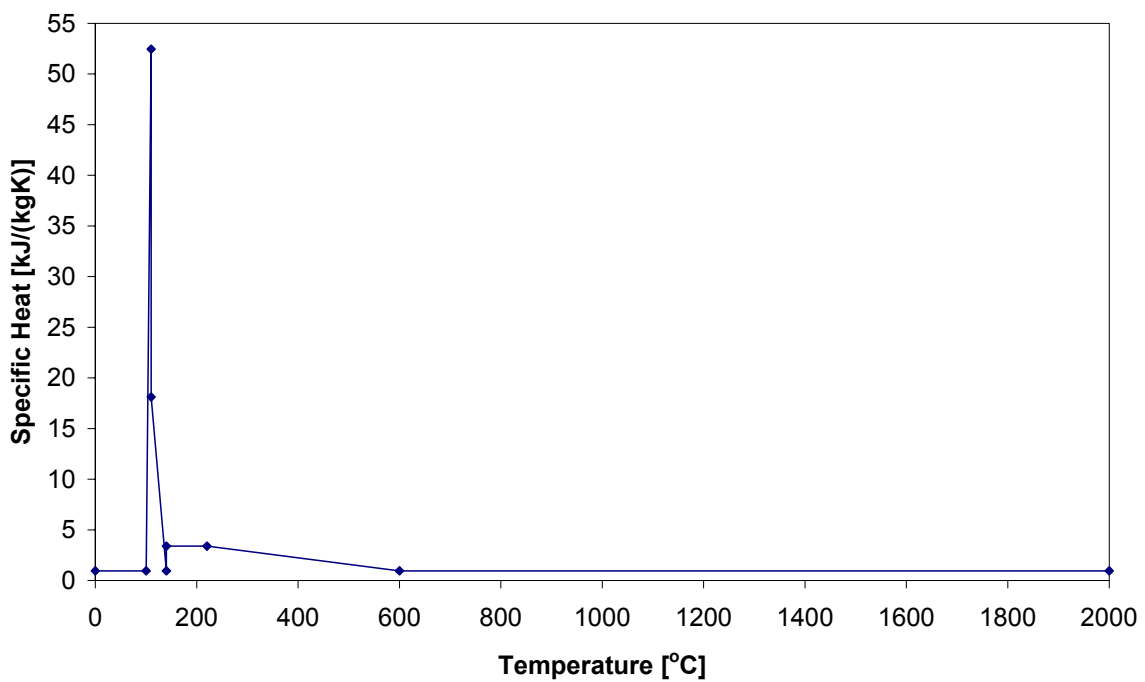


Figure 2.6 Revised specific heat as used (Reproduced from Thomas (2002))

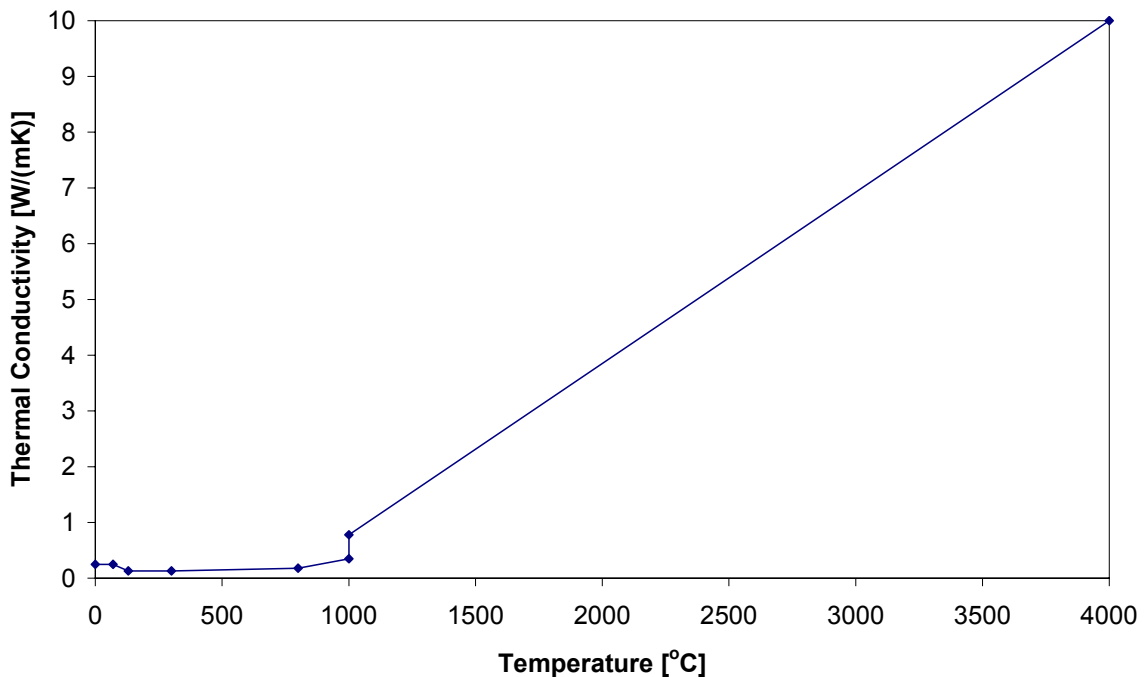


Figure 2.7 Revised thermal conductivity as used (Reproduced from Thomas (2002))

2.1.6 Goncalves et al (1996)

The mechanical properties of gypsum plasterboard subjected to fire are also required when modelling the fire performance of wall assemblies. Goncalves et al (1996) reported the behaviour of plasterboard in ambient and fire conditions, so as to quantify the effect of high temperatures on properties such as strength, stiffness, expansions and shrinkage behaviour of plasterboard. Goncalves et al (1996) observed ablation or spalling at a time less than 15 minutes in the fire when the core temperature in the boards reached 500°C – 650°C. The tensile strength characteristics and modulus of elasticity of plasterboard at 300°C and 500°C tests are summarized in Table 2.2. These results are based on the tests of three Australian manufactured plasterboards; Boral, C.S.R and Pioneer. Stanish (1994) also conducted similar research investigating the plasterboard's mechanical behaviour at a level of detail with New Zealand manufactured plasterboards.

Table 2.2 Mechanical properties of Australian manufactured plasterboards

Board Type	Failure Stress at 300°C [MPa]	Failure Stress at 500°C [MPa]	MOE at 300°C [MPa]	MOE at 500°C [MPa]
Boral	0.121	0.098	8.5 – 18.8	6.0 – 9.9
C.S.R	0.163	0.098		
Pioneer	0.107	0.117		

2.1.7 National Research Council of Canada

National Research Council's Institute for Research in Construction had published a number of papers reporting how various factors affect the fire resistance performance of floor and wall assemblies in different types of dwellings. The most recently paper that has been published was conducted by three researchers; Benichou, Sultan and Kodur presenting the effects of a number of design parameters on lightweight framed wall assemblies. Benichou et al (2003) described the main factors that affected the performance of stud wall assemblies were the type of insulation, stud spacing, the number of gypsum board layers and the addition of a shear membrane. The data collected from the experimental program was used to produce generic fire resistance rating listings for codes, key design trends and to develop fire resistance models for assessing the fire resistance of wood and steel stud wall assemblies.

2.2 Fire Modeling

With the advent of performance based building codes and performance based fire safety design options, there is a need to develop validated fire resistance models for assessing the wall and floor building assemblies. These models have become essential due to the drawbacks of the test methods such as high costs and time consuming, limitations of specimen geometry and loading and repeatability. With the development of fire resistance models, these methods would facilitate a faster design process, more cost-effective and flexible design options.

2.2.1 Mehaffey et al (1994)

Mehaffey et al (1994) presented a simple two dimensional computer model, which is written in Microsoft FORTRAN in order to predict the heat transfer through gypsum plasterboard/wood-stud walls exposed to fire. Predictions were validated with four small-scale and two full-scale fire resistance tests and a good agreement was shown, in particular, for the finish ratings, the time to onset of charring of the studs and the time to failure of the assembly due to heat transmission.

2.2.2 Gerlich (1995)

Gerlich (1995) used a commercially available computer program, Temperature Analysis of Structures Exposed to Fire (TASEF), to predict heat transfer through light steel frame walls exposed to fire. To evaluate the performance of loadbearing LSF wall systems, three fire tests including two standard ISO834 and one non-standard full-scale were performed at BRANZ. Gerlich reported that TASEF yields non-conservative stud temperature predictions toward the end of the fire tests when a realistic fire profile was applied to the model. This was due to the fact that TASEF was unable to account for the mass loss during fire conditions, degradation of joints opening, cracking and ablation of fire-exposed gypsum plasterboard lining. However, when the system was modelled to standard fire, the model could have an 80% – 90% accuracy of predicting the performance of the systems exposed to standard conditions.

2.2.3 Sultan (1996)

Sultan (1996) described a one dimensional mathematical model to predict heat transfer through steel-stud, non-insulated and non-loadbearing gypsum plasterboard wall assemblies. Two non-insulated and non-loadbearing full-scale fire resistance tests were conducted to validate model predictions. The comparisons showed that the model provides reasonably conservative fire resistance predictions, approximately 3% lower than the experimental measured values. The reason for these conservative predictions is due to the several simplified assumptions made by Sultan such as considering heat transfer only in one dimension across the cavity and that the heat

leaving the fire exposed lining and entering the cavity was considered to be completely absorbed by the gypsum plasterboard surface on the opposite of the cavity.

2.2.4 Cooper (1997)

Cooper (1997) developed a methodology and an associated FORTRAN subroutine, GYPST, to simulate the thermal response of fire-environment exposed steel-stud/gypsum plasterboard assemblies. Two full-scale ASTM E119 furnace tests were conducted to validate model predictions. Good agreement was found between the model predictions and experimental results. However the GYPST models use is limited to steel stud/gypsum plasterboard wall constructions exposed to standard fire conditions only.

2.2.5 Takeda and Mehaffey (1998)

Takeda and Mehaffey (1998) presented a two dimensional computer model, WALL2D, to predict heat transfer through non-insulated wood-stud walls with the protection of gypsum plasterboard. WALL2D is a continual work from Mehaffey et al (1994) that the previous model was further incorporated with three sub-models describing heat transfer through gypsum plasterboards, through wood studs and across the cavity. The comparisons between the model predictions for time-dependent temperature profiles in wood-stud walls and the results of both small and full-scale standard fire tests were made and shown to be in reasonable agreement. However, no validation of the model was made for non-standard fire tests.

2.2.6 McGraw (1998)

McGraw (1998) used an existing flame spread model developed by Quintiere and coworkers to evaluate the potential for flame spread on painted gypsum plasterboards exposed to fire. In order for this evaluation to be achieved, the data obtained in the cone calorimeter is needed such as the heat release rate, material burning duration, ignition time and total heat released. Various numbers of coats of interior latex paint were applied to the surface of 16 mm thick Type-X

gypsum board. McGraw also developed a two step dehydration model into a Microsoft Excel spreadsheet template based on a finite difference formulation to simulate the heating and dehydration of gypsum plasterboard. The numerical model developed provides fairly representative temperature predictions within the gypsum samples. McGraw concluded that the depth of the calcination planes is a function of the exposure condition and length of exposure to fire.

2.2.7 Jones (2001)

Jones (2001) used a commercially available finite element program, SAFIR, which is capable of analysing and predicting thermal behaviour of light framed gypsum plasterboard assemblies, subjected to both ISO834 and realistic time-temperature curves. One standard and four non-standard non-loadbearing small-scale furnace tests were conducted to validate predictions from the model. Jones determined that the model calibrated to results from standard ISO834 furnace testing provides predictions of temperatures within assemblies exposed to a moderate fire with reasonable accuracy. But the temperature predictions of assemblies exposed to more severe fires were relatively poor. SAFIR was also unable to model moisture movement, ablation and shrinkage of plasterboard linings.

2.2.8 Thomas (2002)

Thomas (2002) developed a finite element heat transfer model using the computer program TASEF and the finite element program ABAQUS to predict heat transfer through light timber frame wall and floor assemblies. Jones recommended the values for specific heat, mass loss rate and thermal conductivity for gypsum plasterboard that are suitable for use in finite element heat transfer modelling. The heat transfer model was validated with a number of furnace tests including wall tests, floor tests, tests with non-standard time-temperature curves and a realistic fire. The model predicted the wall and floor temperature profiles well and is found conservative

for fast, hot fires. However, the prediction was not that accurate for temperature profiles in specimens subjected to temperature histories with rapid and abrupt changes.

2.3 Post-flashover Analysis

Fire investigators often see the results of calcination or dehydration, which is a chemical and physical change in the nature of common gypsum plasterboard. It can be a particularly useful tool as investigators can use this fire patterns on gypsum plasterboard to determine a number of issues regarding the extent of damage, likely origin and possible fire initiation after a fire has occurred. Unfortunately, only few research papers have been published in past years which address the use of calcination of gypsum plasterboard as a useful fire investigative tool.

2.3.1 Posey and Posey (1983)

The earliest published research paper using the calcination of gypsum plasterboard in post-incident analysis or investigation to reveal fire damage patterns was published by Posey and Posey (1983). The rate of calcination was found as a function of time and temperature and the authors had observed the layers of calcination of varying degrees of sharpness; single sharply defined line, two or more distinct lines and not well defined line. Comparisons were made between the calcination layers within the room and from one room to another. The authors described the comparison of the two calcined layers on either side of the gypsum plasterboard can be a useful in pinpointing fires which start within wall spaces and spread from there out into the room. Deeper or thicker calcination planes were found to indicate longer exposure and/or more intense heat. Although the layers of calcination were unable to be clearly defined, the authors concluded the relative depths of the calcined layer were alone useful as a fire investigative tool.

2.3.2 McGraw (1998)

McGraw (1998) described a method of determining the depth of calcination or dehydration by using visual observation and a vernier calliper rather than “eyeballed” with a ruler. Vernier

callipers would provide greater accuracy and allow for the measurement of the depth at a number of locations where an average value can be obtained. The experiment consisted of exposing the gypsum plasterboard samples at a specific exposure condition and duration, that is, 25, 50, 75 kW/m² and 5, 10, 15 minutes. From his results, exposure durations of 10 minutes produced distinct calcination planes at all exposure heat fluxes tested. McGraw concluded that the depth of calcination planes is a function of the exposure condition and duration to fire and longer exposures and higher heat fluxes would result in deeper development of the calcination plane, however, a correlation for predicting this relationship was not found.

2.3.3 Schroeder and Williamson (2000)

Schroeder and Williamson (2000) reported on how the extent of fire damaged gypsum plasterboard could be used to identify time, temperature and heat flux exposures of the incipient stages of an uncontrolled fire. The experiment involved exposing gypsum plasterboard samples in the cone calorimeter subjected to various heat flux exposures and time intervals. Schroeder and Williamson put two internal thermocouples at 4 mm and 12 mm under the exposed sample surface in the cone calorimeter experiments so to determine the time for the two measurement depths to reach the desired isotherm temperatures. The desired isotherm temperatures were 80°C which is the approximate temperature at which the gypsum begins to lose water, 200°C where the hemihydrate crystal structure begins to form and the temperature corresponding to the beginning of the formation of the anhydrous crystal structure, 500°C. The results of the experiments allowed a plot of time against depth penetration of phase changes in gypsum plasterboard for different levels of heat flux. Schroeder and Williamson concluded that thermally induced changes in gypsum plasterboard provide a quantifiable method for determining time/temperature regimes and/or heat flux levels of unwanted fire.

2.3.4 Kennedy et al (2003)

Kennedy et al (2003) reported the practical use of measurements of depth of calcination of room-fire exposed gypsum plasterboard under actual fire scene investigation conditions to discover and illustrate movement and intensity of fire patterns for fire origin determination. Kennedy et al used the traditionally “probe survey” method and less often utilized and more cumbersome, “visual cross-section” method for their investigation. The test and data collection were performed on full-scale fire evolutions using ten fire investigators of widely varying experience to make and record the depth of calcination measurements without knowing the actual fire origins. Research test results using the “probe survey” method provided accurate and reproducible fire movement analysis and the use of widely varying skill and experience levels of investigators did not affect the overall depth of calcination analyses results. Findings are comparable between the “probe survey” and visual observation of cross-sections methods. However, Kennedy et al only appeared to be interested in identifying fire movement patterns for fire origin or fire development scenarios while the actual measured depth of calcination itself was of relatively little importance and they did not use any control specimens to verify their results.

Chapter 3 Methods of Measuring Calcination Depth

For a better representative of the actual depth of calcination measurements, there is a need for an advanced measuring tool to be made, which is one of the objectives of the research. This tool also needs to be on-site and easy to use.

3.1 Probe Survey Methods

In Kennedy et al (2003) research paper, one of the suggested methods for determining the depth of calcination of gypsum plasterboard is by using a “probe survey” method. “Probe survey” method has been in use by fire investigators for both calcination and depth of char analyses since the 1950’s. The “probe survey” method uses a piece of calibrated probe calliper-like device to determine the depth of heat treatment to structural lining surfaces such as gypsum plasterboard and charred wood.

Depth gauge and vernier calliper are the two types of probe devices that are often used by fire investigators as shown in Figure 3.1 and 3.2. These instruments are inserted perpendicularly into the surface of the fire-damaged gypsum plasterboard and by feeling the difference between the calcined and non-calcined cross-sections, the depth of calcination is measured. The fire investigators can then identify which measurement points had been exposed to more heat, with the deeper measurements being closer to a single source of heating. Therefore from this information gained, the investigators can formulate conclusions regarding the potential fire origin and development scenarios.

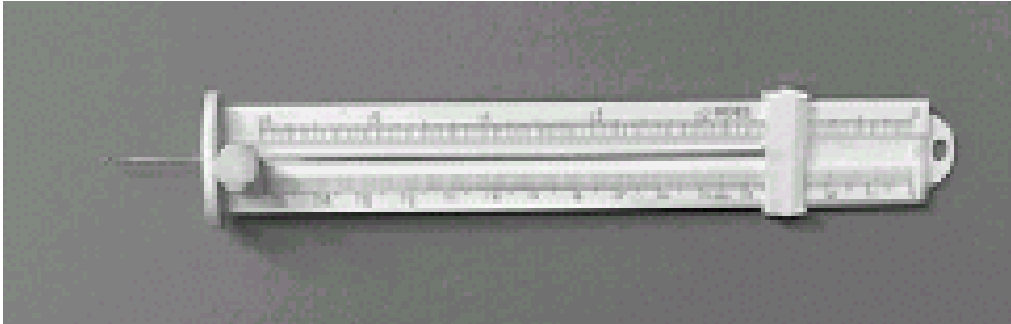


Figure 3.1 Test probe – Depth gauge (Kennedy et al 2003)



Figure 3.2 Test probe – Vernier Calliper

The test probes are easier to use, faster, more practical, considerably less time consuming and labor intensive when compared to the other alternative method, “visual cross-section” method. The “probe” method also does less destruction to the fire-damaged gypsum surface hence leaving the incident place available for further investigations. However, the measurements taken by the test probes have no consistency and may not be a good representative of the actual calcination depth as the measurements taken is dependent on the testing personnel. It requires individual judgment of feeling when the calcination plane is reached and hence different personnel may give different measurements.

3.2 Visual Observation

This method is first introduced by Posey and Posey (1983) as they recognized the rate of calcination was a function of time and temperature and suggested that the depth of calcination could be examined using the naked eye. Fire investigators could systematically cut off the fire-damaged gypsum plasterboard from the wall; break them in half and by looking at its cross-section for any defined lines or subtle colour changes such as from grey to white. The calcinated gypsum would appear as a layer having a different colour, for example, the gypsum plasterboard after exposed to fire in Figure 3.3. The “visual cross-section” method is less often utilized, mainly due to the facts that it is more labour intensive, time consuming, involves observation of poorly defined lines or indistinct colour changes and made more confusing by the presence of impregnated smoke staining in the gypsum from the burning paper backing.



Figure 3.3 Examining the depth of calcination using the naked eye

3.3 Hand Scraping

The gypsum plasterboard begins to undergo the calcination or dehydration process when exposed to heat. The gypsum would start to degrade, losing its strength and softens resulting in two distinct layers of hardness. The depth of calcination could be measured by carefully scraping off the calcined gypsum layer using a flat-headed screwdriver until a reasonable hard plane is reached. The depth of calcination is then measured using a vernier calliper. This “hand scraping”

method can be quite accurate of determining the actual depth of calcination but it does requiring some practice in order to get the feel of the two distinct layers. It is not practical as it requires a lot of labour work and time. However, this method has been used in the research as the basis of verifying the accuracy of measuring the depth of calcination for the proposed measuring tool to be made. No chemical analysis was made to distinguish the boundary between the dihydrate and hemihydrate forms of gypsum.

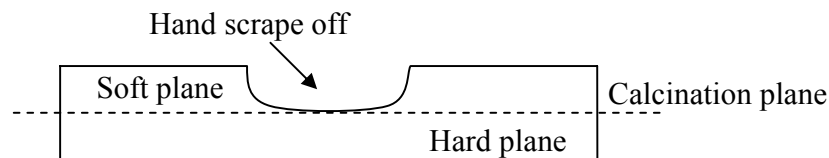


Figure 3.4 Examining the depth of calcination by using “hand scraping” method

3.4 Spring Force Probe

From all of the methods discussed above, each method has their own advantages and disadvantages as an investigative tool for measuring the depth of calcination on gypsum plasterboard. However, there is a need to develop a new measuring tool that can determine the actual depth of calcination. During this period of research study, a new measuring tool was developed which is similar to those test probes; depth gauge and vernier calliper, suggested in “probe survey” method. This newly made tool uses a spring as the force of penetrating the probe into the heat-treated gypsum surface and stops when the probe has insufficient force for more penetration i.e. depth of calcination. The tool is known as “spring-force” probe. The depth of calcination is determined by simply reading the value off the digital meter. Therefore, the testing personnel including those who had never taken calcination probe measurements as well as those who had taken such measurements regularly as part of actual fire investigations would give consistent measurements. The tool consists of an electronic digital calliper, compression spring

Methods of Measuring Calcination Depth

implemented inside the main body, pin at the end of the probe and spiral-like handle. These parts are shown in Figure 3.5, 3.6 and 3.7 respectively.



Figure 3.5 Electronic digital calliper and the main body

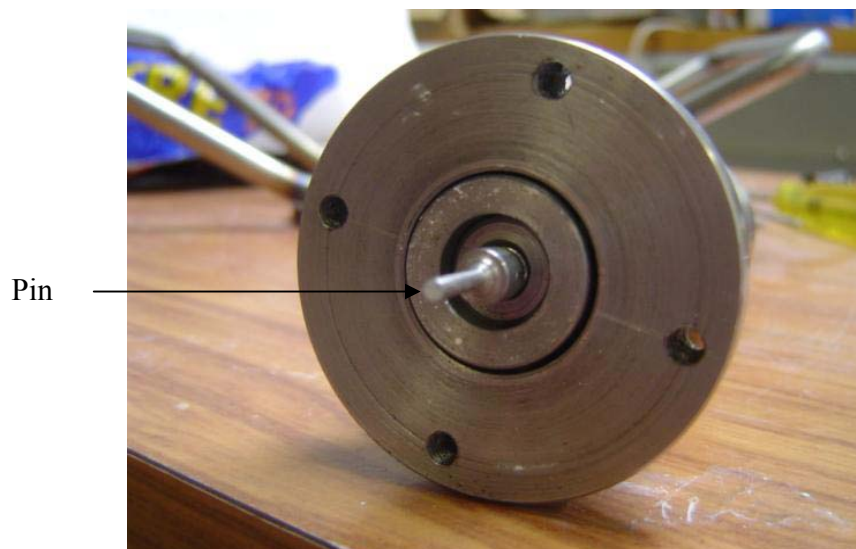


Figure 3.6 Pin attached to the end of the probe with spring inside the main body



Figure 3.7 Complete view of the spring-force probe

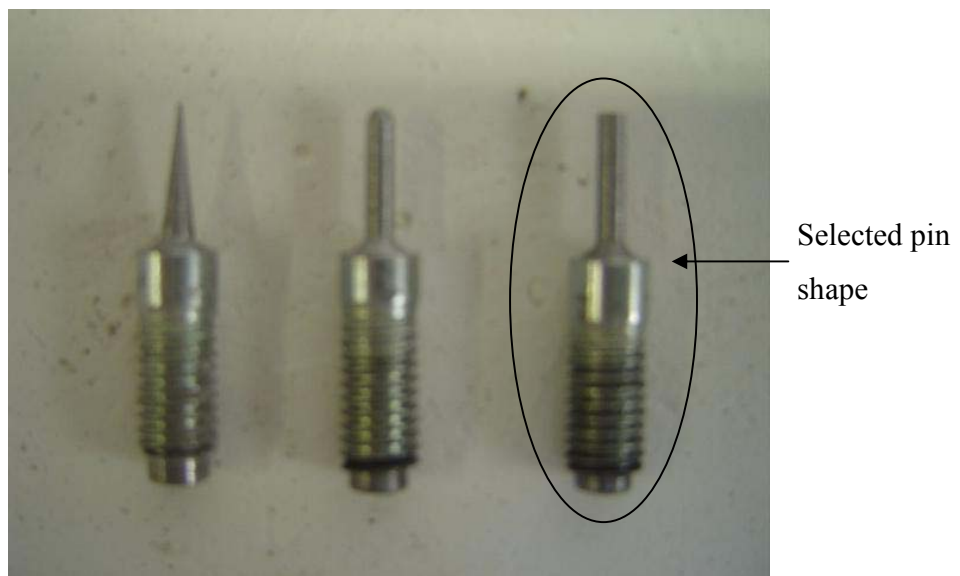


Figure 3.8 Different pin shapes; sharp, blunt and flat (from left to right)

A number of experiments had been carried out by heating the gypsum plasterboard under the cone heater at specific heat flux and time duration in order to test the ability of the tool of determining the actual depth of calcination. Three different pin shapes had been made; sharp, blunt and flat are shown in Figure 3.8, and was concluded to use flat type since the other two shapes were localized, which might not be a good representative of the actual depth of calcination. The results obtained from the tool were verified against hand scraping. These depths of calcination were compared and summarized in Table 3.1 below.

Table 3.1 Depth of calcination measurements by using spring-force probe and hand scraping

Board Type	Fire Duration [min]	Heat Flux [kW/m ²]	Spring-force Probe [mm]	Hand Scraping [mm]
10 mm Standard	15	55	6.749	7.7
10 mm Fyreline	15	55	4.567	6.0
10 mm Noiseline	15	55	1.91	3.25

From the results shown in Table 3.1, the depths of calcination measured by using spring-force probe were lower than the actual depths and was concluded that a stiffer spring hence stronger force was required in order to get more penetration into the heat-treated gypsum surface. In addition, the spring-force probe was found not a very reliable investigative tool to be used as the force exerted is not constant i.e. force increases with more spring compression. This simply means that the probe is required lesser force in order to penetrate through the deeper calcined gypsum. When the gypsum plasterboard is heated at higher heat flux or longer fire duration, more

gypsum is going to be calcined thus the required force to penetrate through the gypsum is different for various board types at different fire conditions i.e. inconsistent measurements. Therefore, the measurements taken from the spring-force probe would not represent the actual depth of calcination.

3.5 Constant Force Probe

The spring-force probe was found inadequate as a tool to measure the actual depth of calcination because the force exerting on the fire damaged gypsum is not constant. In order to apply the same amount of forces through the heat-treated gypsum surface even with different fire conditions, the spring-force probe was modified by replacing the compression spring inside the main body with a constant-force spring. Constant-force springs are a special variety of extension spring (Figure 3.9). They are the only type of springs that truly deflect with a nearly uniform force. They consist of a spiral of strip material with built-in curvature so that each turn of the strip wraps tightly on its inner neighbor. When the strip is extended or deflected, the inherent stress resists the loading force, just as in a common extension spring, but at a nearly constant rate. This is illustrated in the load/deflection curves as shown in Figure 3.10. The materials most often used to make constant-force spring are stainless steel, high carbon steel, beryllium copper and plastic. Among all, Type 301 Stainless Steel has proven to be superior for consistent quality, availability, stress retention and lowest product cost.

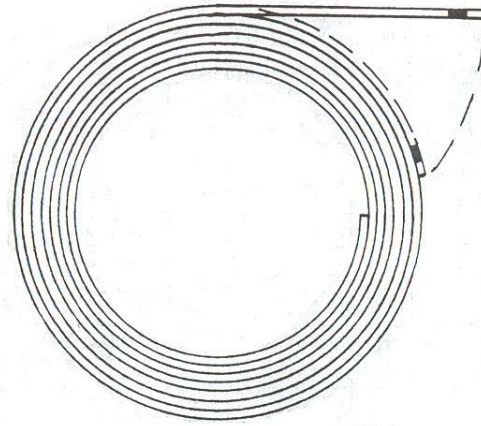


Figure 3.9 Constant-force spring

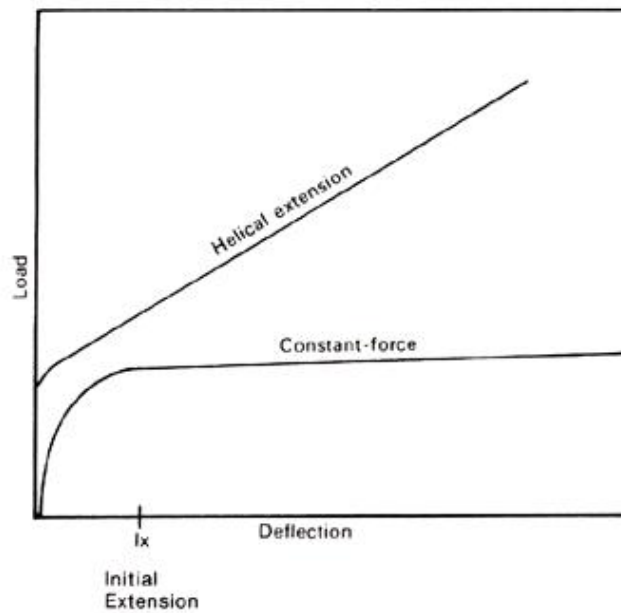


Figure 3.10 Typical load/deflection curves

Constant-force springs are not often used in New Zealand. These springs are not available from any local spring manufacturers and requiring import from overseas. Fortunately, the type of

spring that found inside the measuring tape was constant-force. A slight modification was made to the spring-force probe by replacing the compression spring implemented inside the main body with the constant-force spring pulled out from the measuring tapes. It was found the probe would not have sufficient force to penetrate through the heat-treated gypsum surface to reach the calcination plane. In order to multiply constant-force spring load, multiple constant-force springs could be used in either tandem or back-to-back arrangements as shown in Figure 3.11 below. Back-to-back arrangement was used simply due to the fact that it was easier to modify from the spring-force probe. The constant-force springs were attached to the calliper so to provide the force for the penetration of the probe into the gypsum. This modified piece of tool is then called constant force probe and is shown in Figure 3.12.

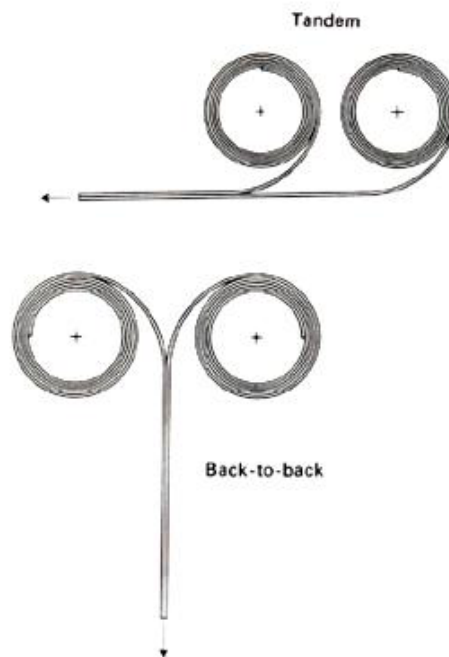


Figure 3.11 Constant-force springs arrangement in order to multiply spring load

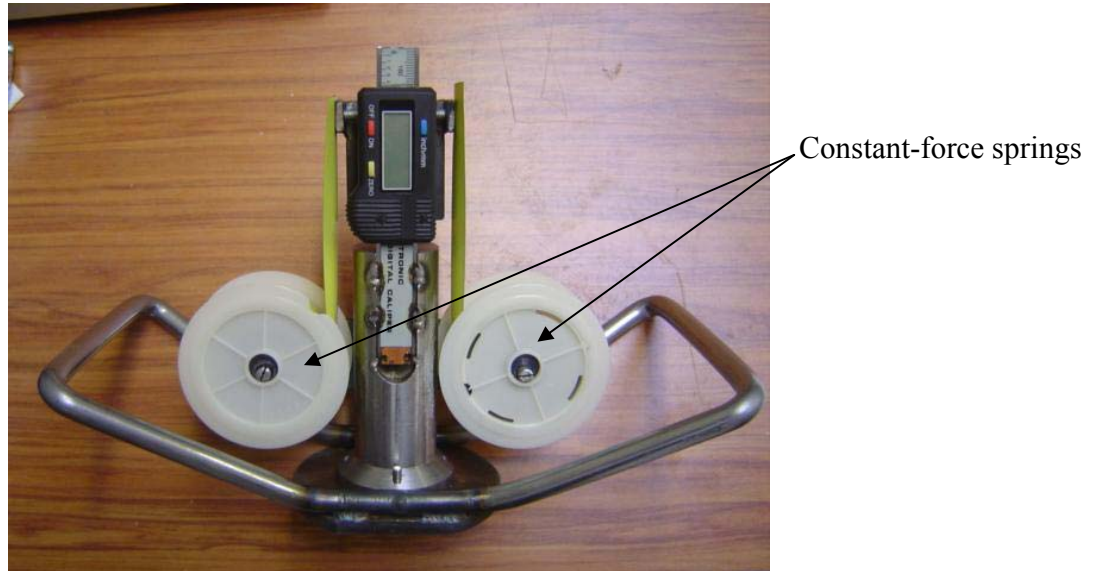


Figure 3.12 Constant force probe made

Spring balance was used to measure the force exerted by the constant-force springs and approximately 3.3 N was recorded for each spring hence giving the constant-force probe a total force of 6.6 N available to measure the depth of calcination. Different probe diameters were also built in order to choose which probe size would give the closest calcination measurements to the hand scraping method. The pressure is a function of force and area, Equation 3.1; hence by doubling the probe diameter (area), it halves the pressure being exerted into the gypsum surface as the force is constant.

$$P = \frac{F}{A} \quad (3.1)$$

Where P is the pressure applied into the heat-treated gypsum [N/mm²]
F is the force applied into the heat-treated gypsum [N]
A is the area of the probe [mm²]

Four different pin diameters; 2.9 mm, 2.05 mm, 1.45 mm and 1.19 mm, were made as shown in Figure 3.13. The pressure applied into the gypsum by each different pin diameter was calculated and summarized in Table 3.2.

Table 3.2 Pressure calculations

Pin Diameter [mm]	Pin Area [mm ²]	Pressure [N/mm ²]
2.19	6.61	1.01
2.05	3.30	2.02
1.45	1.65	4.04
1.19	1.11	6.00

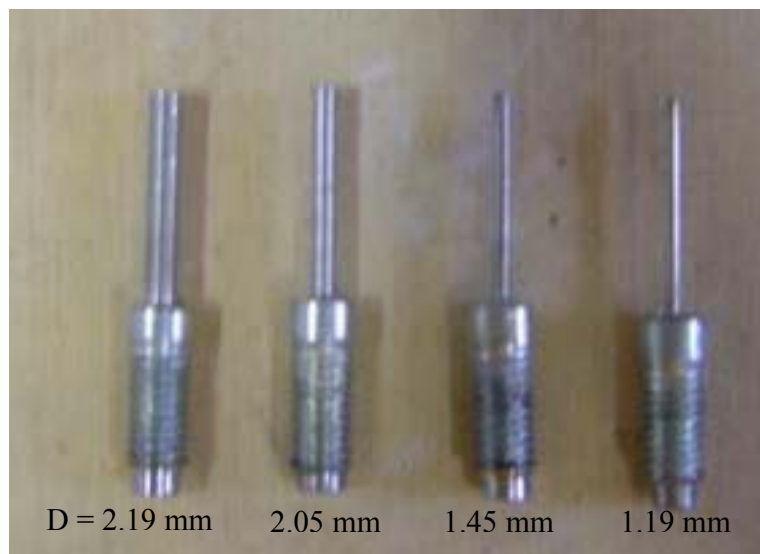


Figure 3.13 Different pin sizes made

Methods of Measuring Calcination Depth

Three fire tests were then constructed with three different types of boards; 10 mm Standard, 10 mm Fyreline and 10 mm Noiseline under the cone heater with heat flux of 50 kW/m^2 and heated for 15 minutes, Table 3.3. After the heating, the depth of calcination for each test was measured using the constant-force probe with each pin diameter and compared with hand scraping method in order to determine the best probe to use. These comparisons were plotted in Figure 3.14, 3.15 and 3.1 respectively.

Table 3.3 Fire tests to determine the depth of calcination by different pin sizes

Probe Test	Board Type	Heat Flux [kW/m^2]	Fire Duration [min]
1	10 mm Standard	50	15
2	10 mm Fyreline	50	15
3	10 mm Noiseline	50	15

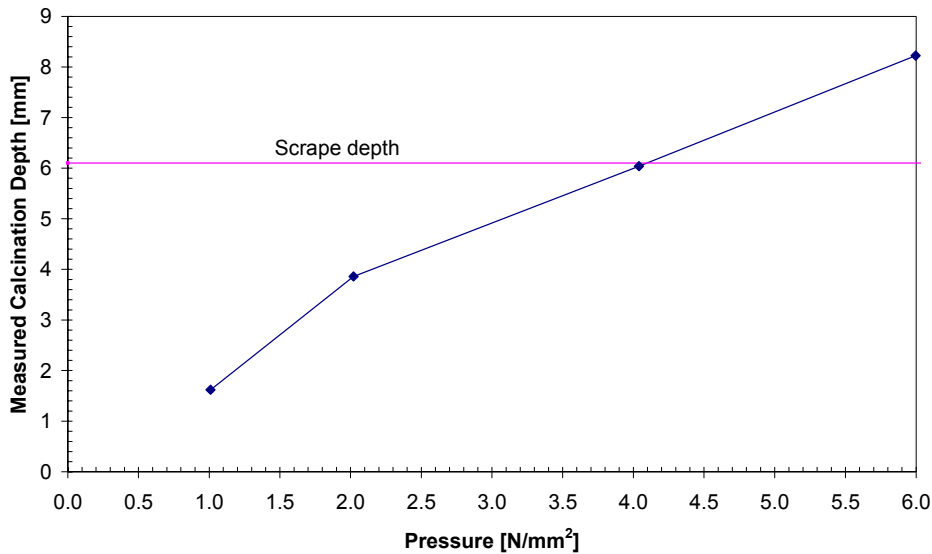


Figure 3.14 Calcination depth measurements at different pressures for probe test 1 – 10 mm Standard board under 50 kW/m^2 and 15 minutes

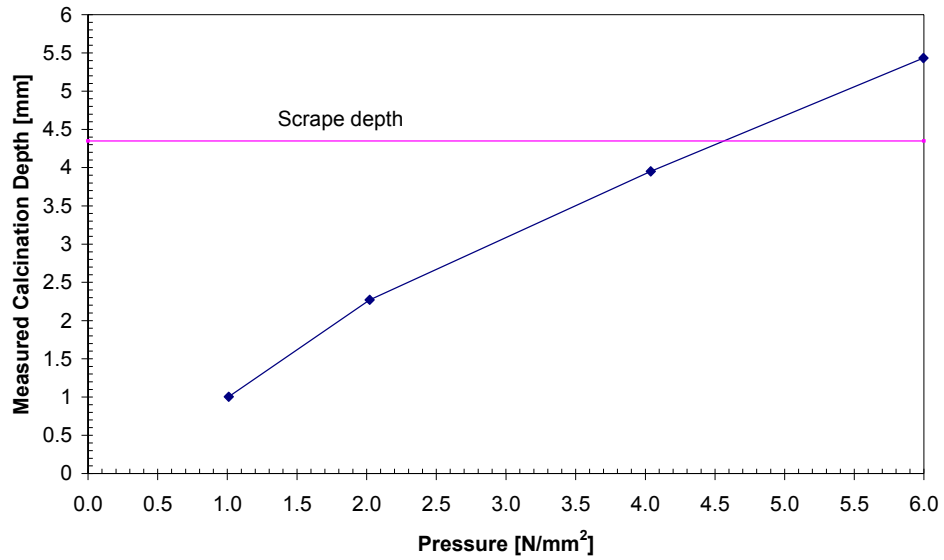


Figure 3.15 Calcination depth measurements at different pressures for probe test 2 – 10 mm Fyreline board under 50 kW/m² and 15 minutes

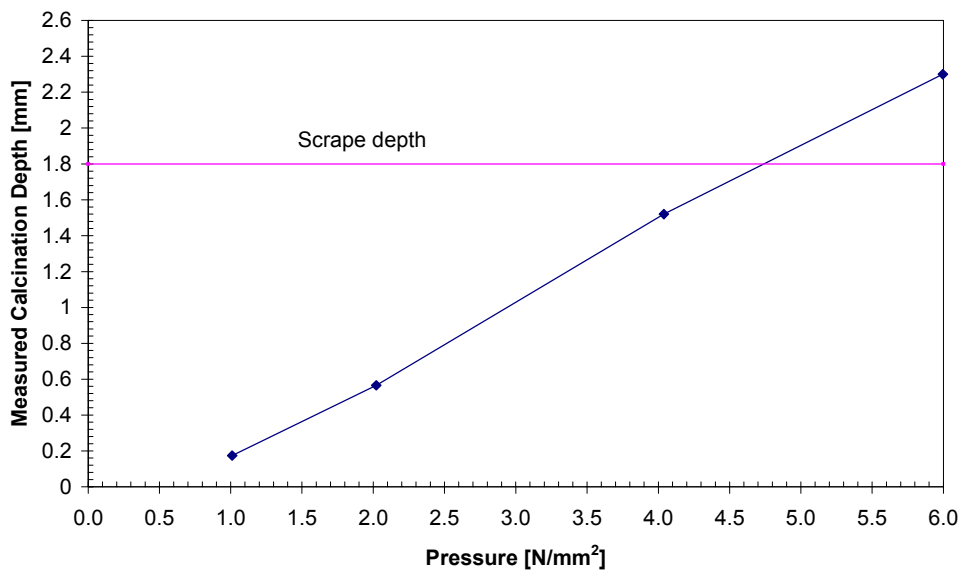


Figure 3.16 Calcination depth measurements at different pressures for probe test 3 – 10 mm Noiseline board under 50 kW/m^2 and 15 minutes

From the above results shown, it was found the pin diameter of 1.45 mm and 4.04 N/mm^2 had the closest measured depth of calcination to the actual depth measured by hand scraping among all the probe sizes. For probe test number 1, the scrape depth (or calcination depth) was 6.1 mm and the measured depth by pin diameter of 1.45 mm (4.04 N/mm^2) was 6.04 mm. For probe test number 2 and 3, even though the agreement between the scrape depth and measured depth by 1.45 mm diameter pin was not as good as observed in probe test number 1, their results were still the nearest one to the scrape depths among the others. In contrast, it was suggested that different pin diameter might be required to measure the depth of calcination on different types of boards. The required pin diameter could be calculated from those graphs as plotted in Figure 3.14 – 3.16 by simply finding the intersection point between the scrape depth and the pressure line. However, this is not included in the research and from now on; the pin diameter of 1.45 mm (4.04 N/mm^2) is chosen for the best pin size of measuring the calcination depth.

3.6 Methods of Measuring Calcination Depth Conclusions

Above all the discussed methods that are available of measuring the depth of calcination, some are already put in use as an investigative tool or technique such as “probe survey” method using depth gauge or vernier calliper and “visual cross-section” method using the naked eye.

Nevertheless these methods have some drawbacks to the practical fire investigation, in particular, only giving the relative changes, increase or decrease in depth of calcination on gypsum plasterboard in which the actual depth of calcination measurements are of little important. For this purposes, the constant-force probe was built as a new fire investigative tool and it has been shown that the measured depths of calcination had reasonable good agreement to the depth of calcination determined by the “hand scraping” method.

Chapter 4 Room Fires

4.1 General

Fire in rooms or compartments are described separately for pre-flashover and post-flashover fires where pre-flashover is the early stage of a fire and post-flashover is the stage when the fire is fully developed. These are the two distinctly different design situations in fire safety engineering design. The emphasis is on the life safety of humans for pre-flashover fires so the design load is characterized by an energy release rate curve where the growth phase of the fire is of most importance. In contrast, the objective design for post-flashover fires is to prevent structural collapse and safety of firefighters. In the post-flashover stage of a fire all the combustible objects in the room are burning and the heat release rate is limited either by the fuel surface area or the available air supply. Therefore, the design load for post-flashover fires is characterized by a temperature-time curve where the fully developed burning phase is of greatest concern. This chapter reviews the behaviour of fires in rooms, the concept of fire severity and the available design fires for structural design.

4.2 Stages in Enclosure Fire Development

In order to have a better understanding of the concept of fire severity, it is necessary to know the stages of development of a fire in greater details. Fire development in rooms is commonly divided into the following five stages:

- Incipient (or ignition)
- Growth
- Flashover
- Fully developed fire (or post-flashover fire)
- Decay

Figure 4.1 shows an idealized variation of temperature with time to illustrate all these stages of development of a fire.

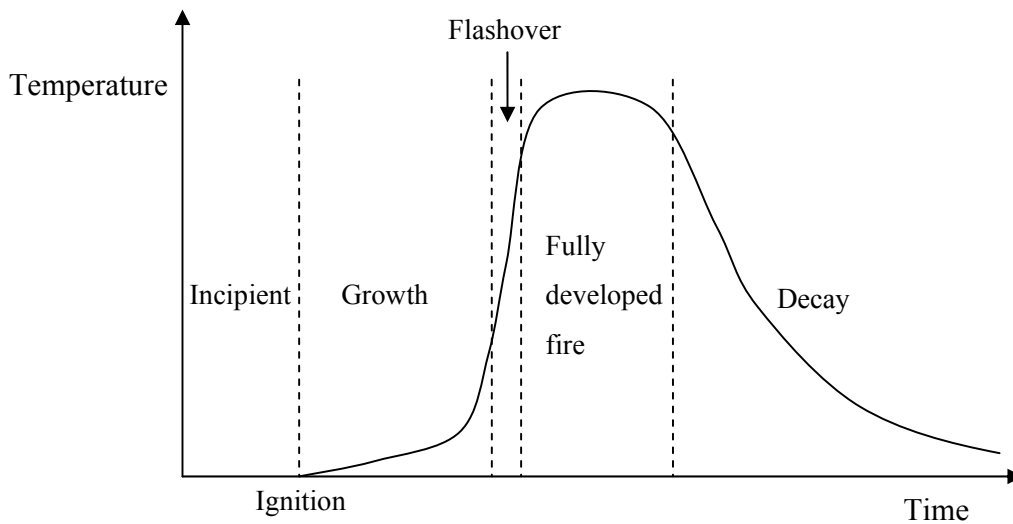


Figure 4.1 Idealized temperature history showing all 5 stages of fire growth

Fire ignition is always preceded by an incipient stage where the incipient stage of a fire can last a few milliseconds to days depending on the initial fuel involved, ambient conditions and ignition sources. Ignition is considered as a process that produces an exothermic reaction characterized by a rapid increase in temperature above the ambient. Ignition normally occurs either by piloted ignition (by flaming match or electrical spark) or by spontaneous ignition (through accumulation of heat in the fuel). An incipient phase can often be detected before ignition occurs due to occupants smelling smoke or by the activation of smoke detector. According to Buchanan (2001b), a fire is in its incipient stage as long as the fire is small enough that radiation is not the dominant form of heat transfer. As a rule of thumb, this is identical to a fire that is of order of 20 kW or less equating to a fire diameter of the order of 0.2 m.

The growth stage is considered to begin when the radiation feedback from the flame governs the burning rate. Fire growth after ignition may be at a slow or fast rate depending on the following factors:

- Type of combustion (smouldering, flaming)
- Type of fuel
- Interaction with the surroundings
- Oxygen available for burning

Smouldering combustion, sometimes refers as flameless combustion, is a particularly slow fire development, which the energy release rate and temperatures are relatively low. This type of combustion is a particular hazard in building fires because insufficient heat or noise is generated to wake sleeping occupants who can be overcome by the production of high quantities of toxic gases and smoke. The growth stage can also occur very rapidly, flaming combustion, where the oxygen levels is sufficient (fuel-controlled) to allow flame spreading over the surface of a combustible fuel and additionally the heat flux from the burning objects is sufficient to ignite adjacent fuel sources.

If the fire continues to grow in an enclosed compartment with a continuing increase in the thickness and temperature of the upper gas layer, a transition will occur between a fire that is dominated by the first burning object to a fire which is dominated by all of the burning combustible fuels in the room. All the exposed surfaces are heated by radiation from the flames, hot surfaces, and the upper layer of smoke and hot gases. This transition is called flashover. Hence, flashover is the transitional stage from the growth period to the fully developed stage in the fire development. Buchanan (2001a) gives the conditions necessary for flashover to occur in a typical room. It occurs when the upper gas layer has reached approximately 600°C or that the radiant heat flux is about 20 kW/m² at floor level.

The behaviour of the fire changes dramatically after flashover. In the fully developed or post-flashover stage of the fire, all of the combustible objects in the compartment are burning and the energy release rate is at its greatest and is often limited by the availability of oxygen. This is called ventilation-controlled burning as opposed to fuel-controlled, and is governed by the size, shape and number of ventilation openings. In ventilation-controlled fires, it is often seen flames sticking out through the openings, as any unburnt gases, which are collected at the ceiling level and leave through the opening will be able to burn due to the new oxygen supply from the outside. The average gas temperature within a compartment during this stage is often very high, can reach up to 1200°C and continues to burn as long as there are sufficient fuel and ventilation. Therefore, the most important information for structural design is the temperature in the room during this fully developed stage.

After a period of fully developed burning, the energy release rate diminishes and hence the average gas temperature in the compartment declines as the fuel is consumed. Once the fuel supply diminishes to a point where it is unable to sustain its maximum burning rate, the fire is then said to be in the decay stage. This type of burning is called fuel-controlled where the rate of burning is controlled by the surface area or availability of fuel remaining within an environment that the oxygen supply is still sufficient. Decay will keep continuing until all the fuel is consumed or the fire goes out depending on fuel type. The decay stage can be extremely short with burning thermoplastics and liquid hydrocarbon fuels whereas for cellulosic materials such as wood, it takes much longer.

4.3 Fire Severity

When designing structures for fire safety, the fundamental step is to verify that the fire resistance of an element is greater than the severity of the fire that the building element is exposed i.e. fire resistance \geq fire severity. Buchanan (2001a) gives both definitions of fire resistance and fire severity as the following:

- Fire resistance is the “measure of the ability of the structure to resist collapse, fire spread or other failure during exposure to a fire of specified severity”
- Fire severity is the “measure of the destructive impact of a fire, or the measure of the forces or temperatures which could cause collapse or other failure as a result of the fire”.

Fire severity is often described in terms of a period of exposure to the standard test fire but this is not true for realistic fires which have very distinct characteristics. The most widely used standard time-temperature curve is ISO 834 as shown in the Equation 4.1 below:

$$T = 345 \log(8t + 1) + T_0 \quad (4.1)$$

Where T is the temperature [°C]
t is the time [minutes]
T₀ is the ambient temperature [°C]

The severity of a real fire is determined to be significantly worse than the equivalent early stages of the standard ISO 834 time-temperature relationship. Nyman (2001) has highlighted these corresponding factors in the following:

- Thermoplastic materials and modern furnishings where they burn significantly fast as pool fires with higher heat release rates

- Realistic time-temperature fire histories where some full-scale compartments was burnt and found to fail earlier than that of the standard furnace tests

Many efforts have been put in by fire engineers and researchers to quantify the severity of a real fire. The concept of equivalent fire severity is the one which is most often used, in which it relates the severity of a real fire to the standard test fire. This concept is of importance allowing designers to use published fire resistance ratings from standard tests with estimates of real fire exposure. There are several approaches that have been used to determine the equivalent fire severity as described in Buchanan (2001a). However among all these methods, equal area and time-equivalent concepts are of particularly significance.

4.3.1 Equal Area Concept

Equal area concept was first proposed by Ingberg in 1928, in which he defined the integral or area under the time-temperature curve as the fire severity. Therefore, two fires are considered to have equivalent fire severity if the areas under each curve are equal, above a certain reference temperature. This equal area concept cannot be proved theoretically because the units of area are meaningless. The equal area concept has a problem that it can give a very poor comparison of heat transfer for fires with distinct shapes of time-temperature curves. At high temperatures, heat transfer from a fire to the surface of a structure is dominated by radiation and due to the fact that radiation is proportional to fourth power of the absolute temperature hence taking a direct area under a time-temperature curve cannot truly represent the fire severity. Using such method would underestimate the severity of short hot fire and overestimate long cool fire severity.

Due to the theoretically inappropriate usage of equal area concept in assessing fire severity, Nyman (2001) expanded the concept further to what he called “radiant exposure area correlation” concept. He proposed to use the total energy impinging upon the surface of a structure to establish the severity of a fire, which is expressed as the area under a plot of the emissive power

of the compartment gases against time. The emissive power is given as the equation below where the emissivity of the gases is conservatively taken as 1 for simplicity:

$$\dot{Q}'' = \varepsilon \sigma T^4 \quad (4.2)$$

Where \dot{Q}'' is the radiant heat flux [kW/m²]
 ε is the emissivity of the gases (1) [-]
 σ is the Stefan-Boltzmann constant (5.67×10⁸) [W/m²K⁴]
 T is the absolute temperature [Kelvin]

The area under the emissive power-time curve is therefore expressed mathematically with units of kJ/m² as follows:

$$Area = \int_0^t \dot{Q}'' dt = \varepsilon \sigma \int_0^t T^4 dt \quad (4.3)$$

The radiant exposure area correlation can be used to any fire exposure time-temperature profiles. When the radiant exposure concept is applied to the standard ISO 834 curve, the measure of fire severity at any time on the curve can be determined and this measure of fire severity can then simply equated to a real fire exposure having the same radiant exposure area, which is the equivalent fire severity. For example, if the failure time of an assembly under the exposure of the standard ISO 834 fire is known and a real fire exposure is known or predicted, the failure time of that assembly in real fire exposure can be determined.

There are two assumptions that have been made in this approach in order to correlate the radiation fire severity in each test type; standard furnace and real test fires. The energy characteristics in both the compartment test fires and the standard furnace test fires are assumed

to be identical and also that the convective components of heat transfer to the structure are of equal proportion to the whole energy transfer in both test fires.

4.3.2 Time-Equivalent Concept

Time-equivalent uses the most common approach in quantifying the severity of a fire that is by equating the performance of a structure under a real fire exposure in terms of an equivalent exposure to the standard fire. Buchanan (2001a) includes a number of time-equivalent formulae that have been developed in assessing fire severity and explains in greater details. These time-equivalent formulae are:

- CIB formula, which based on the ventilation parameters of the compartment and the amount of fuel load available for burning
- Law formula, which based on the test carried out in both small scale and larger scale compartments and the formula is similar to CIB
- Eurocode formula, which again similar to CID but with some modifications, introducing the new compartment lining parameter and the horizontal openings in the roof of the compartment is included into the ventilation factor

4.4 Design Fires

Before designing any structural elements exposed to fire, it is necessary as a fire engineers or designers to choose a design fire. The design fire is selected so that it has the best representation to a real fire exposure. Buchanan (2001a) describes the methods that are available of obtaining design fires include hand calculations, published curves and parametric fire equations. Of particular significance are the parametric fire equations, which are explained in greater detail below.

These parametric fire equations are published by the “Eurocode 1 (EC1 1994): Basis of Design and Design Actions on Structures, Part 2-2: Actions on Structures Exposed to Fire”. The Eurocode parametric fire equations allow a time-temperature relationship to be produced from any combination of ventilation openings, fuel load and wall lining materials. These parametric fire equations are derived from:

Equation for burning period:

$$T = 1325(1 - 0.324e^{-0.2t^*} - 0.204e^{-1.7t^*} - 0.472e^{-19t^*}) \quad (4.4)$$

Where T is the temperature of the compartment gases [°C]
 t^* is a fictitious time in hours [hr]

The fictitious time is given by:

$$t^* = \Gamma t \quad (4.5)$$

Where t is time in hours [hr]

And

$$\Gamma = \frac{\left(\frac{F_v}{F_{ref}}\right)^2}{\left(\frac{b}{b_{ref}}\right)^2} \quad (4.6)$$

$$b = \sqrt{k \rho c_p} \quad (4.7)$$

$$F_v = \frac{A_v \sqrt{H_v}}{A_t} \quad (4.8)$$

Room Fires

Where	F_v is the ventilation factor	[-]
	A_v is the area of the window opening	[m ²]
	H_v is the height of the window opening	[m]
	A_t is the total internal surface area	[m ²]
	F_{ref} is the reference value taken as 0.04	[-]
	b_{ref} is the reference value taken as 1160	[Ws ^{0.5} /m ² K]
	b is the thermal inertia	[Ws ^{0.5} /m ² K]
	k is the thermal conductivity of the lining material	[W/mK]
	ρ is the density of the lining material	[kg/m ³]
	c_p is the specific heat of the lining material	[J/kgK]

Duration of burning period:

The equation for the duration of the burning period in the Eurocode is simplified to:

$$t_d = \frac{0.00013 e_t}{F_v} \quad (4.9)$$

Where e_t is the fuel load [MJ/m² total surface area]

Decay rate:

Following the burning period, the Eurocode uses a reference decay rate $(dT/dt)_{ref}$ equal to 625°C per hour for fires with a burning period less than half an hour and 250°C per hour for fires with a burning period greater than two hours. Figure 4.2 shows this reference decay rate curve including the values when the burning period lies between half an hour and two hours.

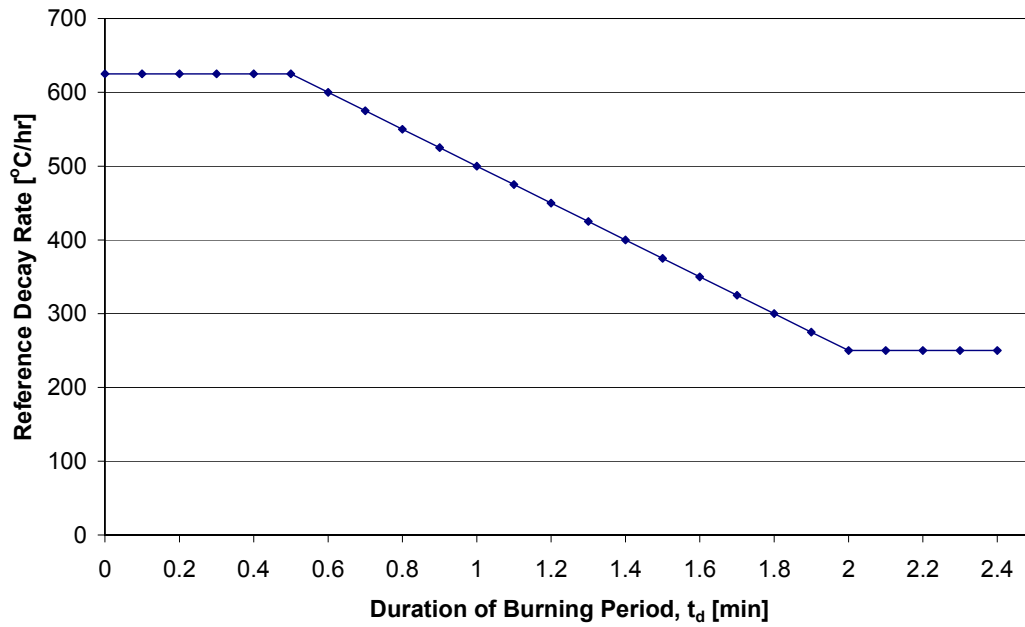


Figure 4.2 Rate of temperature decay in EC1 parametric fires

Therefore, the equation for decay rate is calculated by the following equation:

$$\frac{dT}{dt} = \left(\frac{dT}{dt} \right)_{ref} \frac{\sqrt{F_y/0.04}}{\sqrt{b/1160}} \quad (4.10)$$

Chapter 5 Experimental Program

5.1 General

Cone calorimeter tests were undertaken on different types of gypsum plasterboards exposed to different heat flux (or temperature) and fire duration to determine the depth of calcination and the correlations relating the calcination depths to heat flux and duration. The research was only concerned about the calcination depth measurements and therefore, an ISO ignitability apparatus which is a modification of the cone calorimeter could have been used alternatively to run these experiments and the details of this piece of apparatus shall be obtained from BS 476. The temperature-time history data of thicker gypsum plasterboard at various depths were also measured. This chapter provides an overview of the equipment and methodology used in the research.

5.2 Cone Calorimeter Test

The cone calorimeter from the University of Canterbury Fire Testing Laboratory was used as the testing device for this research project and was shown in Figure 5.1 below. The cone calorimeter has the ability to measure a range of material fire properties such as:

- Rate of heat release
- Total heat release
- Effective heat of combustion
- Mass loss rate
- Time to ignition
- Oxygen consumption
- Carbon dioxide, carbon monoxide and other toxic gases production

- Smoke obscuration

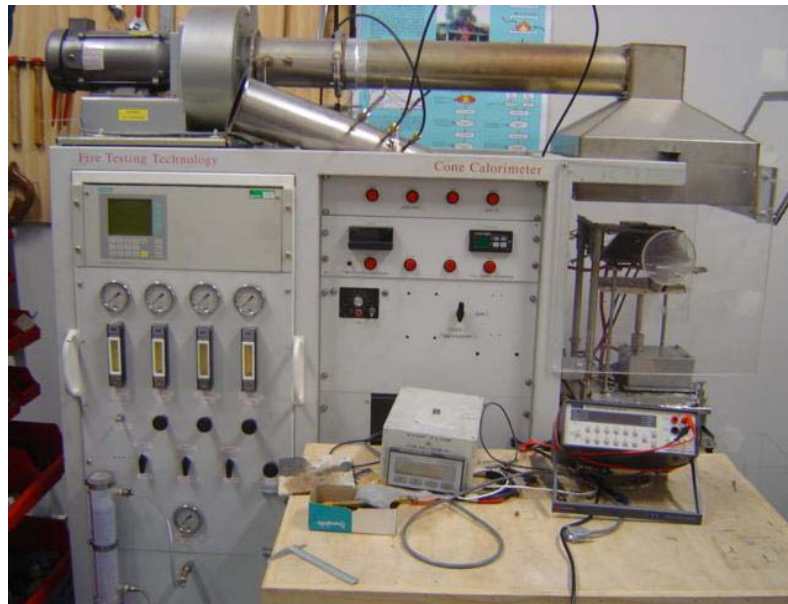


Figure 5.1 The cone calorimeter test apparatus

The cone calorimeter is also able to implement a uniform and repeatable testing procedure under the conical radiator heater where a constant heat flux can be set as the temperatures are measured by the thermocouples within the apparatus and are correlated to a heat flux using a radiometer (heat flux meter). The complete cone calorimeter apparatus is essentially consists of four distinct sections of equipment:

- Conical radiator heater and load cell
- Main and gas control panels
- Gas analysers
- Duct section

Experimental Program

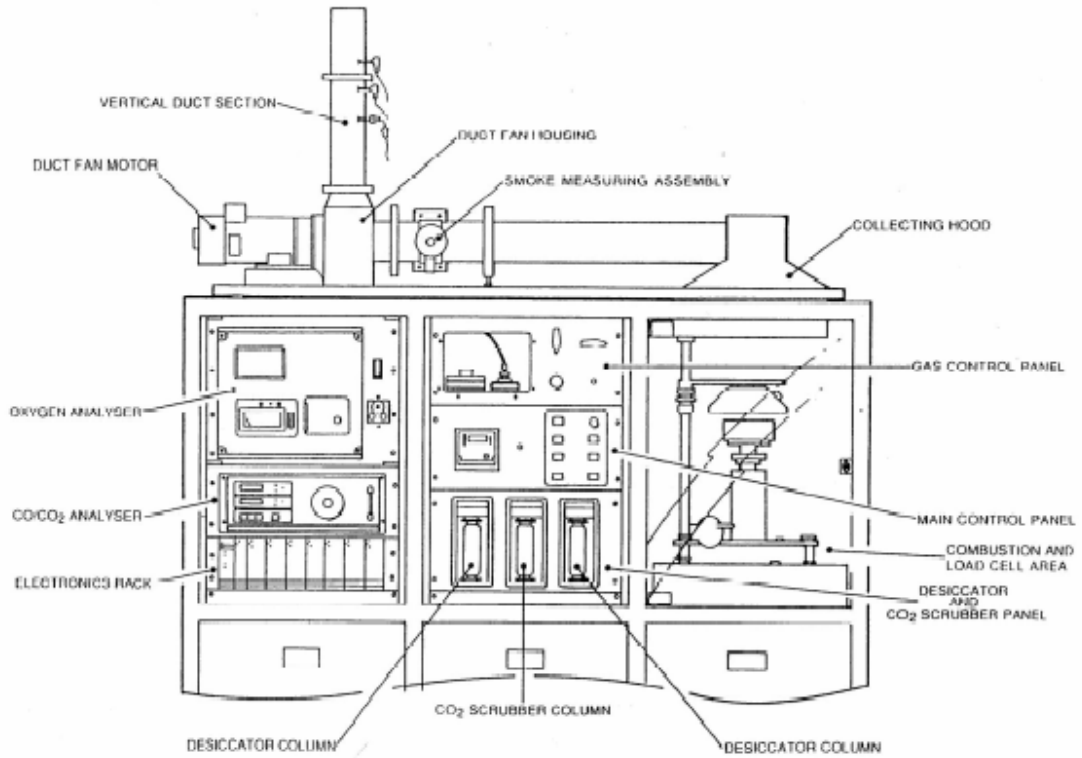


Figure 5.2 Complete schematic representation of the cone calorimeter apparatus (Figure taken from Nyman 2001)

5.2.1 Cone Heater

The cone heater is made up of a heating element that coiled into the shape of a truncated cone and fitted into a shade as shown in Figure 5.3. The purpose of the heating element is to improvise heat fluxes that the items would be exposed to in realistic fires. The conical radiator can be varied from 10 kW/m^2 to 100 kW/m^2 , which basically covers the range from early stages of fires to fully developed fires. In order to ensure the sample is exposed to a constant radiant flux, an electrically powered heating element is used, which has three thermocouples implemented across the coiled heating element measuring the element temperature. The element temperature is then monitored by an electronic controller that keeps taking averages of the three thermocouples readings to ensure the element temperature remains constant. The conical cone radiator section is shown in greater detail in Figure 5.4.

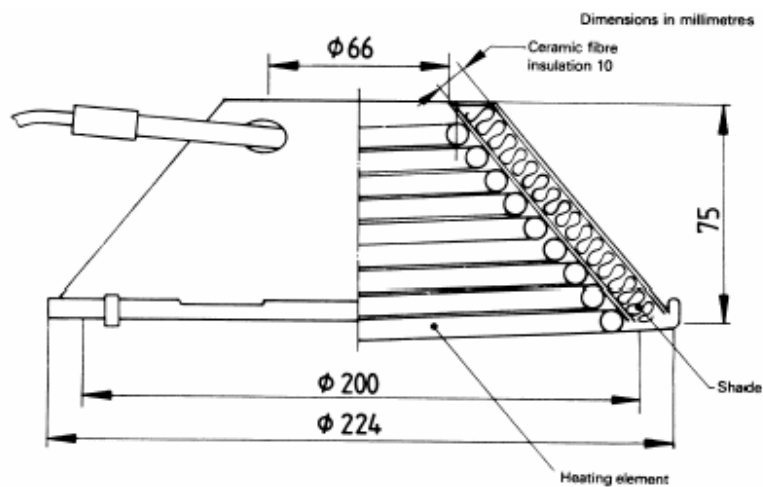


Figure 5.3 Radiator cone (Figure taken from BS 476)

Experimental Program

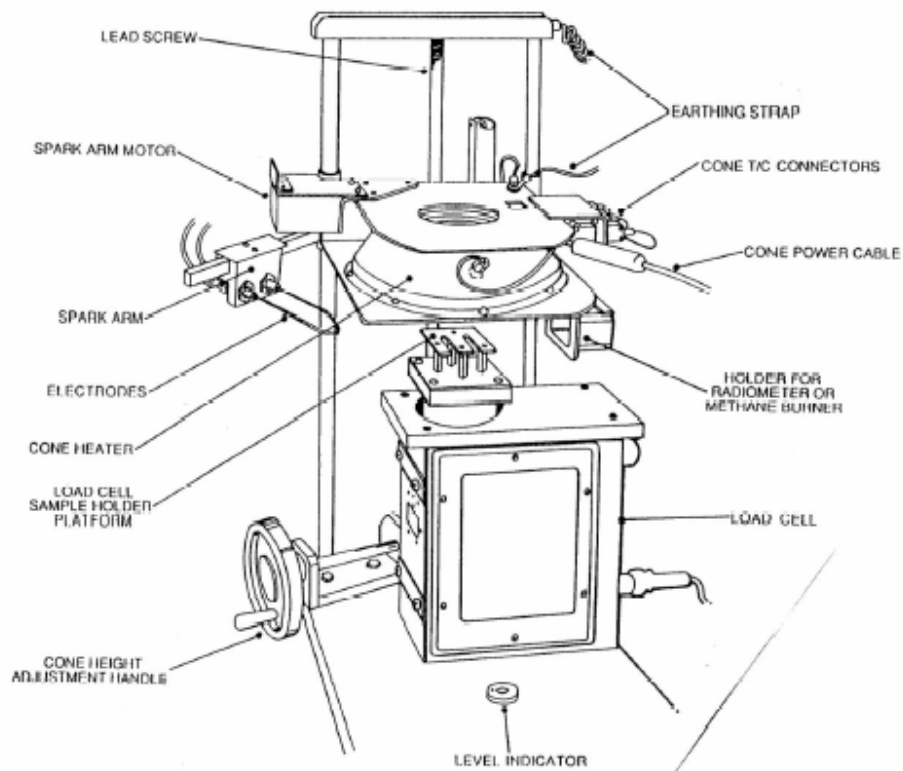


Figure 5.4 Cone heater schematic (Figure taken from Nyman 2001)

5.2.2 Sample Mounting

Samples are mounted on a horizontal orientation platform on the mass scale. The platform height can be adjusted to fit the sample into the cone heater to ensure there is a 25 mm gap between the upper surface of the sample and the bottom of the cone heater. Figure 5.5 shows the illustration of how a piece of gypsum plasterboard sample was mounted under the cone heater. A 100 mm diameter circular opening was cut centrally in the masking plate and positioned over the upper surface of the sample such that a defined area of the upper surface of the specimen is exposed to radiation and reducing any edge effects during testing.

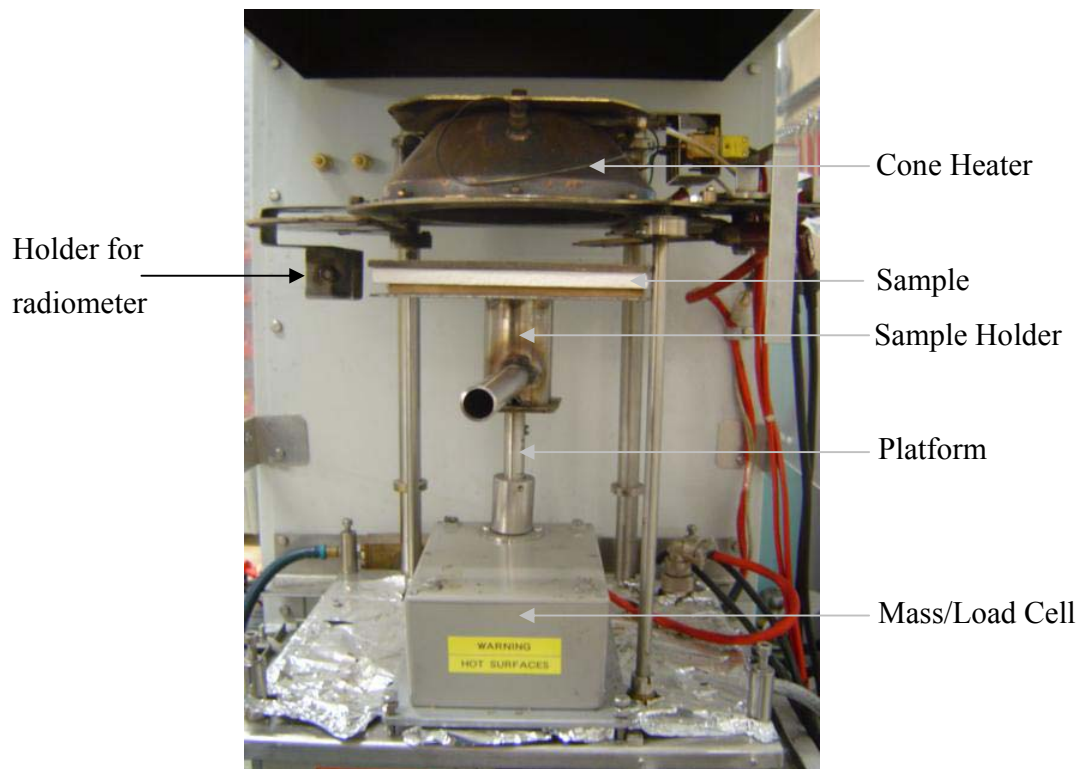


Figure 5.5 Illustration of how the samples were mounted during the fire testing

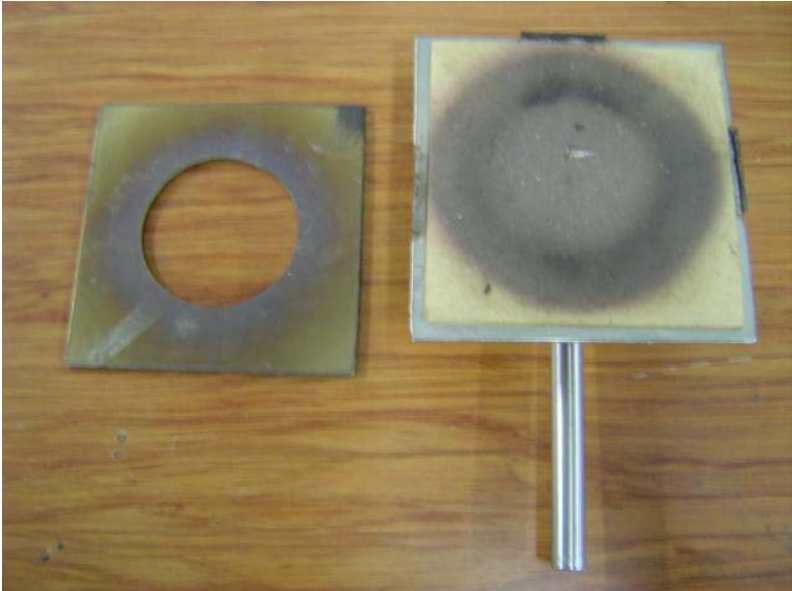


Figure 5.6 Masking plate (left) and sample holder with baseboard (right)

5.3 Experimental Procedures

5.3.1 Calibration

The distribution of irradiance provided by the cone to the sample surface was made such that the variation of irradiance within a circle of 100 mm diameter, drawn from the centre of the masking plate opening, shall be not more than $\pm 5\%$ of that at the centre. The heat flux of the cone heater was calibrated with the use of radiometer or heat flux meter, which was installed in the holder provided as shown in Figure 5.5 above. The radiometer used for the calibration is a Gardon (foil) type with a design range of about 100 kW/m^2 . The radiometer is used to measure the irradiance incident on the surface of a sample and it has a specific calibration curve that converts a voltage to a corresponding heat flux. The full scale output and the responsivity of the radiometer are specified to be 7.46 mV at 100 kW/m^2 and $0.0746 \text{ mV per kW/m}^2$ respectively. This calibration curve is plotted in Figure 5.7 below.

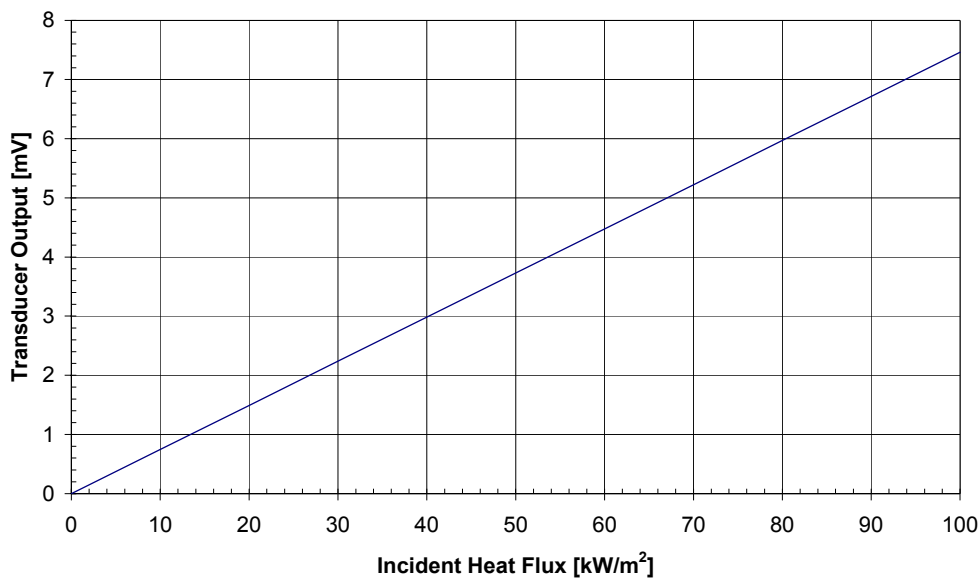


Figure 5.7 Calibration curve for the cone heater

The radiometer was contained within water-cooled body in order to maintain the calibration ambient conditions. Electric supply was then switched on and the temperature settings of the temperature controller were established to produce the required irradiances at the centre of the circular opening in the masking plate. The required irradiances were 20, 35, 50 and 65 kW/m². The measured irradiances of the radiometer were given as a transducer output displayed by the millivolt measuring device. Adjustments near the final setting for the cone heater were followed by a 5 minutes period without further adjustment on the temperature controller to ensure that the cone heater has achieved sufficient temperature equilibrium. These procedures were carried twice, the first time at settings of increasing temperature and the second time at decreasing temperature. Both values shall be repeatable to within $\pm 5^{\circ}\text{C}$ as values outside these limits indicate possible defects in control of monitoring equipment or significant changes in the testing environment. Finally, these calibration data were recorded and tabulated in Table 5.1.

Table 5.1 Calibration data

Required Heat Flux [kW/m ²]	Transducer Output [mV]	Corresponding Temperature [°C]
20	1.492	517
35	2.611	650
50	3.730	743
65	4.849	821

5.3.2 Sample preparation

Three different types of gypsum plasterboards; Standard, Fyreline and Noiseline, with varying thickness were used for the cone calorimeter testing. All samples were cut using a craft knife. Each sample was cut into a square size of 175 mm by 175 mm from the whole board sheet and each was weighed in order to determine the board density. The densities of the gypsum plasterboards were measured and presented in Table 5.2. It should be noted that each of these

board types are separately formulated in different thicknesses by the manufacturer to give the desired range of properties, which explains why the densities are not the same for each type of boards in different thicknesses. All samples were then stored in a cabinet readily for testing.

Table 5.2 Measured densities of gypsum plasterboards

Board Type	Test Density [kg/m^3]
10 mm Standard	631
13 mm Standard	688
10 mm Fyreline	698
13 mm Fyreline	737
16 mm Fyreline	863
19 mm Fyreline	888
10 mm Noiseline	848



Figure 5.8 Samples storage ready for cone calorimeter testing

Experimental Program

A thin steel plate with equivalent size to the sample was made with five circular openings of approximately 5 mm in diameter. These small circular openings were distributed evenly inside a 100 mm diameter as shown in Figure 5.9. The steel plate is used to ensure consistent measurement points are taken by the constant force probe through the openings after the samples have been tested under the cone calorimeter.

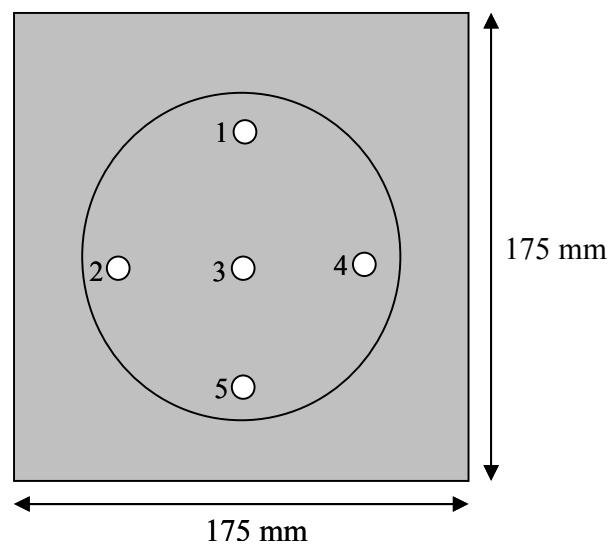


Figure 5.9 Steel plate with five circular openings

Two samples of 19 mm thick Fyrelite plasterboards were used to record the temperature over time. Therefore the samples had been drilled with a series of 2 mm wide holes for the insertion of thermocouples. The depths for the thermocouples insertion were 4 mm, 8 mm, 12 mm and 16 mm below the upper surface of the plasterboard and distributed evenly across the centre. Figure 5.10 shows a schematic representation of the thermocouples placement in the plasterboard.

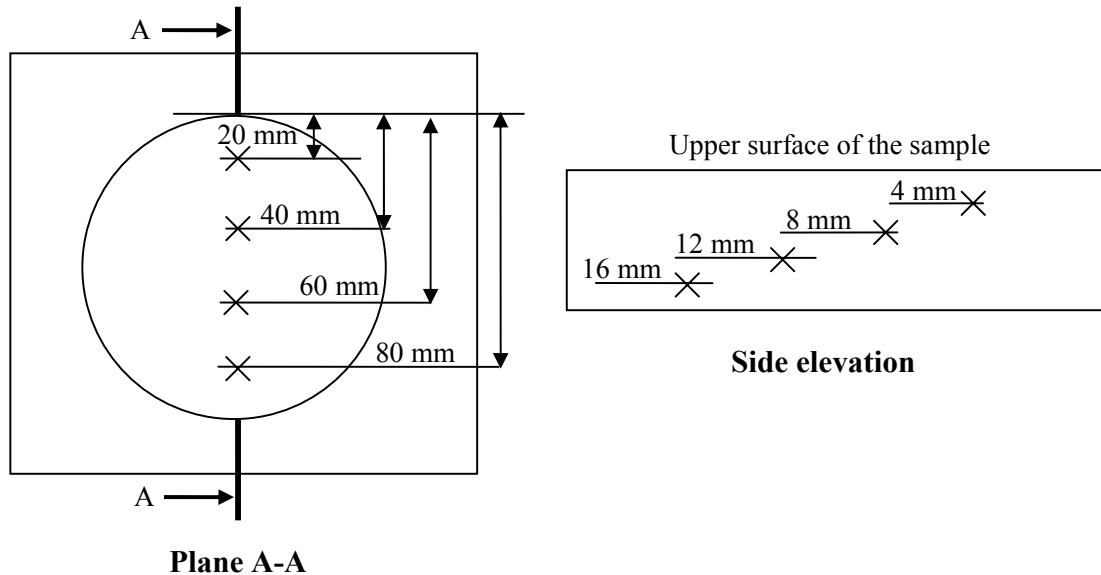


Figure 5.10 Thermocouples placement in thicker gypsum plasterboards

5.3.3 Design of experiments

The aim of the experimental design was to realistically represent a range of potential fire conditions that gypsum plasterboard might be exposed to fire. The gypsum plasterboard samples were each assigned a specific exposure condition (heat flux) and fire duration. Table 5.3 shows the specifications and number of experiments to be carried out under the cone heater. Appendix A outlines the specific scenario for each of the tests.

For thermocouple data, another two tests were carried out with 19 mm Fyrelite plasterboards exposing to two different heat fluxes; 50 kW/m^2 and 65 kW/m^2 , and the exposure durations were approximately two hours. Therefore, there are altogether 72 experimental tests to be carried out in this research.

Table 5.3 Matrix of sample specifications for testing

Board Type	Board Thickness [mm]	Heat Flux [kW/m ²]	Exposure Time [minutes]	No. of Tests
Standard	10	35, 50, 65	2, 5, 10, 15, 30	15
	10	20	15	1
	13	50	15	1
Fyreline	10	35, 50, 65	2, 5, 10, 15, 30	15
	13	50	15	1
	16	50	15	1
	19	35, 50, 65	2, 5, 10, 15, 30, 45, 60	21
Noiseline	10	35, 50, 65	2, 5, 10, 15, 30	15
			Total Tests Required	70

5.3.4 Testing procedure

The cone calorimeter testing was carried out at ambient temperature and humidity conditions. The tests were carried out with a cone heater radiant heat flux and exposure durations as shown in Table 5.3 above for each different types of gypsum plasterboards. The power to cone calorimeter apparatus and cone heater was turned on and the cone temperature was allowed to come up to 200°C and left the cone for five to ten minutes to allow preheating. The cone temperature was then adjusted to 400°C and allowed the cone to stay at this temperature for another five minutes. During these preheating periods, the ceramic fibre wool was used as a dummy specimen board placing over the load cell platform in order to prevent the heat from damaging the load cell. The fan of the collecting hood was also turned on to exhaust all the smokes produced during the samples burning.

While the cone was preheating, the first sample ready for testing was weighed and recorded in order to determine the total mass lost during the test. Sample was then located in a tests sample

holder with the baseboard placed beneath as an insulated backing material and the masking plate was put over the upper surface of the samples. This prepared sample-baseboard combination was ready for testing after the cone heater has been set up.

When the cone heater had been preheated, the cone heater was set to the desired heat flux by adjusting the temperature setting of the controller to the desired temperature established by the calibration procedure as presented in Table 5.1. Once the cone temperature had reached the desired temperature, the cone heater was left for few minutes to attain equilibrium. The next four steps were conducted in rapid succession (approximately 15 seconds) after the cone heater had attained the temperature equilibrium:

- The shielding plate underneath the cone heater was closed over the orifice.
- The dummy specimen board from the load cell platform under the cone heater was removed.
- The prepared sample-baseboard combination was placed onto the platform such that the upper surface of the sample is 25 mm from the base of the heating element.
- The shielding plate was opened and at the same time, the timer (stopwatch) was started.

Upon reaching the end of the test duration, the timer was stopped and closed the shielding plate over the orifice. The sample and holder were then removed quickly from the cone heater test chamber, replaced by the dummy specimen board and opened the shielding plate again. The sample was re-weighed and after that the thin steel plate with five small openings was placed on the upper surface of the sample for calcination measurements. Before taking any measurements, the constant force probe was required to be set to zero by pressing the pin into a hard surface such as table. The constant force probe was then penetrated into the sample at these five specific locations as numbered previously in Figure 5.9. The depths of calcinations of the heat-treated sample were then recorded by reading the value off the digital vernier calliper. The next sample was then carried out in the similar procedure but with different temperature setting, exposure time

Experimental Program

and types of boards. The summary of mass loss and calcination depths for all the tests was presented in Appendix B.

The thermocouple data was recorded and stored by the computer system that had been set up and the same procedure was followed. However, this time each 19 mm Fyrelite plasterboard was left under the cone heater for two hours at a heat flux of 50 kW/m² and 65 kW/m².

When finished all experiments for the day, the cone temperature was reduced to 400°C and cooled at 400°C for five minutes. After the cooling, the cone temperature was further reduced to 200°C and waited for the cone to cool to 300°C before shutting down the cone power. The fan and main power of the cone calorimeter apparatus was then turned off.

Chapter 6 Analysis of Results

6.1 Analysis Procedures and Calculations

The raw data collected from the research was recorded and presented in Appendix B. This section outlines the procedures and calculations that are used for data analysis.

6.1.1 Mass Loss

The mass of each sample was determined prior to testing and after the burning of the sample so the total mass loss can be calculated. Each test with different types of boards, heat flux and exposure duration, the graphs are plotted to depict how the duration of exposure corresponds to the total mass lost from the samples.

6.1.2 Calcination Depth

The depth of calcination was measured using the constant force probe after heating the sample through the five circular openings of the thin plate. The measured calcination depths from each tested sample are averaged. Using the “radiant exposure area correlation” concept described by Nyman (2001), the fire severity which has units of kJ/m^2 can be calculated for each test by simply multiplying the corresponding heat flux (energy impinging upon the surface of the sample from the cone heater) and exposure duration i.e. $\text{kJ}/\text{m}^2 = \text{kJ}/\text{s m}^2 \times \text{s}$. Therefore, a correlation between the depth of calcination and fire severity can be plotted as shown in next section. Such a correlation can be used to identify the predicted calcination depth when exposed to Eurocode parametric fires. These parametric equations were given in Equation 4.1 – 4.10, Chapter 4. The radiant exposure area method is then applied to convert the time-temperature curve obtained from parametric fire to fire severity curve since the severity of a fire is expressed as the area under a plot of the emissive power of the compartment gases against time. This conversion is illustrated in Figure 6.1.

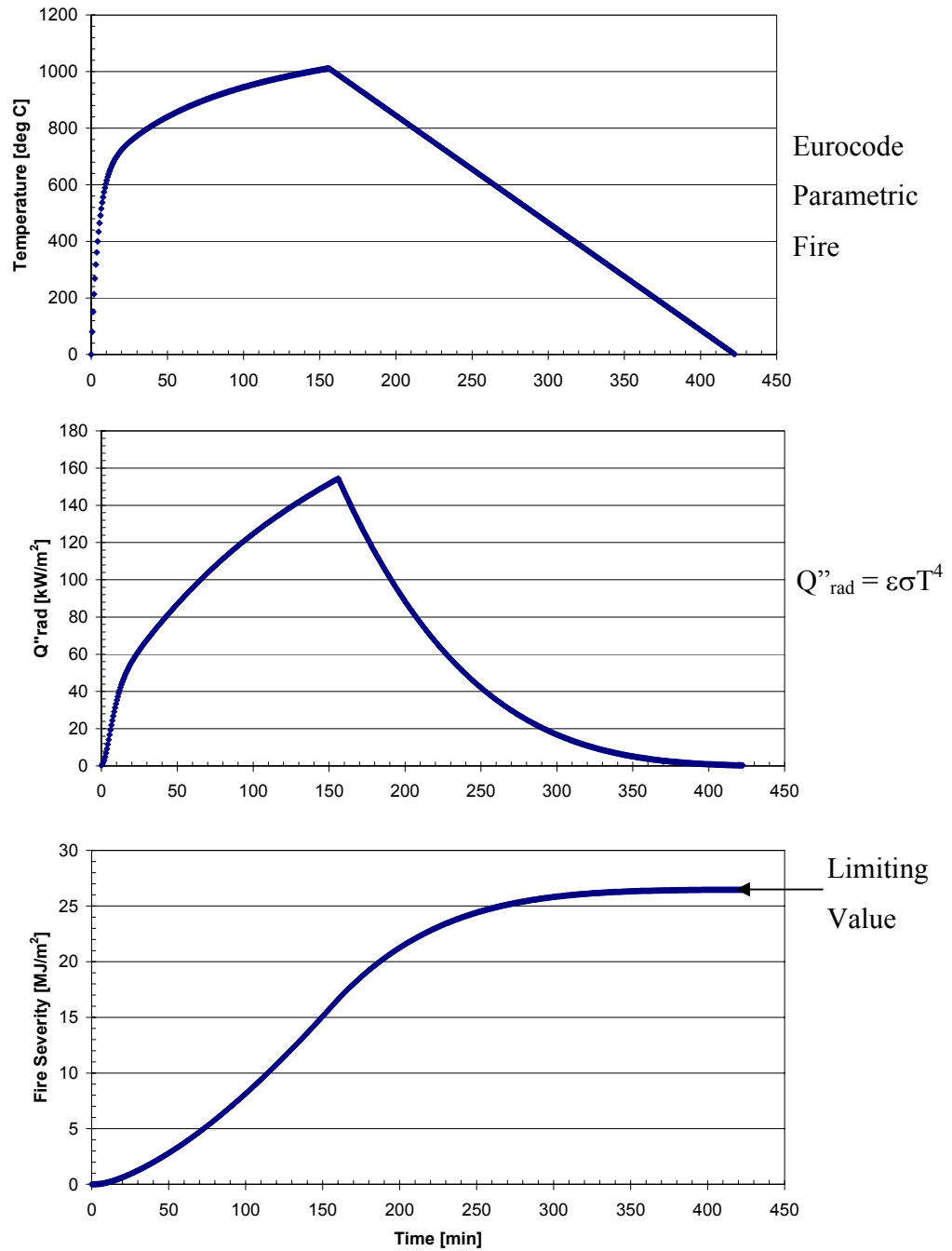


Figure 6.1 Radiant exposure area correlation

Since Eurocode parametric fires only allow a time-temperature relationship during the burning and decay periods, it ignores the pre-flashover i.e. fire growth stage. Therefore, it is necessary to verify the significance of the calcination depth during this pre-flashover period exposed to the total accumulated fire severity before the post-flashover stage. The verification method used is rather crude using the Thomas's flashover criterion and t-squared fires together with some assumptions.

Pre-flashover Stage:

Thomas's flashover criterion states the critical value of heat release, Q_{fo} [MW] for flashover to occur is given:

$$Q_{fo} = 0.0078 A_t + 0.378 A_v \sqrt{H_v} \quad (6.1)$$

Where A_t is the total internal surface of the room [m²]
 A_v is the area of the opening [m]
 H_v is the height of the opening [m]

A standard ISO compartment room size of 2.4 m (width) by 2.4 m (height) by 3.6 m (length) is assumed with gypsum plasterboard linings. The ventilation factor, F_v is given in Equation 4.8 and with this equation, Equation 6.1 can be rearranged in terms of A_t and F_v as follows:

$$Q_{fo} = 0.0078 A_t + 0.378 F_v A_t \quad (6.2)$$

The parabolic curve known as a t-squared fire is assumed to be the fire growth rate such that the heat release rate is proportional to the time squared, Equation 6.3. This equation can then be arranged to determine the time for flashover, t_{fo} [s] to occur by substituting Equation 6.2 into Equation 6.4 where the value of α is given in Table 6.1 for different fire growth rate.

$$Q = \alpha t^2 \quad (6.3)$$

$$t_{fo} = \sqrt{\frac{Q_{fo}}{\alpha}} \quad (6.4)$$

Table 6.1 Fire growth rates for t^2 fires

Fire Growth Rate	Fire Intensity Coefficient, α [MW/s ²]
Slow	0.00293
Medium	0.0117
Fast	0.0466
Ultrafast	0.1874

In a typical room, flashover occurs when the hot gas layer temperature is approximately 600°C i.e. $T_{fo} = 600^\circ\text{C}$. Therefore with this known flashover temperature and the time for flashover to occur, the next step is to assume the time-temperature relationship before flashover is parabolic i.e. temperature = constant \times time² or $T = \beta t^2$. This parabolic fitting from time at zero to the flashover occurrence point is illustrated in Figure 6.2. The severity of the fire during pre-flashover stage is then calculated using the radiant exposure area correlation. Thus the calcination depth during pre-flashover can be determined by substituting its fire severity into the correlation found experimentally between the depth of calcination and fire severity.

Post-flashover Stage:

From the time-fire severity relationship as shown in Figure 6.1, the fire severity increases with increasing exposure duration to a limiting value. This limiting fire severity value is used to predict the calcination depth for a complete burnout of a compartment using the “Power” correlation of calcination depth and fire severity determined from the experimental data.

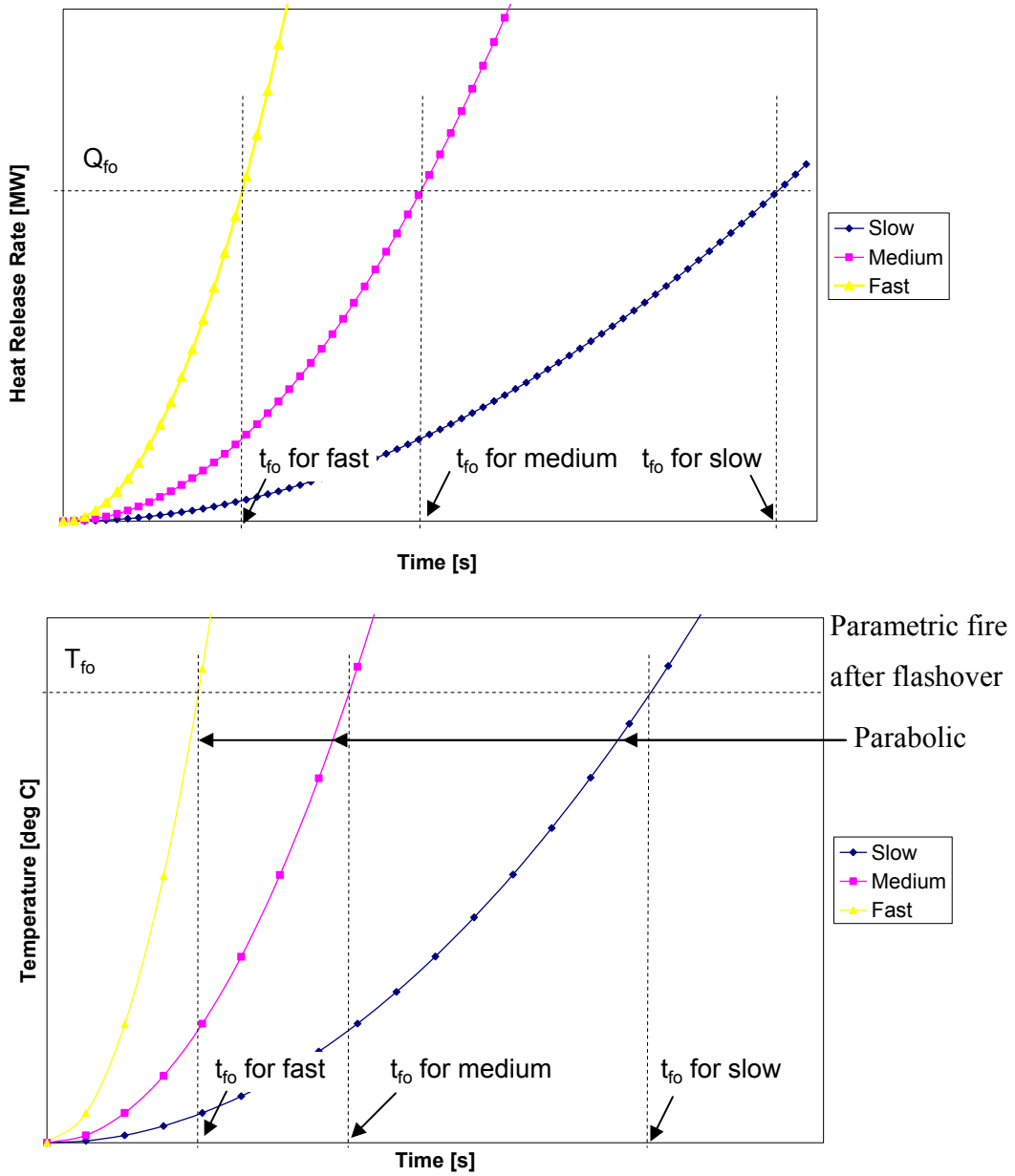


Figure 6.2 Determining the fire severity for pre-flashover period

6.1.3 Temperature profile

From the thermocouples data recorded by the computer, the time-temperature curves at different depth are plotted and presented in the next section.

6.2 Results

6.2.1 Mass Loss

Figure 6.3 depicts how the duration of exposure corresponds to the total mass loss from the 10 mm Fyrelime samples exposed to heat flux of 35 kW/m^2 , 50 kW/m^2 and 65 kW/m^2 . The mass loss curves for each heat flux were observed to increase with exposure duration to a limiting value and the higher heat fluxes resulted in greater amount of mass loss. This similar trend was also observed for other gypsum samples tested as shown in Appendix C.

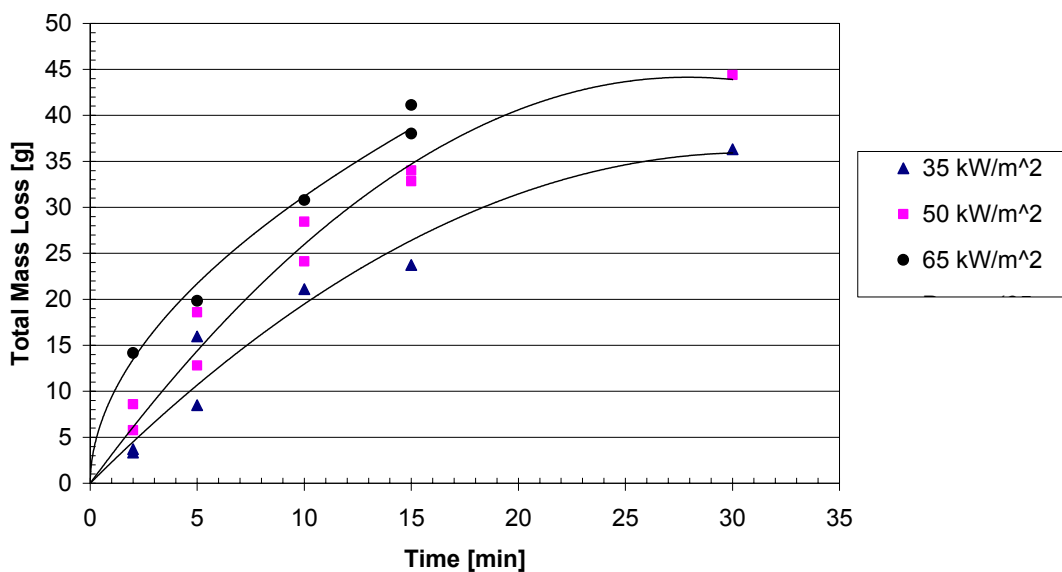


Figure 6.3 Influence of exposure duration on mass loss for 10 mm Fyrelime Board

Analysis of Results

The total mass of the samples during heating and cooling were recorded and plotted in Figure 6.4 below. The samples used were 10 mm Standard under fire exposure of 50 kW/m^2 . During the heating period (time up to 15 minutes), sample mass decreased as exposure duration increased. For cooling period, the sample was left on the mass balance and the sample mass was observed to increase slowly with time.

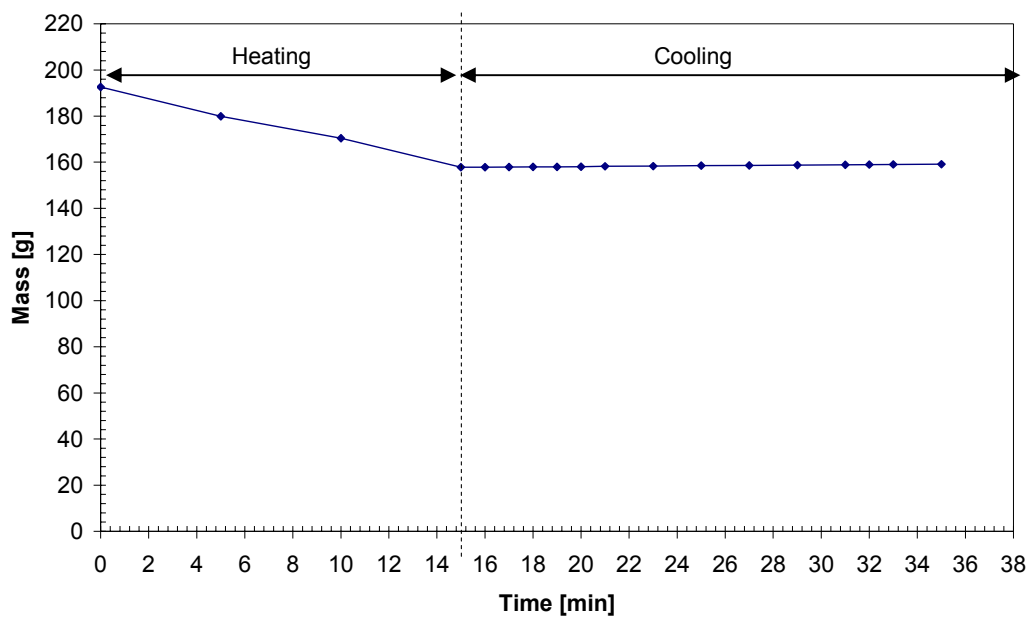


Figure 6.4 Mass loss during heating and cooling under 50 kW/m^2 exposure

6.2.2 Calcination Depth and Fire Severity Correlation

The calcination depth (determined by the constant force probe) for each type of gypsum plasterboard was plotted against the fire severity i.e. multiply the heat flux and exposure time, and shown in Figure 6.5 – 6.8. All these figures depicted the similar trend with the depth of calcination increased as the fire severity also increased but eventually came to limiting value. The “Power” relationship was found to be a best fit curve through these data. The power relationship

Analysis of Results

is the result of empirical curve fitting with no theoretical physical basis. These equations of correlations for each type of gypsum plasterboard are summarized in Table 6.2.

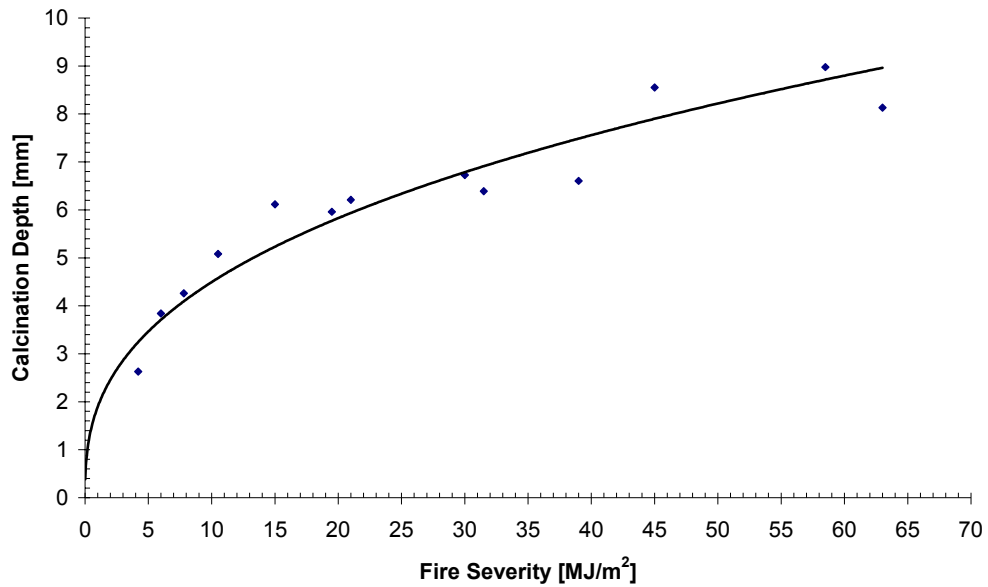


Figure 6.5 Correlation between calcination depth and fire severity for 10 mm Standard Board

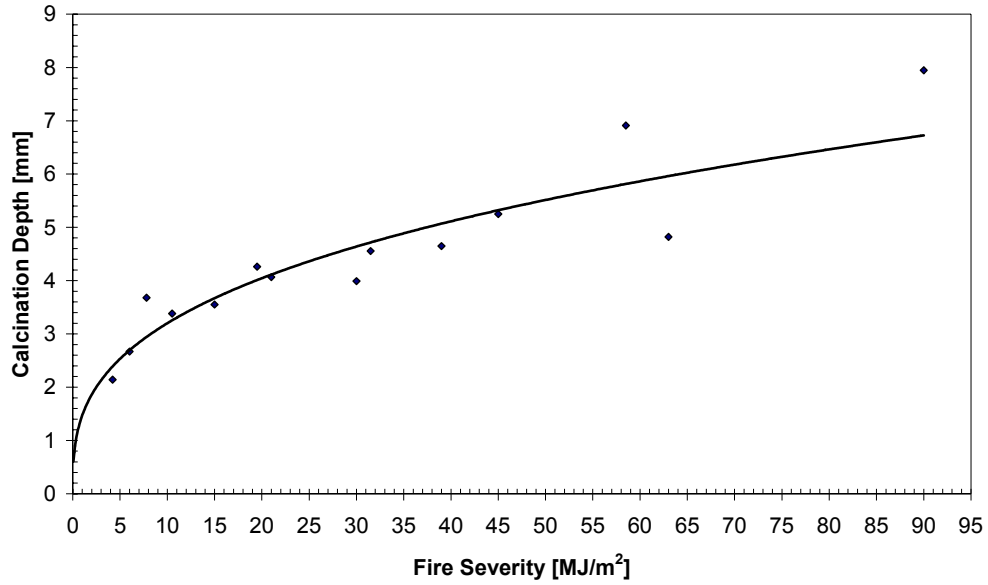


Figure 6.6 Correlation between calcination depth and fire severity for 10 mm Fyrelite Board

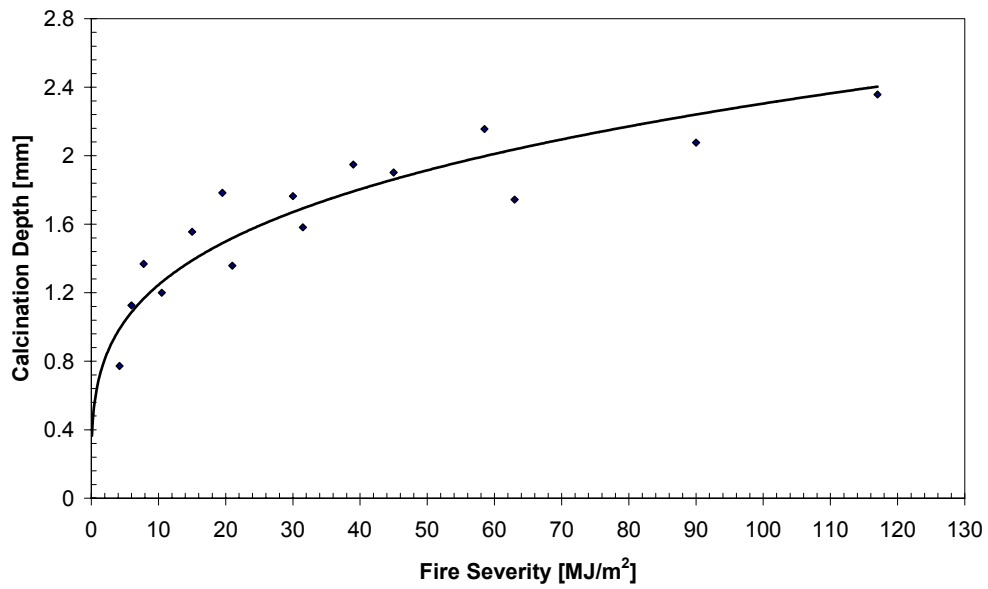


Figure 6.7 Correlation between calcination depth and fire severity for 10 mm Noiseline Board

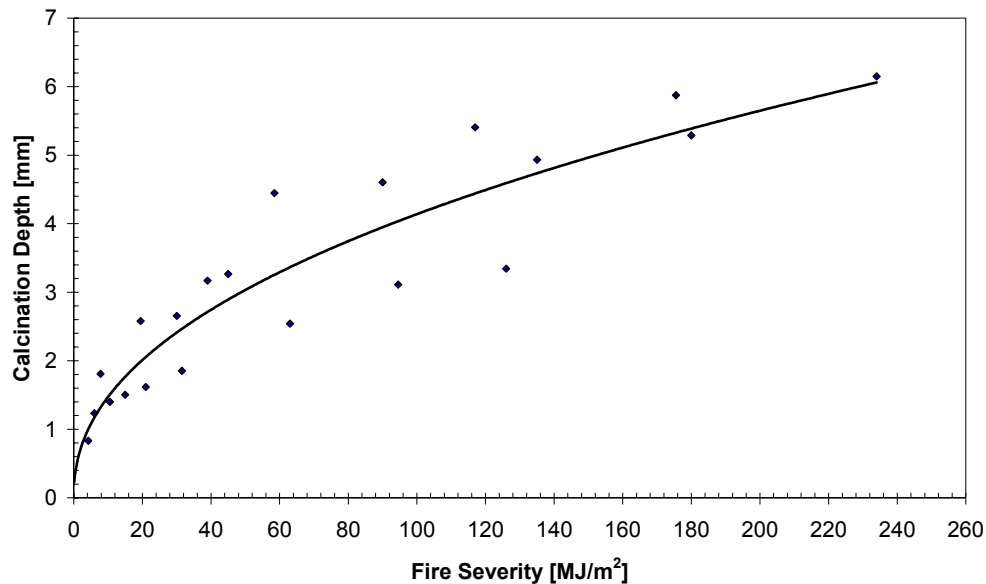


Figure 6.8 Correlation between calcination depth and fire severity for 19 mm Fyreline Board

Table 6.2 The relationship between the calcination depth and fire severity

Board Type	Correlation ($C = \text{Calcination Depth in mm} \ \& \ S = \text{Fire Severity in MJ/m}^2$)
10 mm Standard	$C = 1.90 \times S^{0.38}$
10 mm Fyreline	$C = 1.47 \times S^{0.35}$
10 mm Noiseline	$C = 0.67 \times S^{0.27}$
19 mm Fyreline	$C = 0.52 \times S^{0.45}$

6.2.3 Calcination Depth in Pre-flashover Stage

The calcination depth during the pre-flashover period was calculated and presented in the Table 6.3 – 6.6 for ventilation factor, F_v of 0.02, 0.04, 0.08 and 0.12. Although the values of calcination depth were different for different fire growth rate, types of boards and ventilation factors, they all shared similar characteristics. The calcination depth decreased when the fire growth rate changed from slow to fast. The calcination depths calculated for both 10 mm Standard and Fyreline boards

Analysis of Results

were almost identical and greater than the other two boards. 19 mm Fyrelite was found to have the lowest calcination depth among other boards.

Ventilation factor of 0.02:

Table 6.3 Determined calcination depth before flashover occurs for ventilation factor of 0.02

Fire Growth Rate	Calcination Depth [mm]			
	10 mm Standard	10 mm Fyrelite	10 mm Noiseline	19 mm Fyrelite
Slow	0.17	0.16	0.12	0.03
Medium	0.13	0.13	0.10	0.02
Fast	0.10	0.10	0.08	0.02

Ventilation factor of 0.04:

Table 6.4 Determined calcination depth before flashover occurs for ventilation factor of 0.04

Fire Growth Rate	Calcination Depth [mm]			
	10 mm Standard	10 mm Fyrelite	10 mm Noiseline	19 mm Fyrelite
Slow	0.18	0.17	0.12	0.03
Medium	0.14	0.14	0.10	0.02
Fast	0.11	0.11	0.09	0.02

Ventilation factor of 0.08:

Table 6.5 Determined calcination depth before flashover occurs for ventilation factor of 0.08

Fire Growth Rate	Calcination Depth [mm]			
	10 mm Standard	10 mm Fyrelite	10 mm Noiseline	19 mm Fyrelite
Slow	0.20	0.20	0.19	0.04
Medium	0.15	0.15	0.11	0.03
Fast	0.12	0.12	0.09	0.02

Analysis of Results

Ventilation factor of 0.12:

Table 6.6 Determined calcination depth before flashover occurs for ventilation factor of 0.12

Fire Growth Rate	Calcination Depth [mm]			
	10 mm Standard	10 mm Fyreline	10 mm Noiseline	19 mm Fyreline
Slow	0.21	0.20	0.14	0.04
Medium	0.16	0.16	0.12	0.03
Fast	0.13	0.13	0.10	0.02

6.2.4 Calcination Depth in Post-flashover Stage

Figure 6.9 – 6.12 showed the fire severity determined at different ventilation factors (0.02, 0.04, 0.08, and 0.12) and fuel loads (400, 800, and 1200 MJ/m²), which was derived by applying the radiant exposure area correlation to the parametric time-temperature relationship. All figures depicted the convergence of fire severity to a limiting value and the higher fuel load resulted in more severe of the fire.

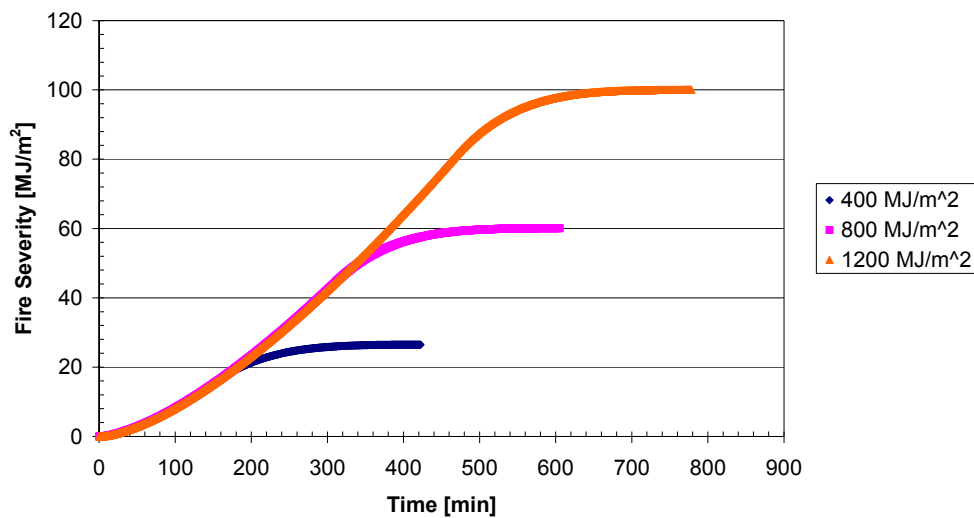


Figure 6.9 Fire severity curves for ventilation factor of 0.02 and different fuel loads

Analysis of Results

For a ventilation factor of 0.02, Figure 6.9 gave the limiting values of fire severity as 26, 60 and 100 MJ/m² for fuel loads of 400, 800 and 1200 MJ/m² respectively. These limiting values changed when the ventilation factor of 0.02 was increased to 0.04 as shown in Figure 6.10. The corresponding limiting values with ventilation factor of 0.04 were 17, 46 and 73 MJ/m² for fuel loads of 400, 800 and 1200 MJ/m² respectively.

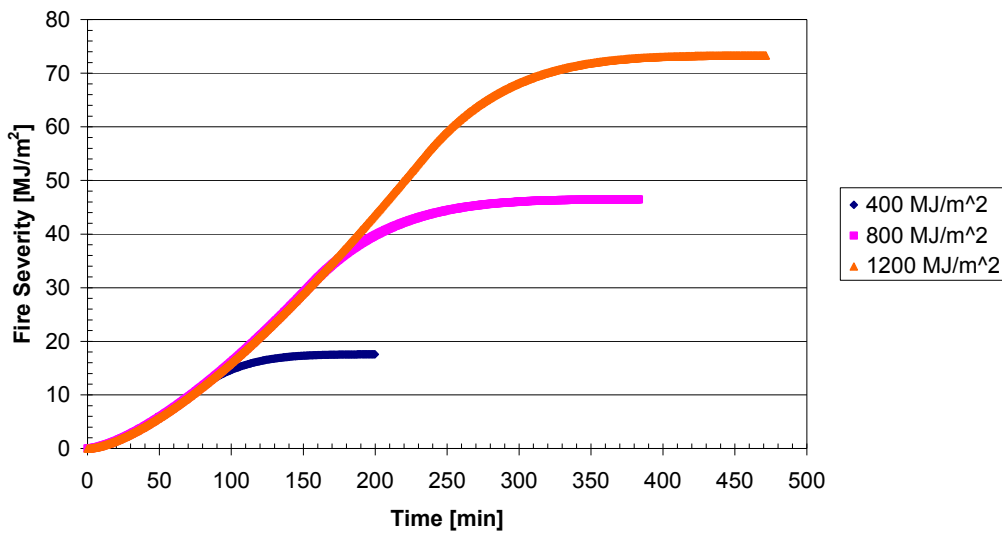


Figure 6.10 Fire severity curves for ventilation factor of 0.04 and different fuel loads

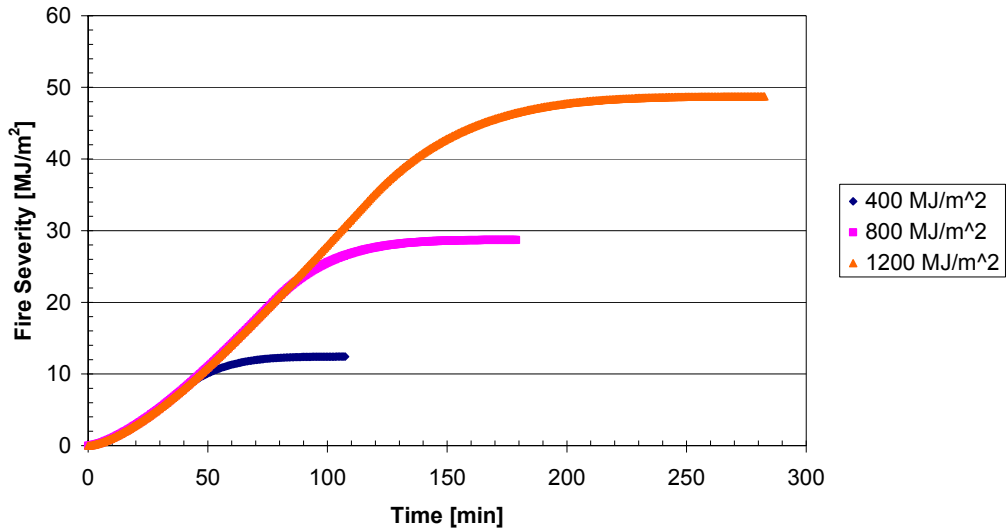


Figure 6.11 Fire severity curves for ventilation factor of 0.08 and different fuel loads

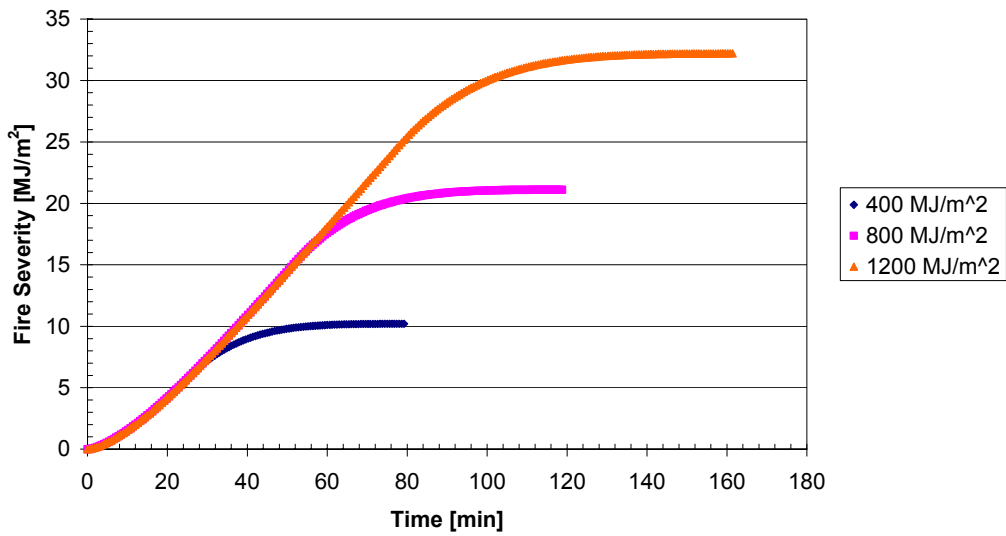


Figure 6.12 Fire severity curves for ventilation factor of 0.12 and different fuel loads

Analysis of Results

For a ventilation factor of 0.08 as shown in Figure 6.11, the limiting values of fire severity were determined to be 12, 28 and 48 MJ/m² correspond to fuel loads of 400, 800 and 1200 MJ/m². The limiting values with ventilation factor of 0.12 were found in Figure 6.12, with values of 10, 21 and 32 MJ/m² for fuel loads of 400, 800 and 1200 MJ/m² respectively.

All the limiting values of fire severity determined for different ventilation factors and fuel loads were used to determine the predicted calcination depth for complete burnout of a compartment. For a compartment room with certain ventilation opening size, the amount of fuel load available for burning, gypsum plasterboards as lining material and using Eurocode parametric fires, the variation of calcination depth with fire duration can be determined. This time-calcination depth relationship exhibited similar characteristics as found in time-fire severity curves i.e. converging to a limiting value as exposure time increases. Most residential houses use 10 mm standard gypsum plasterboard as linings and the common ventilation factor are 0.04 and 0.08. These time-calcination depth curves were plotted in Figure 6.13 – 6.14 below.

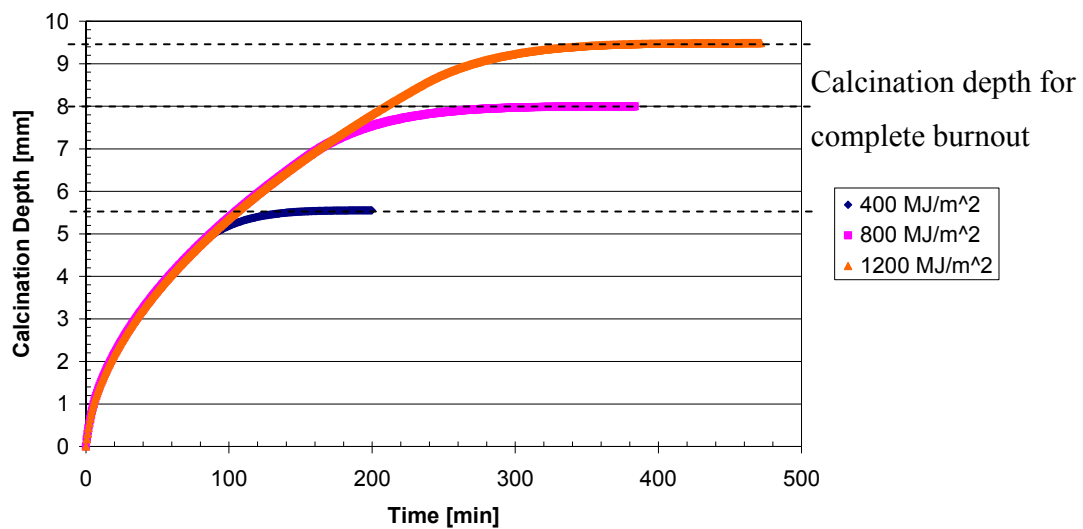


Figure 6.13 Calcination depth curves for 10 mm Standard board with ventilation factor of 0.04

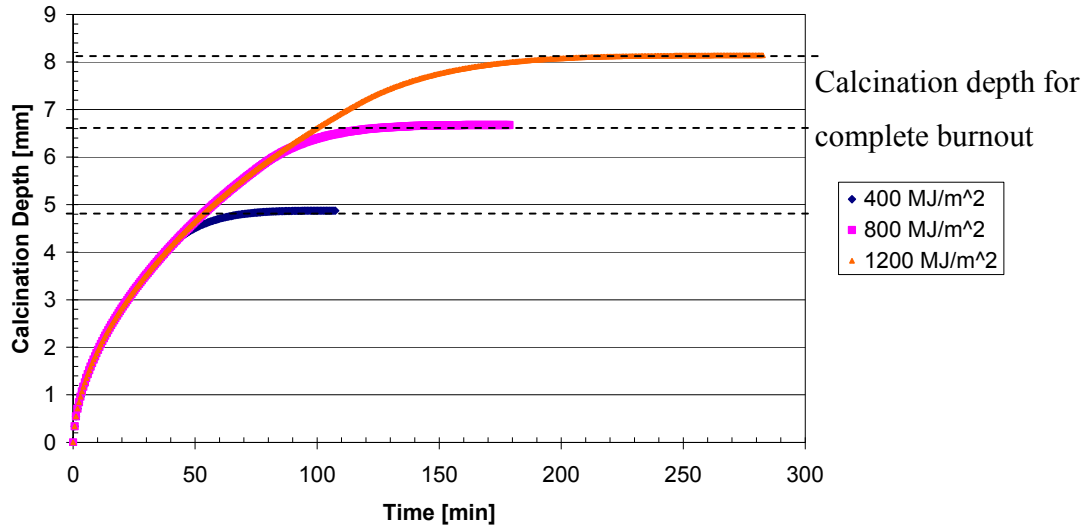


Figure 6.14 Calcination depth curves for 10 mm Standard board with ventilation factor of 0.08

Table 6.7 – 6.10 summarized all the predicted calcination depth for complete burnout for each type of gypsum plasterboard with different ventilation factors and fuel loads. The depth of calcination was found to increase with fuel load and decrease with ventilation factor. This trend was observed for each different type of gypsum plasterboard.

Table 6.7 Predicted calcination depth of 10 mm Standard board for complete room burnout

Fuel Load, e_t [MJ/m ² floor area]	Ventilation factor, F_v			
	0.02	0.04	0.08	0.12
400	6.5	5.6	4.9	4.5
800	8.8	8.0	6.7	5.9
1200	10	9.5	8.1	7.0

Table 6.8 Predicted calcination depth of 10 mm Fyrelite board for complete room burnout

Analysis of Results

Fuel Load, e_t [MJ/m ² floor area]	Ventilation factor, F_v			
	0.02	0.04	0.08	0.12
400	4.4	3.9	3.4	3.2
800	5.9	5.4	4.6	4.1
1200	7.0	6.3	5.5	4.8

Table 6.9 Predicted calcination depth of 10 mm Noiseline board for complete room burnout

Fuel Load, e_t [MJ/m ² floor area]	Ventilation factor, F_v			
	0.02	0.04	0.08	0.12
400	1.6	1.4	1.3	1.3
800	2.0	1.9	1.7	1.5
1200	2.3	2.1	1.9	1.7

Table 6.10 Predicted calcination depth of 19 mm Fyreline board for complete room burnout

Fuel Load, e_t [MJ/m ² floor area]	Ventilation factor, F_v			
	0.02	0.04	0.08	0.12
400	2.3	1.9	1.6	1.5
800	3.3	2.9	2.4	2.1
1200	4.1	3.6	3.0	2.5

6.2.5 Temperature profile

Figure 6.15 and 6.16 illustrated how the node temperatures vary with time over the 19 mm thick Fyreline board under fire exposure of 50 and 65 kW/m² respectively. The node location where the thermocouples were inserted into the thick sample was explained in Figure 5.10, Chapter 5.

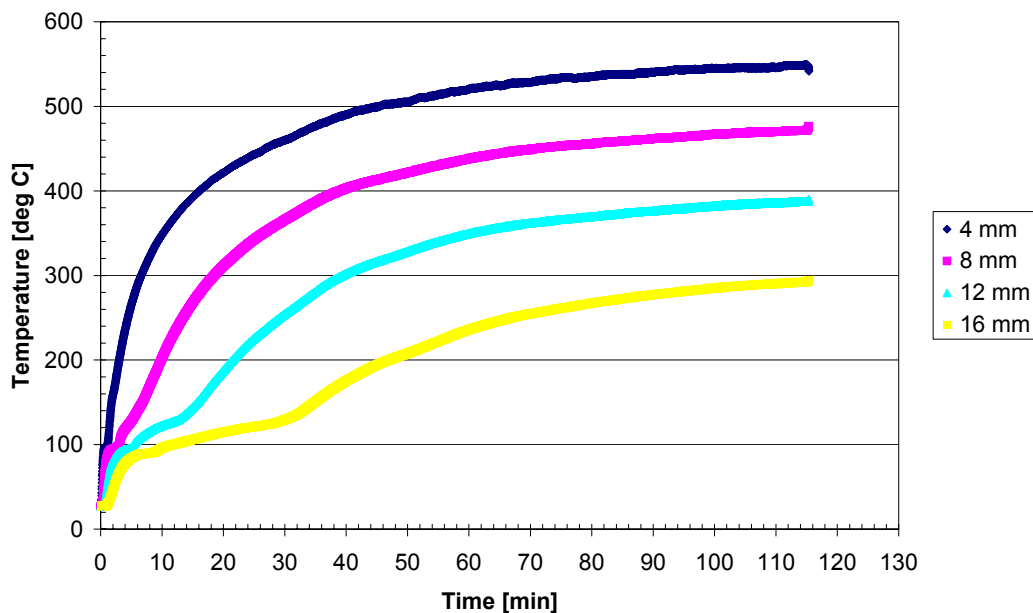


Figure 6.15 Thermocouples data collected at different depth below the upper surface of the sample under 50 kW/m² fire exposure

The temperatures at these four different nodes shown in Figure 6.15; 4 mm, 8 mm, 12 mm and 16 mm below the upper surface, were observed to have similar trends. The temperatures exhibited a sudden increase especially in the first few minutes but as time went along, the temperatures were observed to converge to limiting values i.e. at time around 2 hours. The highest temperature

Analysis of Results

profile was the node with thermocouple implemented at the 4 mm below the sample surface, followed by 8, 12, and 16 mm below the surface. The temperatures were converged to 550, 470, 390 and 300°C correspondingly for 4, 8, 12 and 16 mm below the surface.

For fire exposure of 65 kW/m², Figure 6.16 depicted the same characteristics for the sample being exposed to 50 kW/m² but with higher temperature values were observed, approximately 50°C higher than previous case. The limiting temperature values for thermocouples at 4, 8, 12 and 16 mm below the surface were determined to be 610, 530, 420 and 340°C respectively.

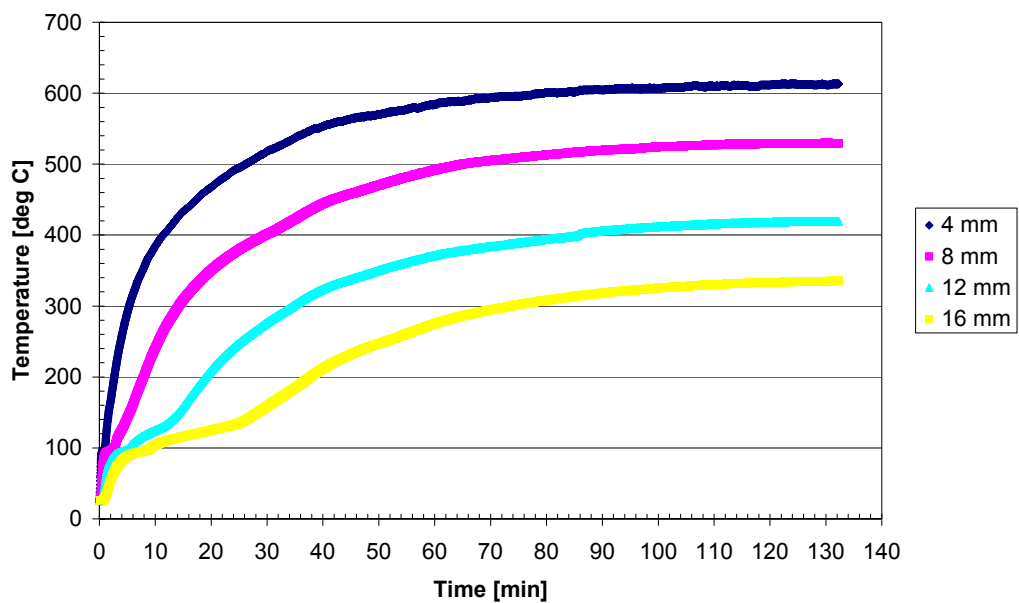


Figure 6.16 Thermocouples data collected at different depth below the upper surface of the sample under 65 kW/m² fire exposure

Chapter 7 Discussion

7.1 Mass Loss

Greater amounts of mass loss from the gypsum samples were results from longer exposure durations and higher heat fluxes. This was expected as more water being driven off the samples at the higher heat fluxes and heated for longer time period. The mass lost from the samples increased rapidly within the first few minutes of fire exposure and leveled off to a final value until all the water being dehydrated. This mass loss relationship with time was also found from the work done by McGraw (1998). At lower heat fluxes for short exposure durations, more mass lost from the sample was came from the paper as the dehydration reaction did not occur until the sample reached the temperature of approximately 120°C. Large amount of heat energy resulted in higher heat fluxes and longer durations was required so that the water would have sufficient energy to overcome the strong crystalline bonding with calcium sulphate and evaporated.

Another aspect regarding about time-mass loss relationship was that the total mass of the sample was observed to increase slowly when it was taken out from the cone heater and cooling off. This indicated the heat-treated sample was actually absorbed the water back from the surroundings. However, this increase of mass was considered as insignificant when compared to the enormous mass lost during the heating. The sample mass was determined to increase by a rate of about 0.065 g/min giving only a mass increase of 4 grams in one hour. Further investigation was recommended to carry out to determine the significance of this cooling period on the depth of calcination.

7.2 Correlation between Calcination Depth and Fire Severity

Heat fluxes and exposure durations that the samples being exposed were multiplied together to obtain the severity of the fire, which was the total impinging energy upon the surface of the samples. The calcination depth obtained from the experimental testing was then correlated to

their corresponding fire severity. A power law correlation was observed to have the best fit through the data for all four gypsum plasterboards tested. This correlation would be useful in predicting the depth of calcination of that particular type of gypsum plasterboard used as the lining materials of a compartment given that the fire severity is known.

Among all four graphs (four different gypsum plasterboards) shown in Figure 6.5 – 6.8, Chapter 6, the data points for 10 mm Standard board was found least scattered enabling a smooth curve to fit well through the points. Possible explanation for this might be due to the difference in properties for standard gypsum plasterboards to Fyrelite, Noiseline and etc. Standard plasterboard consists of pure gypsum plaster with water whereas other better fire resistant boards such as Fyrelite contain glass fibres, vermiculites, starch or other additives. These properties difference would affect the demarcation between the calcined and non-calcined gypsum. These additives would also serve as obstacles for the constant force probe in assessing the depth of calcination.

Therefore, care must be taken when applying the calcination depth and fire severity correlation to gypsum plasterboards other than standard board. According to the information given by Winstone Wallboard Ltd, the 10 mm standard board was found the most commonly used lining material in New Zealand especially in residential buildings, in which approximately 65% of all gypsum plasterboards production was came from manufacturing standard board each year. However, in order to make the power correlation more reliable to use, particularly for other boards such as 10 mm Fyrelite, 10 mm Noiseline, and 19 mm Fyrelite etc, the repeatability test shall be carried out i.e. 3 – 5 tests for each fire exposure and duration.

7.3 Effect of Pre-flashover Stage on Calcination Depth

Since emphasis was often given to post-flashover fires which provide the greatest threat to structural members and other fire resistant elements, the effect of pre-flashover fires on the amount of gypsum calcining was expected to be insignificant. A crude calculation method (as

explained in Chapter 6) had been carried out to estimate the severity of pre-flashover fire using the radiant exposure area correlation. The calcination depth during the pre-flashover period was then calculated by substituting the pre-flashover fire severity into the power correlation obtained from the experimental data.

However, the biggest unknown in the calculation method was the time-temperature relationship before flashover as this was required to determine the fire severity. This time-temperature relationship was then assumed to be fitted by a parabolic curve i.e. $T = \beta t^2$. The other major assumption made was to characterize all the burning objects in a room by a t-squared design fire and using Thomas's flashover criterion to calculate the time to flashover. Thomas's flashover criterion itself was a very approximate correlation, depending on the size, shape and lining materials of the room and even the location of the fire within the room.

From the calculation results shown, the contribution of the severity of a pre-flashover fire to calcine the gypsum plasterboard was trivial that it could be ignored. The highest calcination depth during the pre-flashover was calculated to be about 0.2 mm, which was insignificant compared to the experimental measurements. Slower the fire growth rate and larger the ventilation factor resulted in greater amount of calcination. The fire took longer time to flashover with slower fire growth making the fire more severe as the area under the time-temperature (also $Q'' = \epsilon \sigma T^4$ versus time curve) was greater compared to fast growth rate fires. On the other hand the fires tend to burn hotter due to the higher ventilation factor thus providing higher fire severity.

7.4 Effect of Post-flashover Stage on Calcination Depth

Most calcination depth of gypsum plasterboard was proved to take place after the flashover i.e. when all the objects in the room were fully involved in fire. In real fire situation often the fire is unknown but for a room in which the lining materials is gypsum plasterboard, the depth of calcination on the fire damaged gypsum plasterboard can be measured using the constant force

probe hence calculate the fire severity that the gypsum plasterboard being exposed by substituting the measured calcination depth into the power correlation. However, this calculated fire severity did not provide any useful information since the correlation obtained was based on the cone heater experimental data and so the fire severity did not represent the actual fires.

A more realistic design fire, Eurocode parametric fire, was used to represent the actual fire inside a compartment room and by applying the radiant exposure area correlation, the fire severity to cause complete burnout of a compartment was obtained. This information was then used to predict the calcination depth of particular type of gypsum plasterboard for complete burnout as shown in Table 6.7 – 6.10. Often the fuel load can be estimated according to the objects present in the room and the size of ventilation opening can be measured, the depth of calcination for complete room burnout can therefore be predicted. Higher fuel load for small ventilation factor resulted in greatest amount of calcination due to the higher fire severity as there were more fuels to burn and the fire would last longer.

The predicted calcination depth for complete burnout (or the calcination depth data collected) had proved that Fyreline (fire performance board) had less calcination than Standard due to the enhanced fire properties such as fibre glass, vermiculite and other additives. Among the four gypsum plasterboards tested, 19 mm Fyreline had the highest density of 888 kg/m^3 followed by 10 mm Noiseline (848 kg/m^3), 10 mm Fyreline (698 kg/m^3) and 10 mm Standard (631 kg/m^3). In general from the results shown, higher density boards acquired less calcination, in particular for the Standard and Fyreline boards. In contrast, 10 mm Noiseline with density of 848 kg/m^3 which was lower than 19 mm Fyreline was surprisingly to have less calcination. Consequently, this indicated that the presence of other factors such as additives type, quantity or arrangement within the board itself would have the effect on gypsum calcination. This could lead to another research area of interest.

Above all, another useful finding was established by converting the fire severity of a parametric fire into time-calcination depth relationship. This was performed by substituting the fire severity value into the power correlation found experimentally. This illustration was shown in Figure 7.1 below. This time-calcination depth relationship can be useful to predict the time when the fire has been put out. After the fire incident, the calcination depth can be assessed and according to the relationship shown in Figure 7.1, the time of fire extinguishment can be predicted. For example, with 4 mm calcination depth measured on the fire damaged board this predicted the fire has been burning for approximately 38 minutes. This relationship can be easily produced for each board type with different fuel loads and ventilation factors.

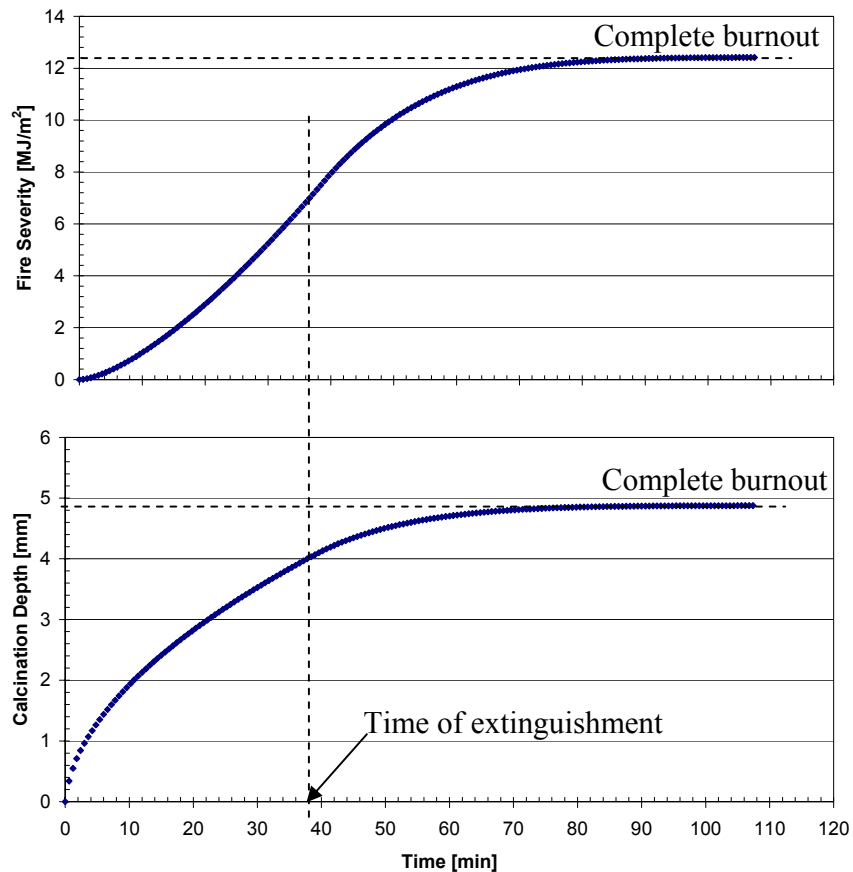


Figure 7.1 Illustration in determining the time of fire extinguishment

All the information gained from the research especially the predicted calcination depth for complete burnout and the time of fire extinguishment, emphasis is given that these findings were based on two approximations. First, the power correlation between the calcination depth and fire severity based on the cone heater testing and furthermore the Eurocode parametric fires as the fires burning inside a compartment room. Further validation is required to determine the reliability of these predictions by carrying out some full scale compartment tests.

The calcination depth measurements taken by using constant force probe developed can also be used to investigate the fire severity on local effects inside the compartment. More calcination measured at that particular location would simply mean that it has been exposed to a greater fire severity or more intense fire. This enables fire investigators to predict the place where the fire first started i.e. fire origin. The relative changes of calcination depth measured locally at different locations would show some thoughts how the fire scenarios have been developed inside the compartment room

One of the research's objectives to apply the depth of calcination of gypsum plasterboard in real fires as an indicator of fire severity was not accomplished as no real fire data was collected. The above calculations are a conceptual demonstration of the methodology, because no compartment fire tests were conducted. For this purpose, compartment testing should be carried out and using the same approach in deriving the correlation from cone heater testing, the calcination depth as an indicator of fire severity in real fires can be determined.

7.5 Temperature Profile

With thermocouples inserted at different depths below the upper surface of the gypsum plasterboard, of course, the temperature profile at the depth nearest to the exposure surface i.e. 4 mm below the surface would result in a higher temperature value compared to other nodes throughout the sample. The higher heat flux also resulted in a steeper temperature rise at the nodes.

Interestingly the temperature data showed a horizontal line at the temperature of around 100°C, which is the boiling point of water. This particular section of the graph was enlarged as shown in Figure 7.2. This proved the occurrence of dehydration of water i.e. calcination as written in literature, the temperature between 100°C and 120°C. The temperature would remain constant until the dehydration reaction was completed. The dehydration reaction was observed to complete faster with nodes closer to the upper surface due to the steeper temperature rise and hotter temperature.

Although in the mean time no particular application was obtained, this thermocouples data still provided an understanding of how temperatures vary with time inside the board and could be useful in numerical analysis or computer modelling in predicting heat transfer throughout the board.

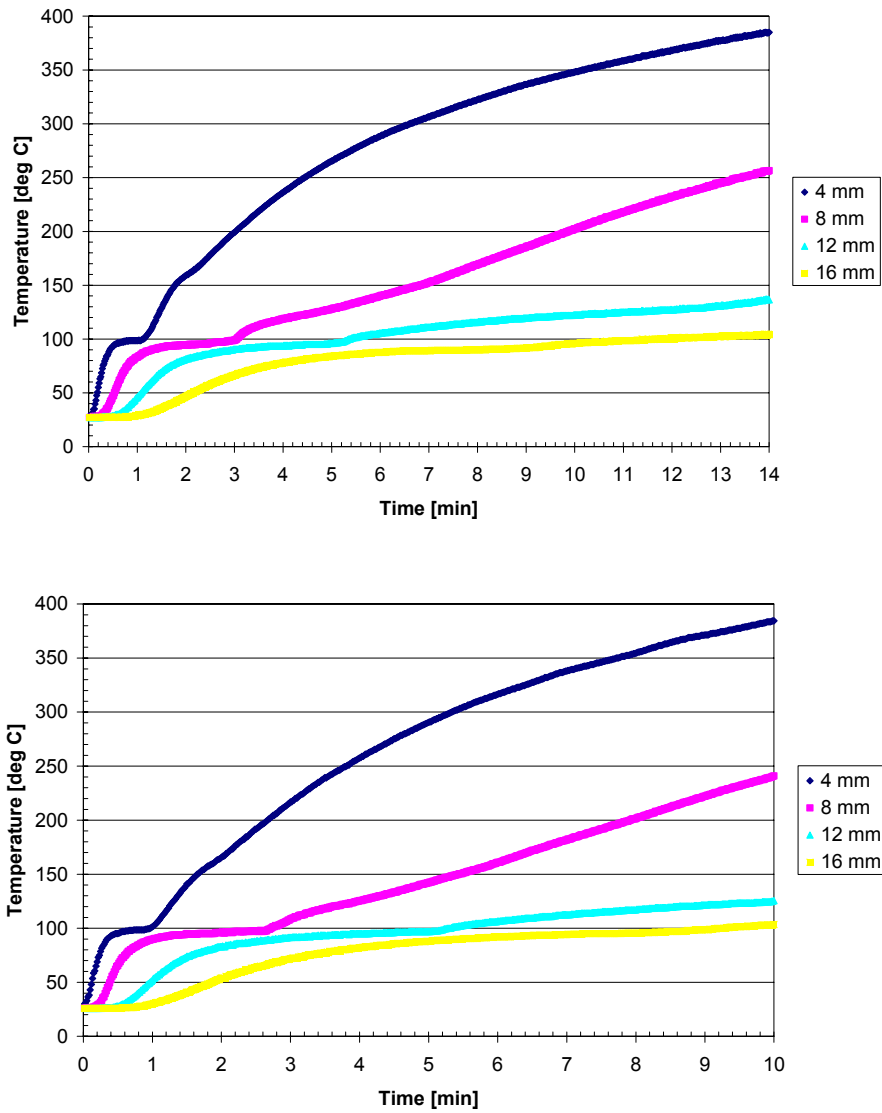


Figure 7.2 Horizontal lines showing water dehydration; Top (50 kW/m²) and Bottom (65 kW/m²)

Chapter 8 Conclusions

8.1 Conclusions

The following are conclusions that have been found from the research:

- A literature review was performed to identify existing tools and techniques used to measure the depth of calcination of gypsum plasterboard, in particular, the “probe survey” and “visual cross-section” methods. Due to the drawbacks of these methods in practical fire investigation, a new measuring tool called the “constant force probe” was developed and was found to have good agreement to the calcination depth determined by the “hand scraping” method.
- The constant force probe was used to quantify the depth of calcination in a large number of cone calorimeter tests conducted on various types of gypsum plaster board.
- Generally, deeper formation of the calcination plane within a sample thickness was correlated with high heat fluxes and greater lengths of exposure. The calcination depth was found to have an empirical power correlation with the fire severity (units of kJ/m^2).
- Higher heat fluxes and longer exposure durations result in greater amounts of mass loss. Interestingly, the mass of the sample increased slowly after being tested as a small amount of water was absorbed back into the specimen during the cooling period.
- The first dehydration reaction (calcination) within the sample was shown to occur at the water boiling point of 100°C as shown from the thermocouples data collected.

Conclusions

- Considering the total radiant heat exposure during a post-flashover fire, a method was developed for predicting the expected calcination depth during exposure to Eurocode parametric fires or other realistic fire exposures.
- The calcination depth correlation derived from this study could be used with the constant force probe in a post-fire investigation, to estimate the time when the fire had been put out or how long the gypsum plasterboard had been exposed to fire.
- More calcination at one local position inside the burnout compartment would produce some evidence as to the location of the fire origin and, according to the relative calcination changes, how the spread of fire might be identified.
- The calculated effect of pre-flashover fires on the depth of calcination was found to be insignificant and was hence ignored in the analysis because most calcination takes place in the post-flashover stage, not considering local effects near the fire origin.
- In this study, it was not possible to verify the depth of calcination of gypsum plasterboard in real fires as an indicator of fire severity because no full scale compartment testing was performed.

8.2 Recommendations

The following are recommendations for further development and investigation in the area of calcination depth of gypsum plasterboard:

- Each test carried under the cone heater should be repeated, at least 3 – 5 times, in order to check the repeatability of testing and gain more confidence with the correlation determined between the calcination depths and fire severity, hence improving the reliability of using the analysis to determine the time of fire extinguishment and the predicted calcination depth for complete burnout.
- In order to use the calcination depth in real fires as an indicator of the severity of fire, full scale compartment tests should be conducted so the calcination depth measurements using the constant force probe can be obtained from real fires. Also from the full scale compartment tests, the predictions for the time when the fire has been put out and the calcination depth for complete burnout found from the experimental data can be validated.
- Different types of gypsum plasterboards having distinct material properties such as the board density, types of additives and their composition, seemed to have a significant effect on the calcination depth, so this is recommended for further investigation.

Chapter 9 References

(Alfawakhiri et al 1999), F Alfawakhiri, M A Sultan, D H MacKinnon, *Fire Resistance of Loadbearing Steel-Stud Walls Protected with Gypsum Board: A Review*, Fire Technology, Vol. 35(4), 308-335, 1999.

(Benichou et al 2003), Nouredine Benichou, Mohamed A Sultan, Venkatesh R Kodur, *Fire Resistance Performance of Lightweight Framed Wall Assemblies: Effects of Various Parameters, Key Design Considerations and Numerical Modeling*”, Conference Papers, Fire and Materials 2003, Interscience Communications, London, UK, 2003.

(BS 476), British Standard BS 476, *Fire Tests on Building Materials and Structures, Part 13: Method of measuring the ignitability of products subjected to thermal irradiance*, FRS Division, BRE, 1987.

(Buchanan 2001a), A H Buchanan, *Structural Design for Fire Safety*, John Wiley & Sons, HK, 2001.

(Buchanan 2001b), A H Buchanan, *Fire Engineering Design Guide*, Centre for Advanced Engineering, Christchurch, New Zealand, 2001.

(Buchanan and Gerlich 1997), A H Buchanan, J T Gerlich, *Fire Performance of Gypsum Plasterboard*, Proceedings, 1997 IPENZ Conference, Wellington.

(Carlson 1978), H Carlson, *Spring Designer's Handbook*, Marcel Dekker, Inc., New York, 1978.

References

(Carlson 1980), H Carlson, *Springs: Troubleshooting and Failure Analysis*, Marcel Dekker, Inc., New York, 1980.

(Clifton 1973), J R Clifton, *Some Aspects of the Setting and Hardening of Gypsum Plaster*, BBS Technical Note 755, National Bureau of Standards, Washington, 1973.

(Cooper 1997), L Y Cooper, *The Thermal Response of Gypsum-Panel / Steel-Stud Wall Systems Exposed to Fire Environments – A Simulation for Use in Zone-Type Fire Models*, NISTIR 6027, Building and Fire Research Laboratory, National Institute of Standards and Technology, Gaithersburg, Maryland, June 1997.

(Gerlich 1995), Gerlich J T, *Design of Loadbearing Light Steel Frame Walls for Fire Resistance*, Fire Engineering Research Report 95/3, University of Canterbury, Christchurch, New Zealand, 1995.

(Goncalves et al 1996), T Goncalves, P Clancy, W Poynter, *Mechanical Properties of Fire Rated Gypsum Board*, Victoria University of Technology, Australia, 1996.

(Hannant 1978), D J Hannant, *Fibre cements and fibre concretes*, John Wiley & Sons, New York, 1978.

(Jones 2001), B H Jones, *Performance of Gypsum Plasterboard Assemblies Exposed to Real Building Fires*, Fire Engineering Research Report 01/4, University of Canterbury, Christchurch, New Zealand, 2001.

(Karlsson and Quintiere 2000), B Karlsson, J G Quintiere, *Enclosure Fire Dynamics*, CRC Press LLC, 2000.

References

(Kennedy et al 2003), Patrick M Kennedy, Kathryn C Kennedy, Ronald L Hopkins, *Depth of Calcination Measurement in Fire Origin Analysis*, Conference Papers, Fire and Materials 2003, Interscience Communications, London, UK, 2003.

(Kirk 2002), John D DeHaan, *Kirk's Fire Investigation*, 5th Edn, Prentice-Hall, New Jersey, 2002.

(Lawson 1977), J R Lawson, *An Evaluation of Fire Properties of Generic Gypsum Board Products*, NBSIR 77-1265, National Bureau of Standards, 1977.

(McGraw 1998), J R McGraw, *Flammability and Dehydration of Painted Gypsum Wallboard Exposed to Fire Heat Fluxes*, University of Maryland, 1998.

(McGraw and Mowrer 1999), J R McGraw, F W Mowrer, *Flammability of Painted Gypsum Wallboard Subjected to Fire Heat Fluxes*, Interflam '99, Interscience Communications Ltd, London, 1999.

(Mehaffey et al 1994), J R Mehaffey, P Cuerrier, G Carisse, *A Model for Predicting Heat Transfer through Gypsum-Board/Wood-Stud Walls Exposed to Fire*, Fire and Materials, Vol. 18, 297-305, 1994.

(Mowrer 2001), F W Mowrer, *Calcination of Gypsum Wallboard in Fire*, NFPA World Fire Safety Congress, Anaheim, California, May 14, 2001.

(Nyman 2001), J Nyman, *Equivalent Fire Resistance Ratings of Construction Elements Exposed to Realistic Fires*, Fire Engineering Research Report 01/13, University of Canterbury, Christchurch, New Zealand, 2001.

References

- (Olsson 1998), Per Ake Olsson, *Bench-scale Testing of Light Timber Frame Walls*, Fire Engineering Research Report, University of Canterbury, Christchurch, New Zealand, 1998.
- (Posey and Posey 1983), James E Posey, Eleanor P Posey, *Using Calcination of Gypsum Wallboard to Reveal Burn Patterns*, The Fire and Arson Investigator, IAAI, St. Louis, MO, 1983.
- (Richardson 2001), L R Richardson, *Thoughts and Observations on Fire-endurance Tests of Wood-frame Assemblies Protected by Gypsum Board*, Fire and Materials, Vol. 25, 223-239, 2001.
- (Ryan 1962), J V Ryan, *Study of gypsum plasters exposed to fire*, Journal of Research of the National Bureau of Standards, Vol. 66C, No. 4, 373-387, 1962.
- (Schroeder and Williamson 2000), R A Schroeder, R B Williamson, *Post-fire Analysis of Construction Materials – Gypsum Wallboard*, Fire and Materials, John Wiley & sons, Ltd., 2000.
- (Stanish 1994), A J Stanish, *Mechanical Properties of Gypsum Plasterboard*, University of Canterbury, 1994.
- (Sultan 1996), M A Sultan, *A model for predicting heat transfer through non-insulated unloaded steel-stud gypsum board wall assemblies exposed to fire*, Fire Technology, Vol. 32, No. 3, 239-259, 1996.
- (Sultan 1998), M A Sultan, *Fire Resistance of Floor Assemblies in Multi-Family Dwellings*, Institute for Research in Construction (IRC), NRC-CNRC, Ottawa, 1998.

References

(Sultan and Lougheed 1994), M A Sultan, G D Lougheed, *The Effects of Insulation on Fire Resistance of Small-scale Gypsum Plasterboard Assemblies*, Proc 3rd International Fire and Material Conference, Washington DC, USA, 1994.

(Sultan and Lougheed 1997), M A Sultan, G D Lougheed, *Fire Resistance of Gypsum Board Wall Assemblies*, Institute for Research in Construction (IRC), NRC-CNRC, Ottawa, 1997.

(Takeda and Mehaffey 1998), Takeda H and Mehaffey J R, *Wall2D: A Model for Predicting Heat Transfer through Wood-Stud Walls Exposed to Fire*, Fire and Materials, Vol. 22, 133 – 140, 1998.

(Thomas 2002), G Thomas, *Thermal Properties of Gypsum Plasterboard at High Temperatures*, Fire and Materials, Vol. 26, 37-45, 2002.

(Winstone Wallboards Ltd 1997), *Penetrations and Closures in Gib® Fire Rated Systems*, Gib® Builders Manual, July 1997.

(Winstone Wallboards Ltd 2000), *Gib® Noise Control Systems*, Gib® Builders Manual, July 2000.

(Winstone Wallboards Ltd 2001), *Gib® Fire Rated Systems*, Gib® Builders Manual, August 2001.

(Winstone Wallboards Ltd 2002), *Gib® Aqualine Wet Area Systems*, Gib® Builders Manual, October 2002.

References

(Winstone Wallboards Ltd 2002), *Gib® Bracing Systems*, Gib® Builders Manual, November 2002.

(Winstone Wallboards Ltd 2003), *Penetrations in Gib® Fire Rated Systems*, Gib® Builders Manual, August 2003.

Appendix A Sample Test Scenarios

Test No.	Test Date	Board Type	Thickness [mm]	Fire Duration [min]	Heat Flux [kW/m ²]
1	16/12/2003	Standard	10	2	35
2	16/12/2003	Standard	10	5	35
3	16/12/2003	Standard	10	10	35
4	16/12/2003	Standard	10	15	35
5	16/12/2003	Standard	10	30	35
6	16/12/2003	Standard	10	2	50
7	16/12/2003	Standard	10	5	50
8	16/12/2003	Standard	10	10	50
9	16/12/2003	Standard	10	15	50
10	18/12/2003	Standard	10	2	65
11	18/12/2003	Standard	10	5	65
12	18/12/2003	Standard	10	10	65
13	18/12/2003	Standard	10	15	65
14	18/12/2003	Fyreline	10	2	65
15	18/12/2003	Fyreline	10	5	65
16	18/12/2003	Fyreline	10	10	65
17	18/12/2003	Fyreline	10	15	65
18	18/12/2003	Fyreline	10	2	50
19	18/12/2003	Fyreline	10	5	50
20	18/12/2003	Fyreline	10	10	50
21	18/12/2003	Fyreline	10	15	50
22	19/12/2003	Fyreline	10	30	50
23	19/12/2003	Fyreline	10	2	35
24	19/12/2003	Fyreline	10	5	35
25	19/12/2003	Fyreline	10	10	35
26	19/12/2003	Fyreline	10	15	35
27	19/12/2003	Fyreline	10	30	35
28	19/12/2003	Noiseline	10	2	35
29	19/12/2003	Noiseline	10	5	35
30	19/12/2003	Noiseline	10	10	35
31	19/12/2003	Noiseline	10	15	35
32	22/12/2003	Noiseline	10	30	35
33	22/12/2003	Noiseline	10	2	50
34	22/12/2003	Noiseline	10	5	50
35	22/12/2003	Noiseline	10	10	50
36	22/12/2003	Noiseline	10	15	50
37	22/12/2003	Noiseline	10	30	50

Appendix A

38	22/12/2003	Noiseline	10	2	65
39	22/12/2003	Noiseline	10	5	65
40	22/12/2003	Noiseline	10	10	65
41	22/12/2003	Noiseline	10	15	65
42	5/01/2004	Noiseline	10	30	65
43	5/01/2004	Fyreline	19	2	35
44	5/01/2004	Fyreline	19	5	35
45	5/01/2004	Fyreline	19	10	35
46	5/01/2004	Fyreline	19	15	35
47	5/01/2004	Fyreline	19	30	35
48	5/01/2004	Fyreline	19	45	35
49	5/01/2004	Fyreline	19	60	35
50	5/01/2004	Fyreline	19	2	50
51	5/01/2004	Fyreline	19	5	50
52	5/01/2004	Fyreline	19	10	50
53	5/01/2004	Fyreline	19	15	50
54	5/01/2004	Fyreline	19	30	50
55	5/01/2004	Fyreline	19	45	50
56	6/01/2004	Fyreline	19	60	50
57	6/01/2004	Fyreline	19	2	65
58	6/01/2004	Fyreline	19	5	65
59	6/01/2004	Fyreline	19	10	65
60	6/01/2004	Fyreline	19	15	65
61	6/01/2004	Fyreline	19	30	65
62	6/01/2004	Fyreline	19	45	65
63	8/01/2004	Fyreline	19	60	65
64	8/01/2004	Fyreline	16	15	50
65	8/01/2004	Fyreline	13	15	50
66	8/01/2004	Standard	13	15	50
67	8/01/2004	Standard	10	15	20

Appendix B Summary of Mass Loss and Calcination Depths

Test No.	Mass Before [g]	Mass After [g]	Total Mass Loss [g]	Depth [mm]					Mean Depth [mm]
				1	2	3	4	5	
1	189.92	185.87	4.05	2.79	2.8	2.52	2.68	2.36	2.63
2	195.69	185.28	10.41	5.05	4.99	4.99	5.24	5.14	5.08
3	192.76	171.98	20.78	5.52	5.62	5.59	5.61	5.19	6.21
	197.83	181.54	16.29	7.17	6.65	6.63	6.95	7.16	
4	194.43	166.37	28.06	5.75	5.32	6.1	5.72	5.62	6.39
	192.81	169.19	23.62	6.9	6.99	7.83	7.33	6.36	
5	193.75	157.08	36.67	7.71	7.98	8.71	8.3	7.96	8.13
6	190.23	182.51	7.72	3.77	4.01	3.57	3.95	3.91	3.84
7	197.61	182.4	15.21	6.47	6.27	6.53	5.96	6.18	6.12
	192.95	179.92	13.03	6.14	5.8	6.03	5.86	5.93	
8	196.05	168.7	27.35	6.45	7.73	7.87	6.78	7.09	6.73
	194.82	170.37	24.45	6.52	6.31	6.29	6.08	6.16	
9	196.87	162.03	34.84	9.31	8.7	8.59	8.1	8.06	8.55
10	191.4	185.7	5.7	4.16	4.23	4.2	4.41	4.38	4.26
	194.95	188.18	6.77	4.22	4.23	4.33	4.2	4.25	
11	193.65	179.43	14.22	5.99	5.65	5.43	5.5	5.71	5.96
	192.25	176.94	15.31	6.25	6.19	6.39	6.09	6.41	
12	194.66	165.44	29.22	6.86	6.37	6.05	7.07	6.67	6.60
13	196.66	158.15	38.51	9.15	8.82	9.21	8.92	8.79	8.98
14	213.67	199.5	14.17	3.9	3.37	3.89	3.73	3.5	3.68
15	214.67	194.83	19.84	4.38	4.48	4.01	3.98	4.45	4.26
16	214.99	184.19	30.8	4.41	4.97	4.07	4.78	5.01	4.65
17	217.38	176.25	41.13	8.5	6.36	8.52	8.18	8.37	6.91
	215.13	177.1	38.03	5.8	6.02	5.87	5.77	5.73	
18	213.89	208.12	5.77	3.08	2.86	2.86	2.69	2.83	2.67
	218.74	210.14	8.6	2.53	2.38	2.54	2.41	2.49	
19	216.84	204.04	12.8	3.86	3.59	4.31	4.04	4.31	3.55
	219.63	201.03	18.6	3.17	2.97	3.02	3.12	3.11	
20	215.6	191.47	24.13	4.33	3.87	4.31	4.64	4.33	3.99
	220.34	191.9	28.44	3.88	3.78	3.72	3.55	3.49	
21	218.68	184.66	34.02	4.74	4.65	5.04	4.87	5.32	5.25
	215.68	182.84	32.84	5.34	5.76	5.82	5.43	5.53	
22	214.52	170.14	44.38	8.31	7.61	8.15	7.99	7.67	7.95
23	212.97	209.26	3.71	2.42	2.38	2.32	2.26	2.14	2.14
	213.63	210.29	3.34	2.04	2.07	2.01	1.89	1.89	
24	215.93	199.96	15.97	3.84	3.66	3.93	4.49	3.84	

Appendix B

	216.8	208.31	8.49	2.99	2.84	2.51	2.86	2.85	3.38
25	215.95	194.84	21.11	4.43	3.8	4.18	4.11	3.81	4.07
26	214.34	190.61	23.73	5.07	4.81	4	4.01	4.88	4.55
27	218.12	181.79	36.33	5.28	5.11	4.74	4.5	4.46	4.82
28	257.83	251.68	6.15	0.87	0.79	0.79	0.7	0.71	0.77
29	259.41	247.02	12.39	1.08	1.2	1.23	1.23	1.26	1.2
30	258.38	238.02	20.36	1.34	1.42	1.38	1.4	1.25	1.36
31	259.81	231.63	28.18	1.6	1.56	1.55	1.48	1.72	1.58
32	257.23	216.57	40.66	1.89	1.53	1.85	1.77	1.68	1.74
33	259.61	254.52	5.09	1.26	1.18	1	1.14	1.05	1.13
34	259.08	247.27	11.81	1.64	1.57	1.53	1.49	1.55	1.56
35	255.17	230.7	24.47	1.79	1.62	1.71	1.93	1.77	1.76
36	266.07	229.61	36.46	2.18	1.93	1.69	1.85	1.86	1.90
37	262.59	210.26	52.33	2.36	2.02	2.11	1.88	2.01	2.08
38	262.2	252.11	10.09	1.4	1.36	1.37	1.37	1.34	1.37
39	259.14	240.82	18.32	1.81	1.78	1.87	1.74	1.72	1.78
40	259.05	226.65	32.4	1.95	1.89	1.99	1.97	1.94	1.95
41	257.33	213	44.33	2.08	2.31	2.36	2.01	2.02	2.16
42	260.72	205.82	54.9	2.5	2.62	2.06	2.25	2.36	2.36
43	511.19	508.17	3.02	0.9	0.9	0.92	0.71	0.73	0.83
44	516.48	509.97	6.51	1.4	1.59	1.46	1.3	1.24	1.40
45	513.89	499.88	14.01	1.72	1.61	1.54	1.62	1.6	1.62
46	506.39	481.56	24.83	2.06	1.72	1.89	1.86	1.73	1.85
47	523.15	477.2	45.95	2.68	2.44	2.53	2.5	2.55	2.54
48	517.56	457.73	59.83	3.07	3.36	3.39	2.8	2.94	3.11
49	517.25	447.03	70.22	3.19	3.19	3.57	3.14	3.63	3.34
50	507.61	504.74	2.87	1.21	1.19	1.27	1.29	1.21	1.23
51	506.08	497.51	8.57	1.48	1.51	1.6	1.49	1.44	1.50
52	520.45	499.01	21.44	2.72	2.6	2.57	2.69	2.7	2.66
53	516.45	482.67	33.78	3.59	3.25	3.13	3.01	3.35	3.27
54	512.97	454.7	58.27	4.82	4.73	4.74	4.4	4.33	4.60
55	512.46	440.05	72.41	4.88	5.04	4.93	4.55	5.27	4.93
56	508.11	430.67	77.44	4.98	5.47	5.77	5.17	5.05	5.29
57	525.13	518.67	6.46	1.84	1.86	1.84	1.85	1.66	1.81
58	526.84	513.16	13.68	2.77	2.49	2.58	2.62	2.44	2.58
59	517.17	489.25	27.92	2.96	3.3	3.4	3.1	3.08	3.17
60	530.01	487.03	42.98	4.63	4.26	4.38	4.57	4.4	4.45
61	514.55	446.29	68.26	5.99	5.2	5.44	5.17	5.24	5.41
62	517.55	435.63	81.92	5.97	6.21	6.16	5.36	5.68	5.88
63	526.48	436.4	90.08	6.24	6.05	6.46	5.98	6.03	6.15
64	419.69	392.75	26.94	2.26	2.51	2.92	2.39	2.31	
	407.22	372.2	35.02	3.34	2.6	2.79	3.49	2.68	2.73

Appendix B

65	295.31 291.52	264.83 259.36	30.48 32.16	4.98 5.87	5.31 5.75	5.43 5.79	5.25 5.91	4.35 5.82	5.45
66	272.01	236.88	35.13	7.49	6.7	7.99	7.29	6.7	7.23
67	197.03	187.36	9.67	5.15	5.01	5.07	5.33	5.08	5.54
	192.11	178.55	13.56	6.03	6.11	5.92	5.77	5.95	

Appendix C Mass Loss Curves

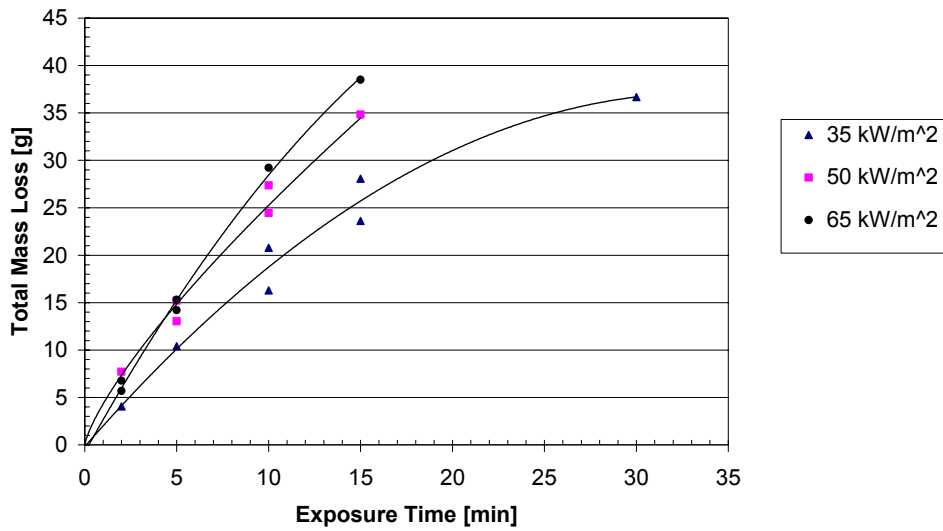


Figure C.1 Mass Loss versus Exposure Duration for 10 mm Standard Board

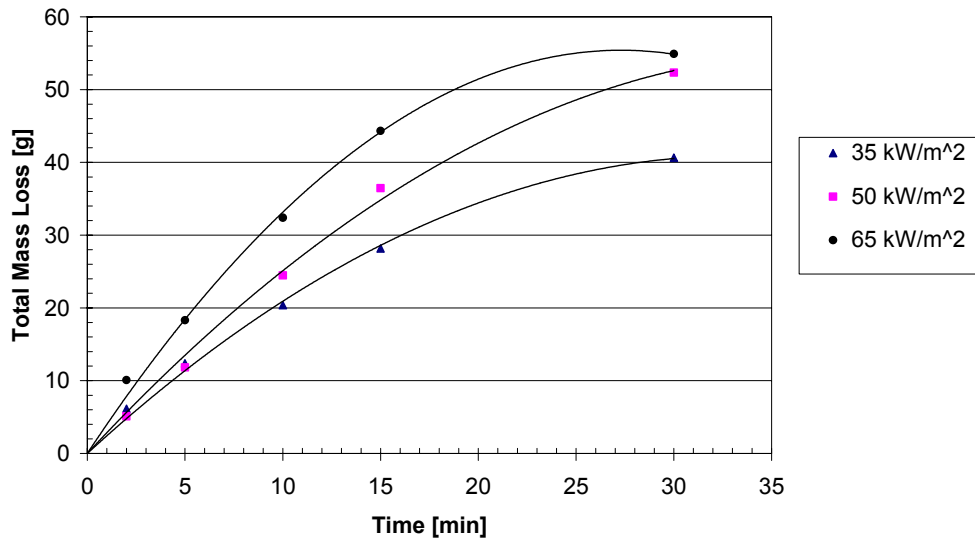


Figure C.2 Mass Loss versus Exposure Duration for 10 mm Noiseline Board

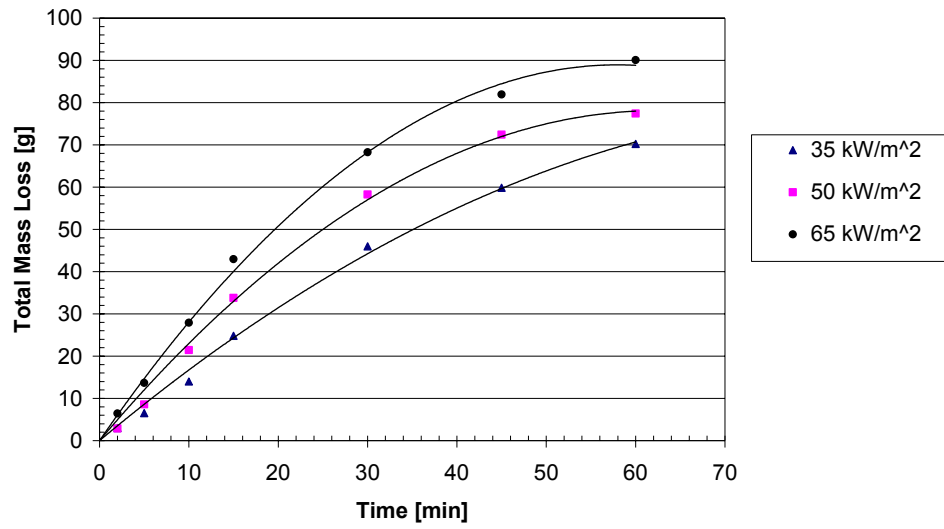


Figure C.3 Mass Loss versus Exposure Duration for 19 mm Fyrelite Board